CHAPTER III

RESULTS AND DISCUSSION

1. The effect of pH on stability of indomethacin

Table 13 shows the stability of IMC in various pH medium. A high performance liquid chromatography (HPLC) assay method was developed to measure IMC quantitatively after it was hydrolyzed by alkaline solution. The results indicated that in aqueous solution, IMC was decomposed by hydrolytic cleavage with a rate constant depending on the pH of the solution. The higher pH, the higher the decomposition is found (Muller and Brauns, 1985). The basic hydrolysis of IMC, an activated amide, converts to p-chlorobenzoate and 2-methyl-5-methoxy-indole-3-acetate (Mathews, McCancy and Cohen, 1984) is shown in Figure 5.

Table 13 Stability of indomethacin in phosphate buffer for agitation time of 12 hours

pH	Percent amount of indomethacin in solution	
	Initial	Shaking time 12 hours
6.0	100.00	83.68
7.4	100.00	71.92
8.0	100.00	47.21

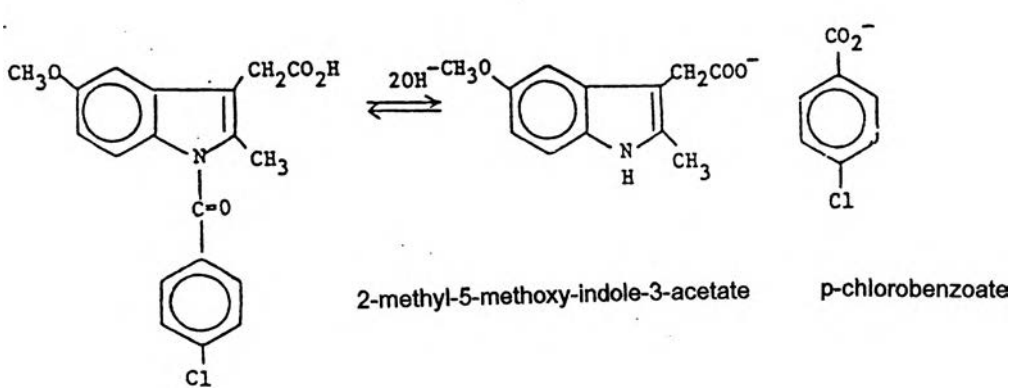

Figure 5 *Decomposition of indomethacin at higher pH*

2. Solubility study

2.1 Solubility study of indomethacin in various pH solutions

The results of the solubility of IMC in solution at various pH values are summarized in Table 14. The solubility of IMC increases as a result of the ionization of the drug when pH of solution increases (Espinar et al., 1992) since the drug is a weak acid (pKa is 4.5).

Table 14 Solubility of indomethacin in various pH solutions for agitation time of 12 hours

pH	Solubility of indomethacin in solution (mg%)
6.0	0.28
7.4	1 03
8.0	1.76

2.2 Solubility study of indomethacin in beta cyclodextrin solution

The construction of phase solubility diagram is used to determine the relationship between the total concentration of dissolved drug and the concentration of added cyclodextrin. Figure 6 and 7 show the solubility plots for the IMC-BCD systems in phosphate buffer pH 7.4 at 37 °C, shaken for 12, 24, 72 and 144 hours and Table 15 shows the solubilities of IMC in various concentration of BCD solution. The optimum shaking time was that when the concentration of IMC became constant. Although the concentrations of BCD were different, 12 hours of shaking time was enough for drug to be dissolved completely (Figure 7). In this study the solubility of IMC in phosphate buffer pH 7.4 without BCD was found to be about 2.89×10^{-5} M and at approximately about 14×10^{-3} M of BCD solution the increased is about 2.5 times the original value (8×10^{-5} M). From a plot of concentration of BCD versus concentration of IMC (Figure 6), the aqueous solubility of the drug increased almost linearly as a function of BCD concentration. It is clearly observed that the solubility of IMC in the presence of BCD can be classified as the A_L type according to Higuchi and Connors (1965).

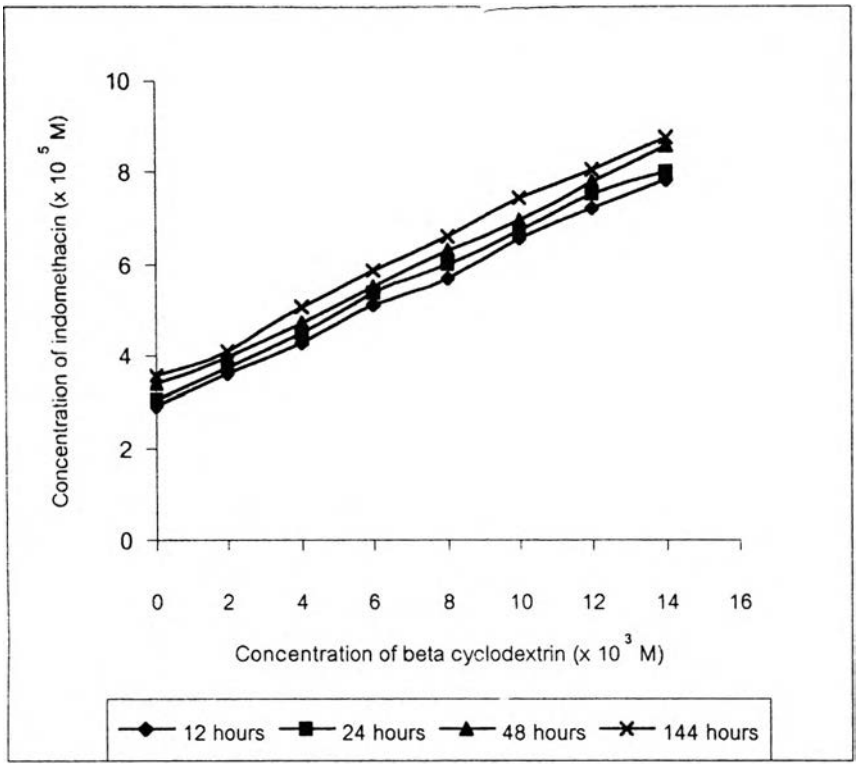

Figure 6 *Phase solubility diagram of indomethacin and beta cyclodextrin in phosphate buffer pH 7.4 at 37±1 °C*

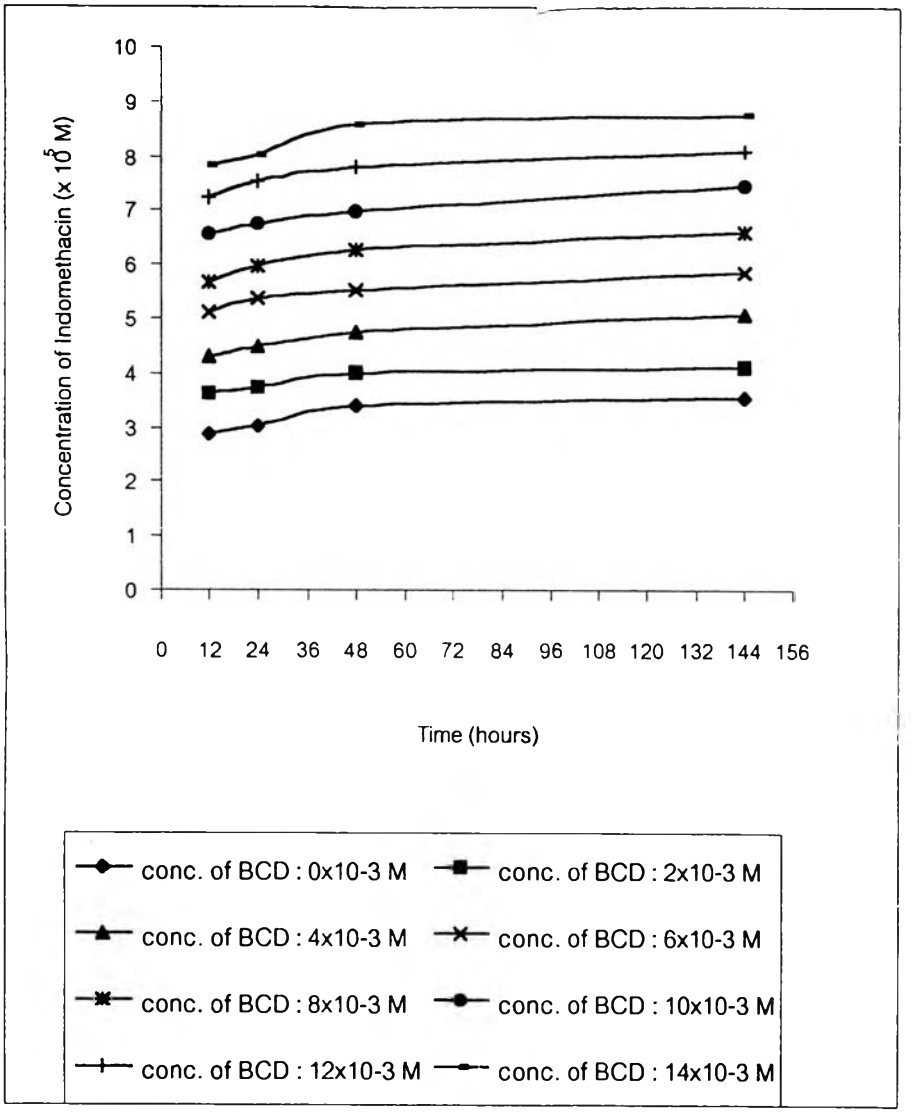

Figure 7 *Solubility of indomethacin at different concentrations of BCD in phosphate buffer pH 7.4 at 37±1 °C*

Table 15 Phase solubility of indomethacin with beta cyclodextrin in phosphate buffer pH 7.4 at 37±1 °C

Concentration of beta cyclodextrin ($\times 10^{-3}$ M)	Solubility of indomethacin ($\times 10^{-5}$ M) (SD)			
	12 hrs.	24 hrs.	48 hrs.	144 hrs.
0	2.89(0.15) ≅ 1.03 mg%	3.02(0.19)	3.41(0.36)	3.56(0.23)
2	3.62(0.08)	3.75(0.19)	3.99(0.21)	4.10(0.03)
4	4.28(0.06)	4.49(0.19)	4.73(0.19)	5.08(0.14)
6	5.11(0.08)	5.36(0.16)	5.52(0.36)	5.87(0.33)
8	5.67(0.15)	5.97(0.18)	6.27(0.45)	6.59(0.16)
10	6.55(0.19)	6.75(0.15)	6.97(0.07)	7.45(0.49)
12	7.23(0.56)	7.53(0.10)	7.81(0.55)	8.08(0.30)
14*	7.82(0.04)	8.02(0.33)	8.60(0.31)	8.77(0.25)

* Solubility limit of beta cyclodextrin

strength of complex and the change in physicochemical properties of guest molecule in the host molecule such as the solubility of guest molecule. The K_c value, within a range of 100 -1000 M^{-1}, shows the possibility of formation of inclusion complex (1:1) which may contribute to the improvement in bioavailability of poorly water-soluble drugs. Smaller stability constants give too weak of an interaction to improve the solubility whereas larger values hinder the absorption process (Higuchi and Connors, 1965). In this study, the average apparent stability was found to be 117 M^{-1}.

$$K_c = \frac{\text{slope}}{S_o(1\text{-slope})}$$

where S_o is the drug solubility (intercept).

This moderate stability constant may be explained on the basis that BCD had a rigid structure due to the presence of intramolecular hydrogen bonds within the hydroxyl groups of C2 and C3 of adjacent glucopyranose units (Moyano et al.,1995). This structure was found to interfere with the insertion of the p-chlorobenzoic part of IMC molecule into the cyclodextrin cavity (Backenfield et al., 1990).

2. Preparation of Indomethacin spray dried samples

2.1 Appearance of spray dried products

The solid IMC/BCD mixtures prepared by spray drying was a yellowish, fine powder. The particles of the spray dried products packed more loosely than each individual material or the physical mixtures due to its bulkiness and high electrostatic charge. The preparation nomenclature, as indication of various spray drying conditions and molar ratios, of spray dried products and physical mixtures are shown in Table 16-18. This classification will be used throughout this study.

2.2 Yield of Production

The yield of spray dried powder is expressed as the weight percentage of the final product harvested with respect to the initial amount of all components in each formulation. The spray dried products were collected from two locations of the spray dryer, the collector and the chamber. The amount of spray dried products from two sources was calculated as the percent yield. The yields of all spray dried products are shown in Table 19.

The average percent yield of spray dried IMC/BCD in every ratios were in the range of 70-80% while the percent yield of spray dried IMC/SLS gave 85-95% and spray dried IMC alone in phosphate buffer pH 7.4 had about 76% percent yield. The calculation of the percent yield of spray dried products were shown in the latter section. These results indicated that the percent yield of the spray dried powder was increased when SLS was used in the preparation due to the lower moisture content (as shown in a comparison of spray dried IMC/SLS with spray dried IMC/BCD in Table 22). The lower moisture content of spray dried powder, the lesser powder adhered in the chamber.

The calculation of the percent yield of spray dried products is being shown in this example (II10B130, Sample A):

The absolute actual solid content of IMC, BCD and 1.782% phosphate buffer in this spray dried powder is 115.64 g. After the spray drying process the residual amounts of these substances in the collector and chamber are 80.58

and 5.99 g, respectively. Each residual solid content divided by the absolute actual solid content are 69.68 and 5.18%, respectively. Thus, the total residual yield included each residual percent yield.

Table 16 Preparation nomenclature for various spray-drying conditions of IMC/BCD products

Ratio of IMC and BCD	Formulation		
	Inlet air temperature (°C)		
	130	140	150
1) 2:1 (indicated by IIB)			
Feed rate : 10 ml/min	II10B130	II10B140	II10B150
15 ml/min	II15B130	II15B140	II15B150
20 ml/min	II20B130	II20B140	II20B150
2) 1:1 (indicated by IB)			
Feed rate : 10 ml/min	I10B130	I10B140	I10B150
15 ml/min	I15B130	I15B140	I15B150
20 ml/min	I20B130	I20B140	I20B150
3) 1:2 (indicated by IBB)			
Feed rate : 10 ml/min	I10BB130	I10BB140	I10BB150
15 ml/min	I15BB130	I15BB140	I15BB150
20 ml/min	I20BB130	I20BB140	I20BB150

Table 17 Preparation nomenclature of IMC/BCD physical mixtures

Ratio of IMC and BCD	Formulation
2:1	IIB(PM)
1:1	IB(PM)
1:2	IBB(PM)

Table 18 Preparation nomenclature of IMC/SLS products

IMC/SLS system	Formulation	
	Spray-drying products at inlet air temperature 140 °C and feed rate 15 ml/min	Physical mixtures
1) IMC+13% SLS	IS13	IS13(PM)
2) IMC+20% SLS	IS20	IS20(PM)
3) IMC+27% SLS	IS27	IS27(PM)
4) IMC+33% SLS	IS33	IS33(PM)

Table 19 The percent yield values of spray-dried IMC/BCD and spray dried IMC/SLS

Formulation	Percent Yield of Production						Average
	A			B			
	Collector	Chamber	Total	Collector	Chamber	Total	
II10B130	69.68	5.18	74.86	73.18	6.33	79.51	77.19
II10B140	77.25	2.31	79.56	74.75	5.69	80.44	80.00
II10B150	78.59	0.39	78.98	78.69	0.26	78.95	78.97
II15B130	77.19	3.84	81.03	78.99	3.56	82.55	81.79
II15B140	80.41	3.04	83.45	82.72	2.31	85.03	84.24
II15B150	81.66	1.41	83.07	81.61	1.21	82.82	82.95
II20B130	57.23	27.41	84.64	52.66	28.71	81.37	83.01
II20B140	68.69	10.01	78.70	55.32	15.94	71.26	74.98
II20B150	73.15	7.91	81.06	74.76	5.34	80.10	80.58
I10B130	64.57	7.78	72.35	78.73	7.09	85.82	79.09
I10B140	69.26	6.67	75.93	67.35	5.58	72.93	74.43
I10B150	68.96	1.23	70.19	67.85	2.31	70.16	70.18
I15B130	72.09	4.03	76.12	71.59	4.67	76.26	76.19
I15B140	71.35	4.11	75.46	73.69	4.15	77.84	76.65
I15B150	75.58	3.34	78.92	77.23	4.01	81.24	80.08
I20B130	64.38	9.34	73.72	61.75	8.67	70.42	72.07

Table 19 (continue) The percent yield values of spray-dried IMC/BCD and spray dried IMC/SLS

Formulation	Percent Yield of Production						Average
	A			B			
	Collector	Chamber	Total	Collector	Chamber	Total	
I20B140	69.42	10.62	80.04	68.52	12.34	80.86	80.45
I20B150	71.31	6.37	77.68	76.30	3.81	80.11	78.90
I10BB130	73.15	4.73	77.88	77.86	5.61	83.47	80.68
I10BB140	77.66	4.25	81.91	79.44	3.61	83.05	82.48
I10BB150	81.10	4.01	85.11	79.56	2.35	81.91	83.51
I15BB130	75.03	5.15	80.18	77.87	6.01	83.88	82.03
I15BB140	79.35	4.94	84.29	78.86	5.97	84.83	84.56
I15BB150	80.61	2.50	83.11	79.95	2.64	82.59	82.85
I20BB130	73.04	5.15	78.19	76.96	4.04	81.00	79.60
I20BB140	76.90	2.86	79.76	72.81	4.05	76.86	78.31
I20BB150	82.97	2.61	85.58	83.57	4.12	87.69	86.64
IS13	73.16	12.71	85.87	76.65	11.69	87.34	86.61
IS20	71.41	17.26	88.67	75.16	17.43	92.59	90.63
IS27	63.52	20.83	84.35	64.48	20.88	85.36	84.86
IS33	63.71	26.87	90.58	62.16	25.92	88.08	89.33
Spray dried IMC	41.05	35.67	76.72	40.97	34.85	75.82	76.27

3. Evaluations of Physiochemical Properties of Spray Dried Powders

3.1 Scanning Electron Microscopy (SEM)

Scanning electron photomicrographs of IMC, buffer and BCD are shown in Figures 8 and 9. IMC and BCD prior to spray drying were irregular in shape, rough surface in various sizes adhering together (Figure 8A and 9A). The physical mixtures in Figure 10 characterized by the presence of crystals of each of the components (BCD and IMC) without modification in the shape or size. In contrast, the photomicrographs of the spray dried powder revealed the effect of the spray drying process. The spray drying process produced powder which were small and more spherical in shape. It was shown that the shape and surface topography of individually spray dried IMC and BCD (Figure 8C and 8D, Figure 9B) were different from the original IMC and BCD crystals, respectively. Figure 8 shows that the spray dried IMC in buffer solution resulted in the small and spherical particles but spray dried IMC in water (Figure 8B) was not different from pure IMC. This was possibly due to the poor solubility of IMC in water (pH 4.5) resulting in the formation of a suspension instead of clear solution and spray dried as individual original particles. IMC in phosphate buffer pH 7.4, however, was ionized and resulted in true solution. For the spray dried BCD (Figure 9B), it was observed to be spherical but with several wells on the surface. This result indicated that BCD was possibly swollen initially and collapse due to the high temperature in the spray drying chamber and then immediately cool down.

The photomicrographs of spray dried powder obtained from IMC in BCD solution at different ratios (2:1, 1:1 and 1:2, respectively) are shown in Figures 11-13. They exhibited a spherical, concave surface similar to that of spray dried BCD. The photomicrographs of spray dried IMC/BCD prepared with various molar ratios and spray-drying conditions, such as temperatures and feed rates, showed no differences in the shape, size and surface topography when observed under SEM.

The microscopic images of SLS before and after spray drying process are shown in Figure 14. SLS prior to spray drying exhibited the agglomeration of small particles, producing the irregular shape with rough creases and fold surface. After spray drying process they exhibited smaller and smoother spherical particles. For the

physical mixtures, photomicrographs (Figures 15) show mainly the crystals of IMC. It can be explained by the way that the mixtures contained very small amounts of SLS compared to IMC used in the system.

The shape and surface topographies of the spray dried powder of IMC prepared by using SLS at the various percentages are shown in Figure 16. The spray dried IMC/SLS was small and spherical with smoother surfaces when compared with spray dried IMC/BCD at different molar ratios and spray drying conditions. These results were possibly due to the more rigid outer shell of the particles of spray dried IMC/SLS when they were compared with the outer shell of the particles of spray dried IMC/BCD. During the spray drying process, water in the particles of IMC/BCD diffused to the dried outer shell of the particles and caused the outer shell to swell reducing the thinness of the shell and increase diffusitivity. Thus, when temperature decreased after spray drying process, the swollen outer shell of IMC/BCD particles collapsed resulting in the concave surface observed. On the other hand, the dried outer surface of the particles of spray dried IMC/SLS were assumed to be much more rigid than IMC/BCD. While water tried to diffuse through the outer shell of particles, there was high pressure build-up in the particles causing cracks and breakage observed in spray dried IMC/SLS.

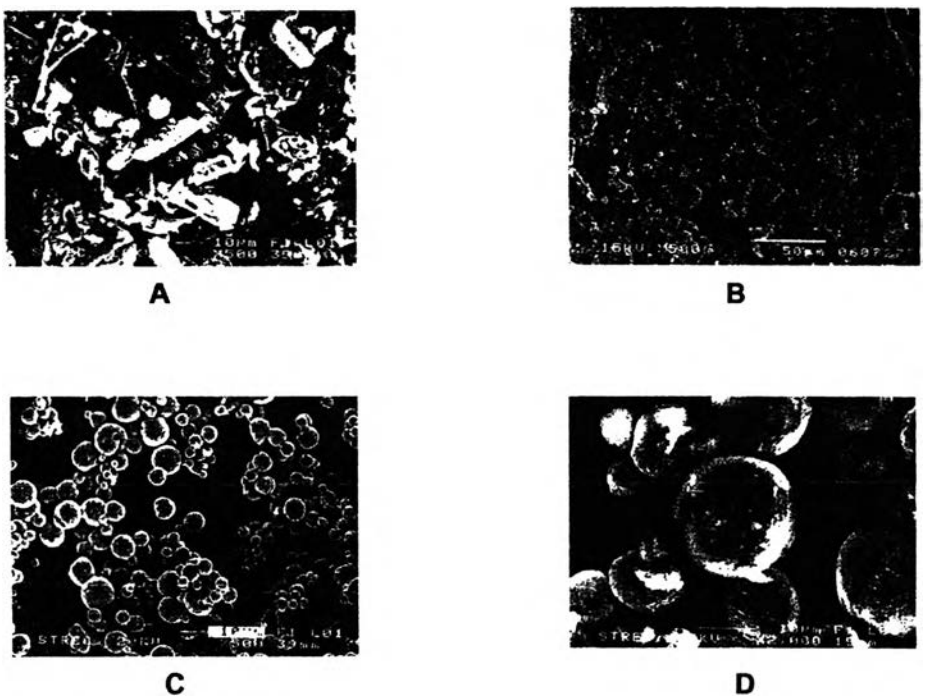

Figure 8 *Scanning electron photomicrographys of (A) IMC; (B) spray dried IMC in water; (C) spray dried IMC in buffer and (D) spray dried buffer*

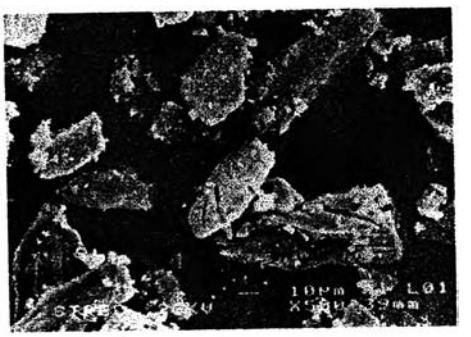

A

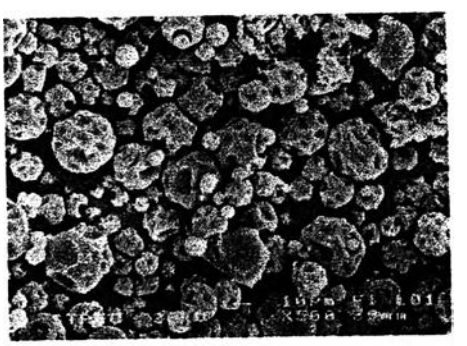

B

Figure 9 *Scanning electron photomicrographs of (A) BCD and (B) spray dried BCD in buffer*

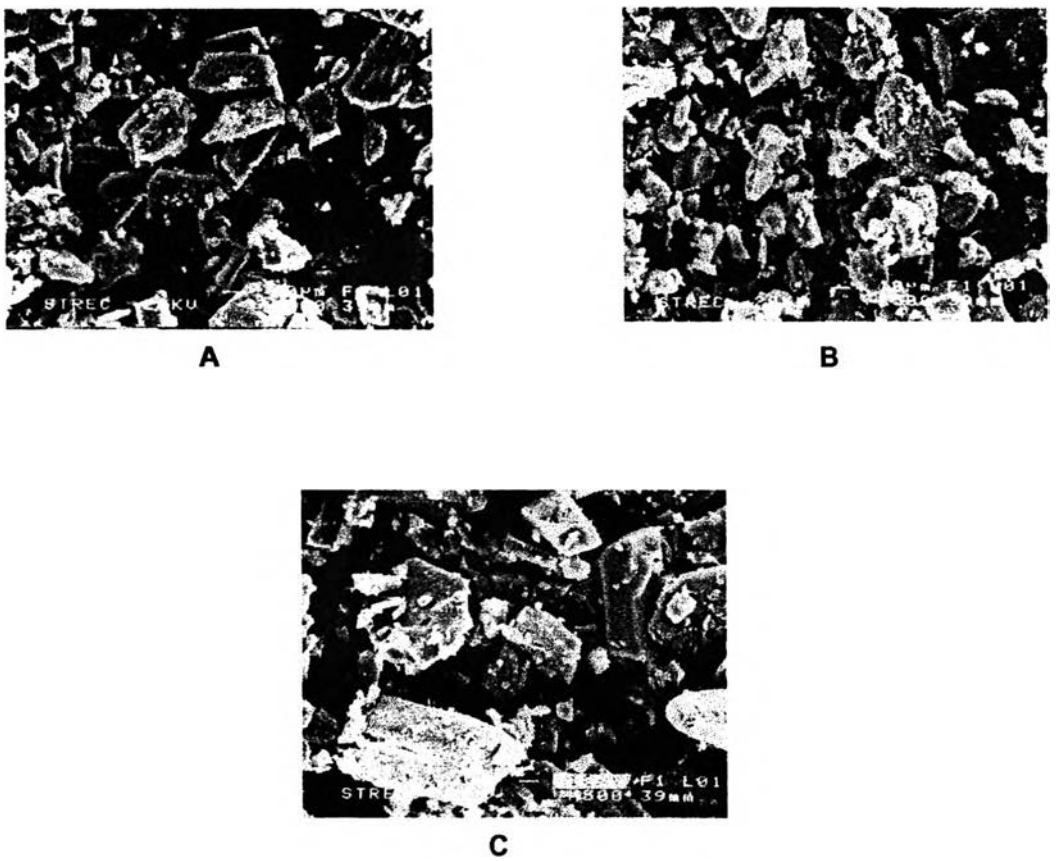

Figure 10 *Scanning electron photomicrographs of indomethacin and beta cyclodextrin physical mixtures : (A) IIB (PM); (B) IB(PM) and (C) IBB (PM)*

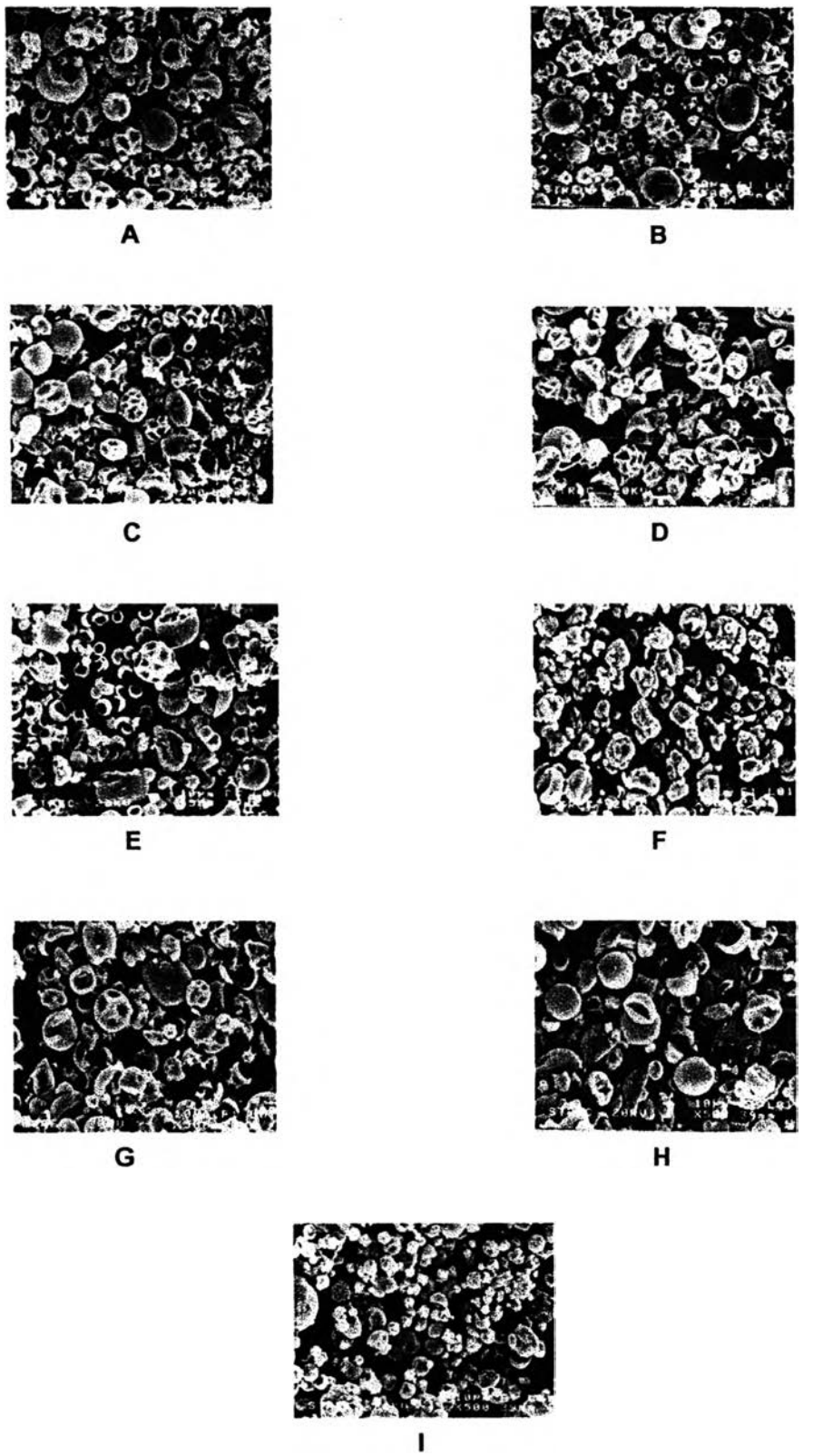

Figure 11 *Scanning electron photomicrographs of spray dried indomethacin and beta cyclodextrin at molar ratio 2:1 [(A) II10B130; (B) II10B140; (C) II10B150; (D) II15B13; (E) II15B140; (F) II15B150; (G) II20B130; (H) II20B140 and (I) II20B150]*

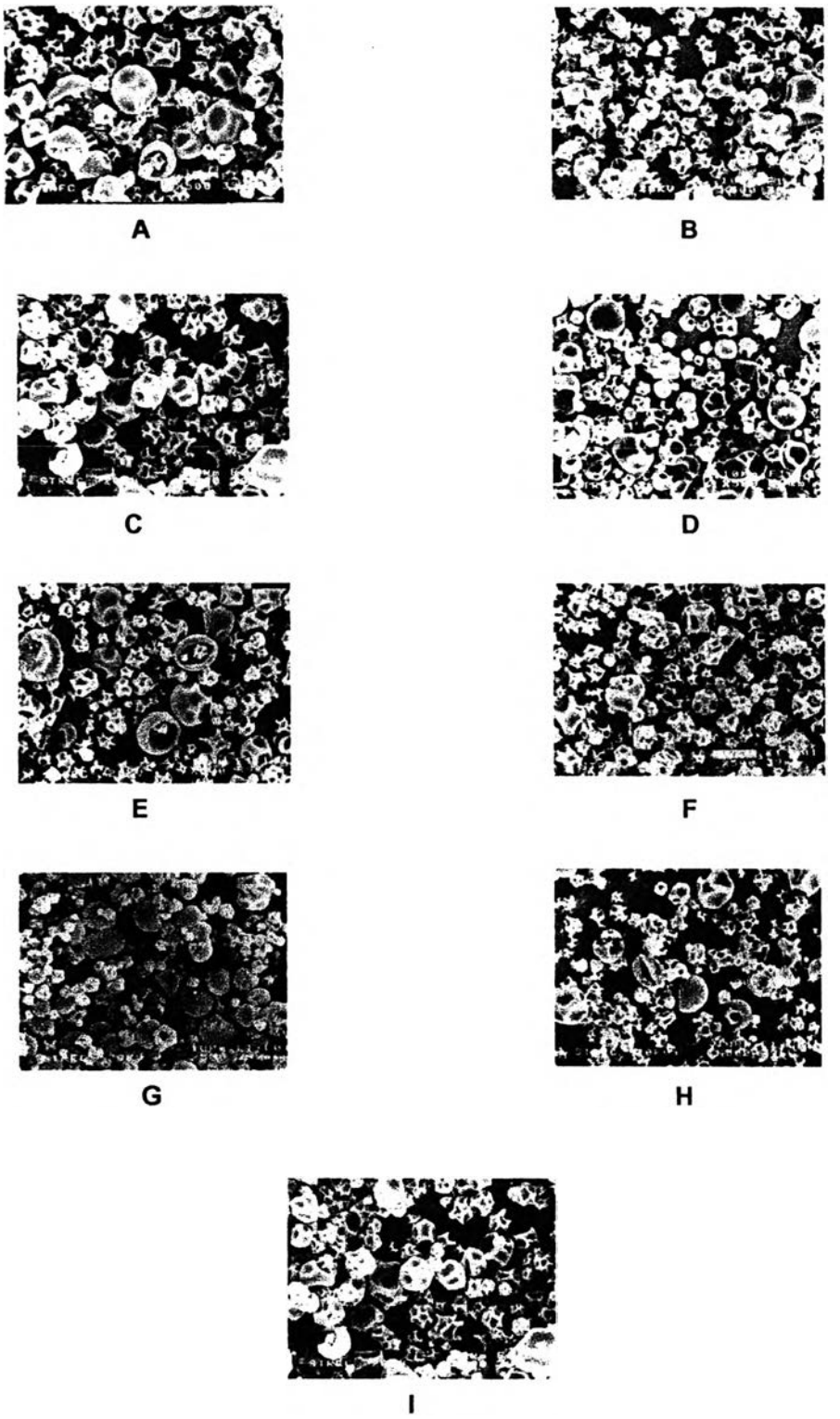

Figure 12 *Scanning electron photomicrographs of spray dried indomethacin and beta cyclodextrin at molar ratio 1:1 [(A) I10B130; (B) I10B140; (C) I10B150; (D) I15B130; (E) I15B140; (F) I15B150;(G) I20B130; (H) I20B140 and (I) I20B150]*

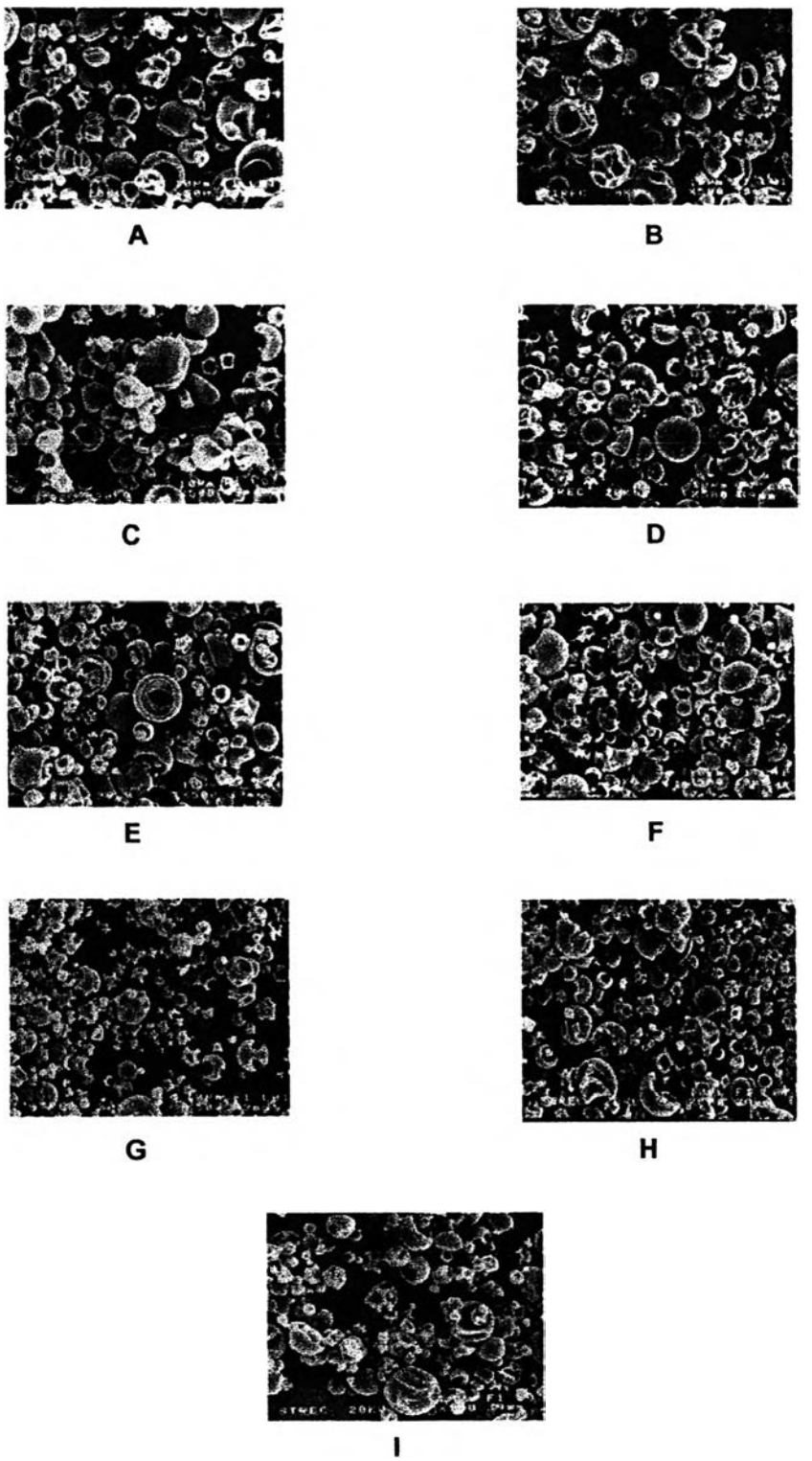

Figure 13 *Scanning electron photomicrographs of spray dried indomethacin and beta cyclodextrin at molar ratio 1:2 [I10BB130; (B) I10BB140; (C) I10BB150; (D)I15BB130; (E) I15BB140; (F) I15BB150; (G) I20BB130; (H) I20BB140 and (I) I20BB150]*

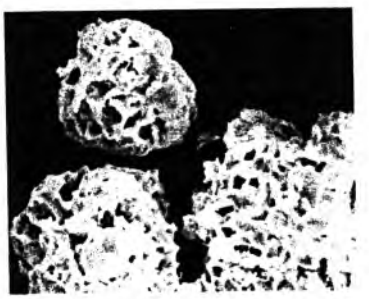

A

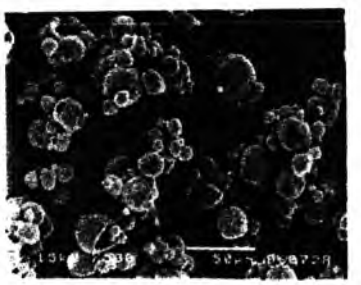

B

Figure 14 *Scanning electron photomicrographs of (A) SLS and (B) spray dried SLS*

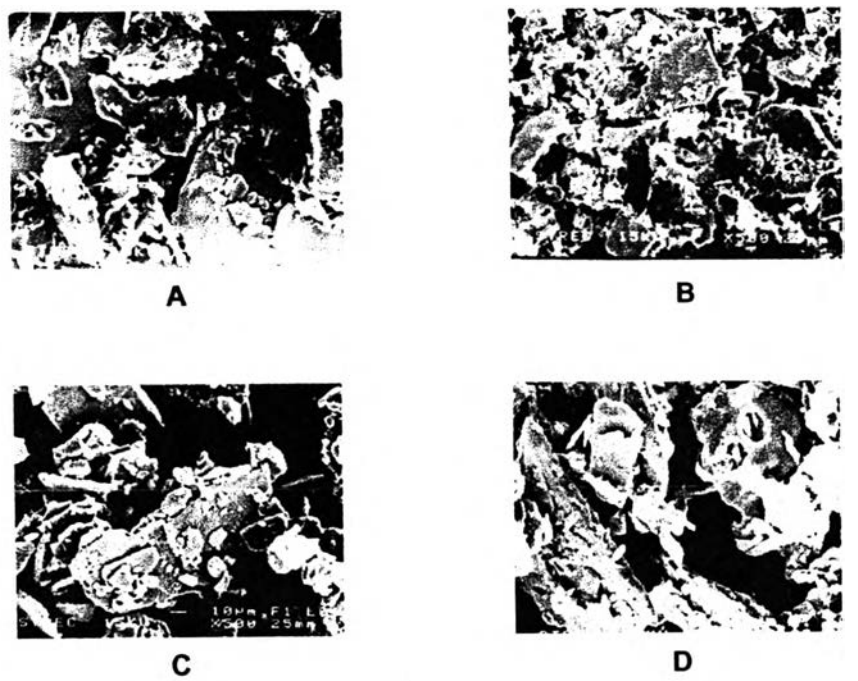

Figure 15 *Scanning electron photomicrographs of indomethacin and sodium lauryl sulfate physical mixtures :(A) IS13 (PM); (B) IS20(PM); (C) IS27(PM) and (D) IS33(PM)*

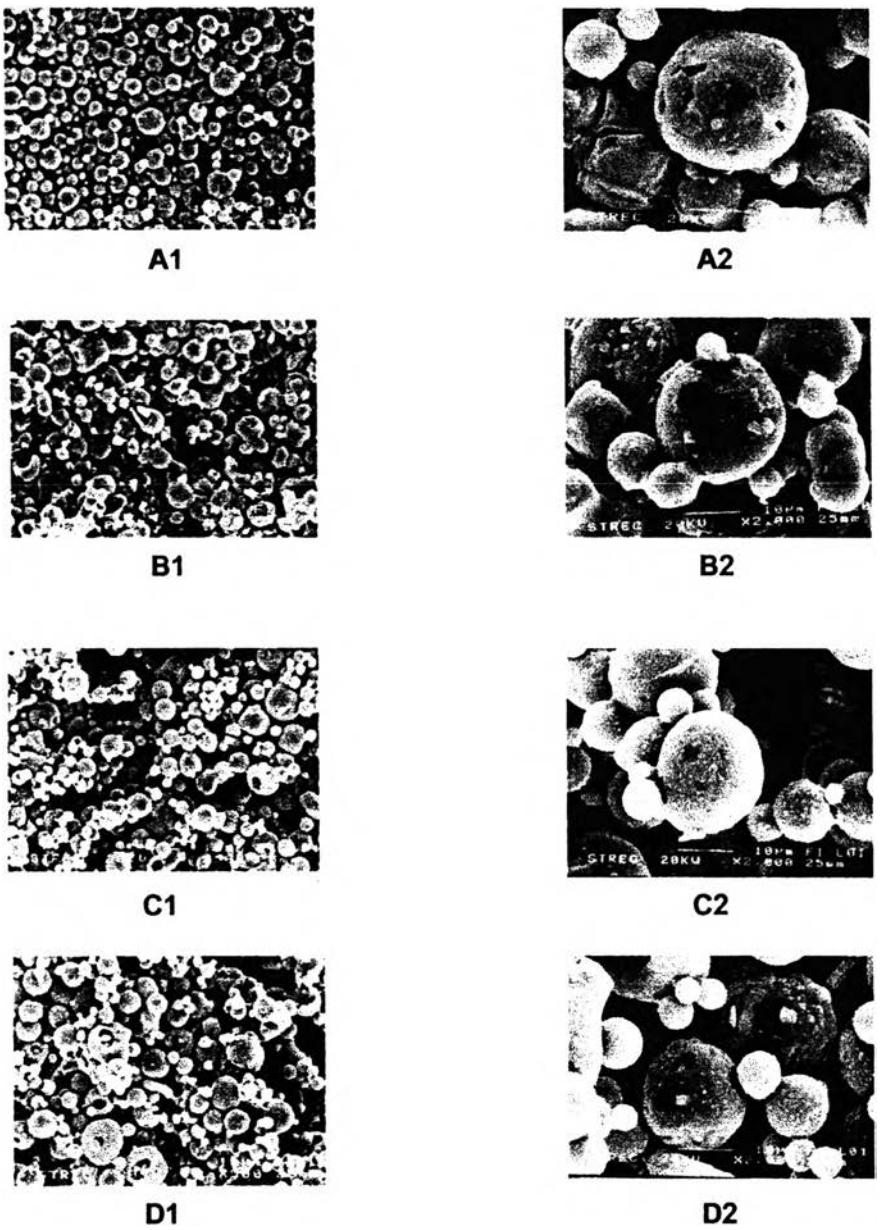

Figure 16 *Scanning electron photomicrographs of spray dried indomethacin and sodium lauryl sulfate prepared by various percentage of SLS [(A1 and A2) IS13; (B1 and B2) IS20; (C1 and C2) IS27 and (D1 and D2) IS33]*

3.2 Flow rate, Bulk Density, Tapped Density and Percent Compressibility

Table 20 shows flow rate, bulk density, tapped density and percent compressibility of spray dried powder prepared from different compositions and spray drying conditions.

The bulk densities varied between 0.4 and 0.6 g/cm^3 while tapped densities ranged between 0.6 and 1.1 g/cm^3. The bulk density is an important parameter used to determine the space required for the storage of bulk drug. It can also influence powder flowability and may influence certain characteristics of the final product (Foster and Leatherman, 1995). Tapped density is used to investigate the packing properties of materials (Grant and Brittain, 1995).

The mean bulk densities of IMC and spray dried IMC were 0.5 and 0.4 g/cm^3, respectively. A comparison of spray dried IMC/BCD (II10B130-I20BB150) and IMC/BCD physical mixtures [IIBB(PM)-IBB(PM)] showed spray dried IMC/BCD had bulk densities of 0.5-0.6 g/cm^3, while IMC/BCD physical mixtures had bulk densities of 0.6-0.7 g/cm^3. These results showed no statistical difference ($p>0.05$). When compared bulk densities of spray dried IMC/SLS (IS13-IS33) of about 0.4 g/ cm^3 and IMC/SLS physical mixtures [IS13(PM)-IS33(PM)] about 0.6 g/ cm^3 it was shown that they are statistically different ($p<0.05$) indicating that the bulk density of IMC/SLS physical mixtures were significantly more than that of spray dried IMC/SLS. This is possibly due to the smaller particle size of spray dried IMC/SLS than that of IMC/SLS physical mixtures (as shown in the particle size determination) which cause it to have high electrostatic charge as can be visually observed resulting in a lower bulk density of spray dried IMC/SLS.

The mean tapped densities of IMC and IS(PM) were not different. When compared tapped density of physical mixtures of IMC/SLS [IS13(PM)-IS33(PM)], about 0.8 g/cm^3, and spray dried IMC/SLS [IS13-IS33], about 1.0 g/cm^3, it was shown that the tapped density of spray dried IMC/SLS was more than that of physical mixture due to the smaller particle size (as indicated in particle size determination in Table 21), producing in the spray drying process.

Compressibility of powder is also related to the flowability of powder. The more flowable the powder the smaller compressibility value. A compressibility value smaller than 20% suggests excellent flowability of powders (Lin and Kao, 1989). Table 20 shows that the compressibility values of pure IMC and spray dried IMC were 28.6 and 33.3%. The high percent compressibility of pure IMC (28.6%) and spray spray dried IMC (33%) were due to the irregular shape of IMC particles and the high electrostatic charge of the smaller particle size, respectively. The percent compressibility values of IIB and IB were not different (about 17%) while the percent compressibility of IBB (about 25%) was higher the other ratios due to the high amount of BCD used (BCD was shown to have high moisture content as will be discussed in TGA determination). The high moisture content in the system caused the powder to be less flowable due to the cohesive powder. The variation of the compressibility values of spray dried IMC/BCD (14-29%) may be due to the variation of particle size of spray dried products (as indicated in SEM) and the high electrostatic charge of the small particle size (as indicated in the appearance of spray dried powder). Thus, the flow of spray dried IMC/BCD can not be concluded by comparison of compressiblity values due to the above variations. A better way to determine the flow of spray dried IMC/BCD should be the determination of the actual flow rate which will be discussed latter.

The compressibility of spray dried IMC/SLS (IS13-IS33) were 44-62% while IMC/SLS physical mixtures [IS13(PM)-IS33(PM)] were all 25%. These results indicated that the average compressibility value of spray dried IMC/SLS was more than 50%. They exhibited a very, very poor flowability of powder according to Foster T. and Leatherman W. due to the high electrostatic charge of spray dried IMC/SLS (as indicated in the appearance of spray dried powder). While the percent compressibility values of each IMC/SLS physical mixture were not different and were small (comparable to that of pure IMC) due to the high amount of IMC relative to SLS in IMC/SLS physical mixtures.

Due to the various factors involving in the compressibility determinations and causing the flowability results to be inconclusive, a better way to determine flowability is measure the actual flow rate. The mean flow rate of pure drug and spray dried IMC were 634.5 and 404.9 mg/sec, respectively. The mean flow rate

of spray dried IMC/BCD which can be tested varied between 155.3 and 796.6 mg/sec while IMC/BCD physical mixtures ranged between 541.1 and 810.6 mg/sec. The flowability of IMC/BCD physical mixtures depended on the amount of BCD in the system. An increased amount of a large particulate BCD in the physical mixtures may improve the flow property of the physical mixtures. In contrast, from the data shown in Table 20 indicated that flowability of spray dried IMC/BCD depended on the amount of IMC in the system (as indicated that the flow rate of IIB was more than that of IB and IBB, respectively). Thus, the higher amount of IMC the better flow of powder. This is possibly due to spray dried BCD having the spherical shape with several rough wells on the surface while comparing to IMC which are smooth spherical particles (as shown in SEM). Thus, the higher amount of IMC the more spherical the particles causing a better flow of spray dried powder. It can also be noted that the flow of pure IMC was approximately equal to that of spray dried IMC/BCD (II10B130, II10B140, II10B150, II15B150, II20B140, I10B130, I10B140, I15B130, I15B150, I20B130, I20B150, I10BB140, I10BB150, I15B130, I20BB140 and I20BB150) and the reason as discussed in the previous section. The above results can be concluded that the mean flow rate order are as the following:

IMC/BCD physical mixtures $\approx$ IMC $\approx$ spray dried IMC/BCD (2:1) > spray dried IMC > spray dried IMC/BCD (1:1) $\approx$ spray dried IMC/BCD (1:2)

Thus, as can be seen that the various ratios of IMC/BCD used in the spray drying process did have significant impact on the overall flowability of spray dried powder.

As shown in Table 20, the flow rate of spray dried IMC/SLS ranged from 547.2 and 562.6 mg/sec while IMC/SLS physical mixtures ranged between 535.0 and 562.9 mg/sec. No statistical difference ($p > 0.05$) was observed between the mean flow rates of spray dried IMC/SLS and IMC/SLS physical mixtures. However, the flow rate of spray dried IMC/SLS was poorer than IMC due to the effect of having residual moisture in spray dried IMC/SLS as indicated by moisture loss in TGA (Figure 22) and the dehydration peak in DSC thermograms (Figure 27 and 28).

Table 20 The bulk density, tapped density and percent compressibility of pure IMC, physical mixtures and spray dried products

Sample	Flow rate (mg/sec)*	Bulk Density* (g/ml)	Tapped Density* (g/ml)	% Compressibility (%)
II10B130	563.3	0.5	0.7	28.6
II10B140	610.2	0.5	0.7	28.6
II10B150	724.5	0.5	0.7	28.6
II15B130	496.3	0.6	0.7	14.3
II15B140	730.0	0.6	0.7	14.3
II15B150	796.6	0.5	0.7	28.6
II20B130	502.5	0.5	0.6	16.7
II20B140	509.4	0.5	0.7	28.6
II20B150	566.2	0.5	0.7	14.3
I10B130	305.4	0.5	0.7	28.6
I10B140	225.4	0.5	0.7	28.6
I10B150	281.4	0.5	0.6	16.7
I15B130	220.3	0.5	0.7	28.6
I15B140	246.2	0.6	0.7	14.3
I15B150	206.8	0.5	0.7	28.6
I20B130	None	0.5	0.7	28.6
I20B140	None	0.5	0.7	16.7
I20B150	None	0.5	0.7	28.6
I10BB130	155.3	0.5	0.6	16.7
I10BB140	156.4	0.5	0.7	28.6
I10BB150	172.4	0.5	0.7	28.6
I15BB130	156.3	0.5	0.7	28.6
I15BB140	156.6	0.6	0.7	14.3
I15BB150	176.5	0.6	0.7	14.3
I20BB130	179.9	0.6	0.7	14.3
I20BB140	178.5	0.6	0.7	28.6

* Average from three determinations

Table 20 (continue) The bulk density, tapped density and percent compressibility of pure IMC, physical mixtures and spray dried products

Sample	Flow rate (mg/sec)*	Bulk Density* (g/ml)	Tapped Density* (g/ml)	% Compressibility (%)
I20BB150	177.7	0.5	0.7	28.6
IIB(PM)	541.1	0.6	0.7	16.7
IB(PM)	695.8	0.6	0.7	16.7
IBB(PM)	810.6	0.6	0.8	25.0
IS13	547.2	0.4	1.1	63.6
IS20	562.6	0.4	1.1	63.6
IS27	553.4	0.5	1.0	50.0
IS33	561.9	0.5	0.9	44.4
IS13(PM)	562.9	0.6	0.8	25.0
IS20(PM)	535.0	0.6	0.8	25.0
IS27(PM)	550.3	0.6	0.8	25.0
IS33(PM)	556.7	0.6	0.8	25.0
IMC	634.5	0.5	0.7	28.6
Spray dried IMC	404.9	0.4	0.6	33.3

* Average from three determination

The above results can be concluded that the spray dried products did not improve the flowability of pure drug. The reasons include the presence of electrostatic charge, small particle size (Table 21), surface morphology and/ or moisture content in the spray dried products (Table 22). But amounts of IMC and BCD affect flow of IMC/BCD spray dried powder. In contrast, amount of SLS did not have significant impact of the flowability of IMC/SLS spray dried powder.

3.3 Particle size determination

The spray dried products were observed to be fairly spherical particles under an optical microscope. From Table 21 it was shown that the average particle size of spray dried IMC was smaller than pure drug.

The average particle size of IIB were in the range of 37.11 to 67.04 μm. From Table 21 indicates the low average particle size of IIB except the average particle size of IIB prepared by inlet air temperature 130 °C and feed rate 15 ml/min. A reason for this result may be due to the high particle size distribution (as indicated by high standard deviation) which affected the average particle size determination by this method.

Table 21 shows that the average particle size of spray dried IB varied between 38.56 and 46.24 μm. The results were that the average particle size of IB were not significantly different ($p>0.05$).

The average particle size of IBB ranged between 38.81 and 59.74 μm. The results from Table 21 shows that feed rate and inlet air temperature affect on the average particle size of IBB. The reasons for the higher average particle size than the IIB and IB were due to the high amount of BCD in the preparations which produced a large rough particles.

IS having the average particle size of 20.93 to 32.43 μm. It was shown that IS33 has possibly the highest average particle size due to the high moisture content of spray dried powder (2.21%), compared with the other spray dried IMC/SLS. Thus, it may be causing particles to agglomerate to the larger particles.

Table 21 Particle size [d(v,0.5)] of indomethacin and spray dried products (micrometer)

Sample	Inlet air temperature °C [SD]		
	130	140	150
1) IIB			
Feed rate : 10 ml/min	38.70[0.18]	42.44[0.58]	42.84[0.13]
15 ml/min	67.04[1.44]	57.04[0.54]	37.11[0.75]
20 ml/min	45.88[0.30]	43.34[0.43]	44.38[0.42]
2) IB			
Feed rate : 10 ml/min	41.78[0.09]	41.27[0.23]	43.47[0.24]
15 ml/min	38.56[0.08]	46.24[0.17]	39.47[0.41]
20 ml/min	40.94[0.28]	43.00[0.48]	39.28[0.36]
3) IBB			
Feed rate : 10 ml/min	38.81[0.70]	54.40[0.48]	59.74[0.23]
15 ml/min	48.86[0.40]	47.51[0.43]	43.96[0.58]
20 ml/min	58.34[0.15]	45.42[0.49]	58.61[0.44]
4) IS13	**	22.32[0.70]	**
IS20	**	20.93[0.23]	**
IS27	**	23.64[0.33]	**
IS33	**	32.43[0.25]	**
5) Spray dried IMC	**	60.69[0.67]	**
6) IMC	151.73[2.11]		

* Average from three determinations

** These spray dried IMC/SLS were not prepared with varying spray drying conditions because the study would like to investigate only the role of SLS concentrations on solubility enhancement of IMC.

3.4 Thermogravimetry

TGA thermograms of spray dried IMC, BCD, SLS and spray dried products prepared with various components according to Table 16-18 are shown in Figures 17-22 and APPENDIX D. Percent weight loss from TGA thermograms of all components and spray dried products are summarized in Table 22. The results from TGA thermograms were used to confirm the results obtained by DSC in checking the location of temperature where endothermic changes occurred and the percent weight loss of the substances compared to that of IMC and BCD.

Weight loss of spray dried IMC in buffer could be seen between the temperature range of 50-100 °C and 183-248 °C (Figure 17). Weight loss of spray dried BCD (Figure 18) was observed to also be in two ranges, 50-120 °C and 220 °C onward. The first range for both instances is indicative of water loss from the samples and the second range is the fusion of remaining solids (confirmed by DSC analysis in Figure 27B). Results in Table 22 indicated that percent moisture content of spray dried IMC/BCD (4-8%) was higher than the spray dried IMC/SLS (moisture content was in the range of 1.29-2.21%). The high moisture content of IIB [Appendix E], IB [Figure 20] and IBB [Appendix E] were in the range of 5-8, 5-10 and 5-8 percent, respectively due mainly to the ability of BCD to absorbed moisture (from Figure 21, BCD contained moisture of 13.64%) and residual water retained from spray drying process.

From the above results weight loss of spray dried SLS (Figure 21) and IS with various percentage of SLS (Figure 22) could be also seen in two ranges (30-120 °C and 160-200 °C). The first range and the second range indicated the same as TGA thermograms of spray dried IMC/BCD mentioned previously. Figure 21 and 22 confirmed the results obtained by DSC analysis shown in Figure 30.

Table 22 Percent moisture content in spray dried products

Sample	Inlet air temperature °C		
	130	140	150
1) IIB			
Feed rate : 10 ml/min	5.180	4.869	4.434
15 ml/min	5.981	6.414	3.917
20 ml/min	6.013	7.511	5.08
2) IB			
Feed rate : 10 ml/min	5.582	5.927	6.155
15 ml/min	9.381	9.459	7.639
20 ml/min	7.485	6.309	5.548
3) IBB			
Feed rate : 10 ml/min	5.732	8.656	6.577
15 ml/min	6.778	6.135	6.002
20 ml/min	7.264	7.652	6.282
4) IS13	*	1.293	*
IS20	*	1.416	*
IS27	*	1.389	*
IS33	*	2.211	*
5) Spray dried IMC	*	4.676	*
6) Spray dried BCD	*	12.194	*
7) Spray dried SLS	*	0.4270	*

* These spray dried IMC/SLS were not prepared with varying spray drying conditions because the study would like to investigate only the role of SLS concentrations on solubility enhancement of IMC.

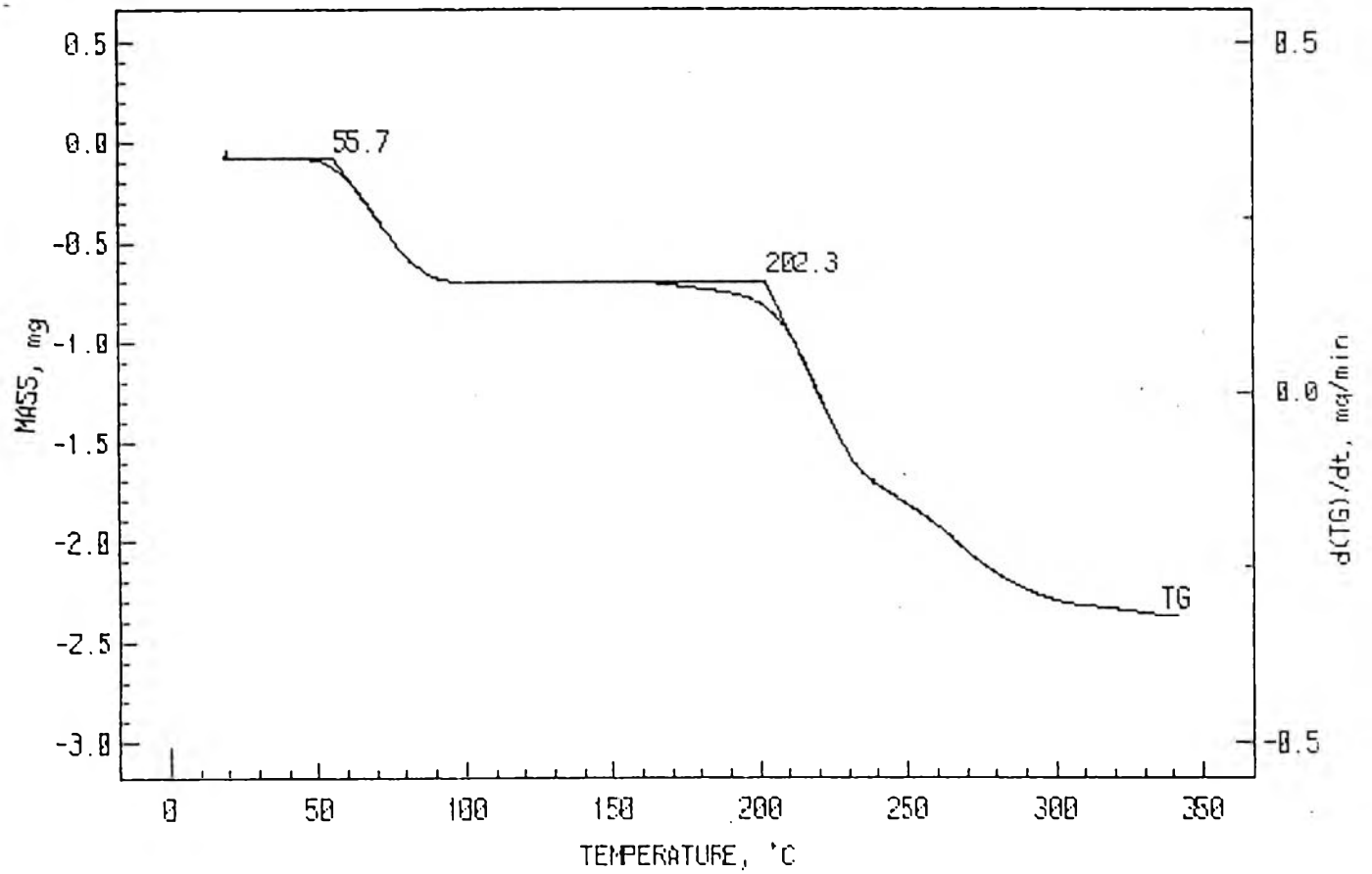

Figure 17 *TGA thermograms of spray dried indomethacin in buffer (spray dried IMC)*

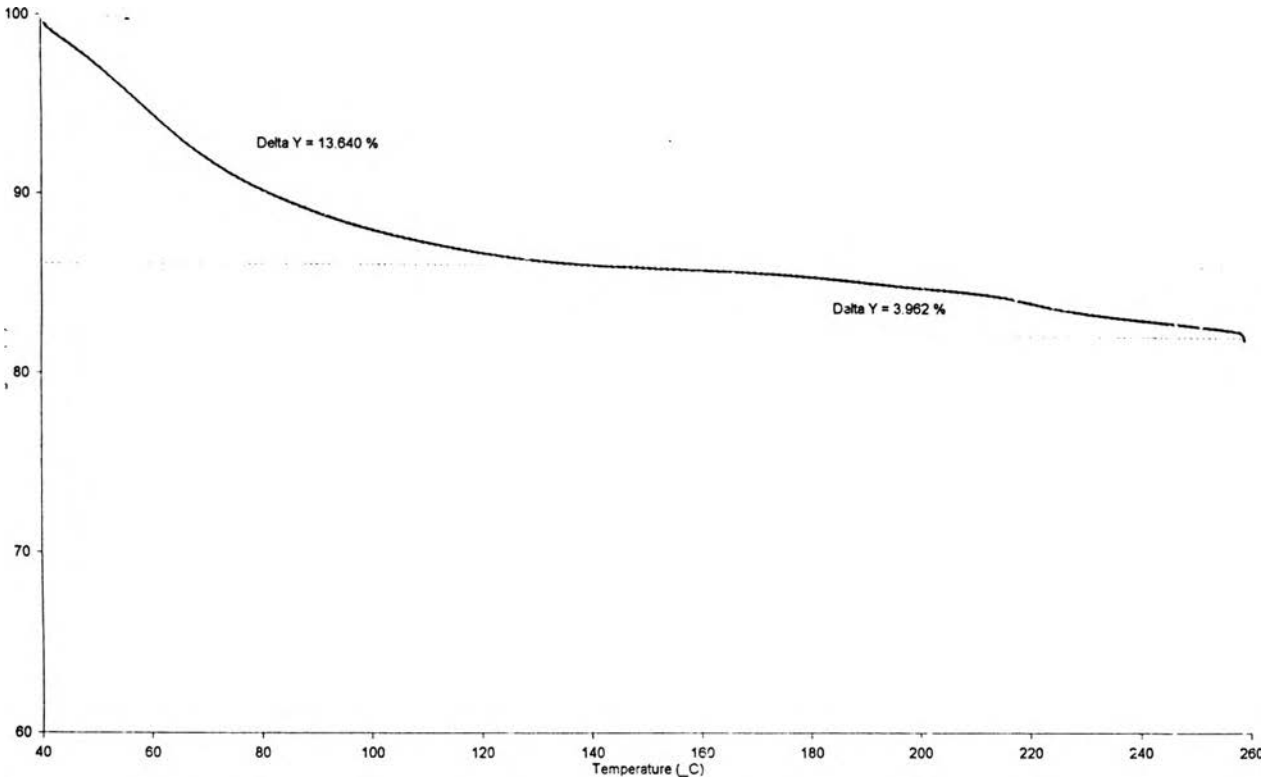

Figure 18 *TGA thermograms of BCD*

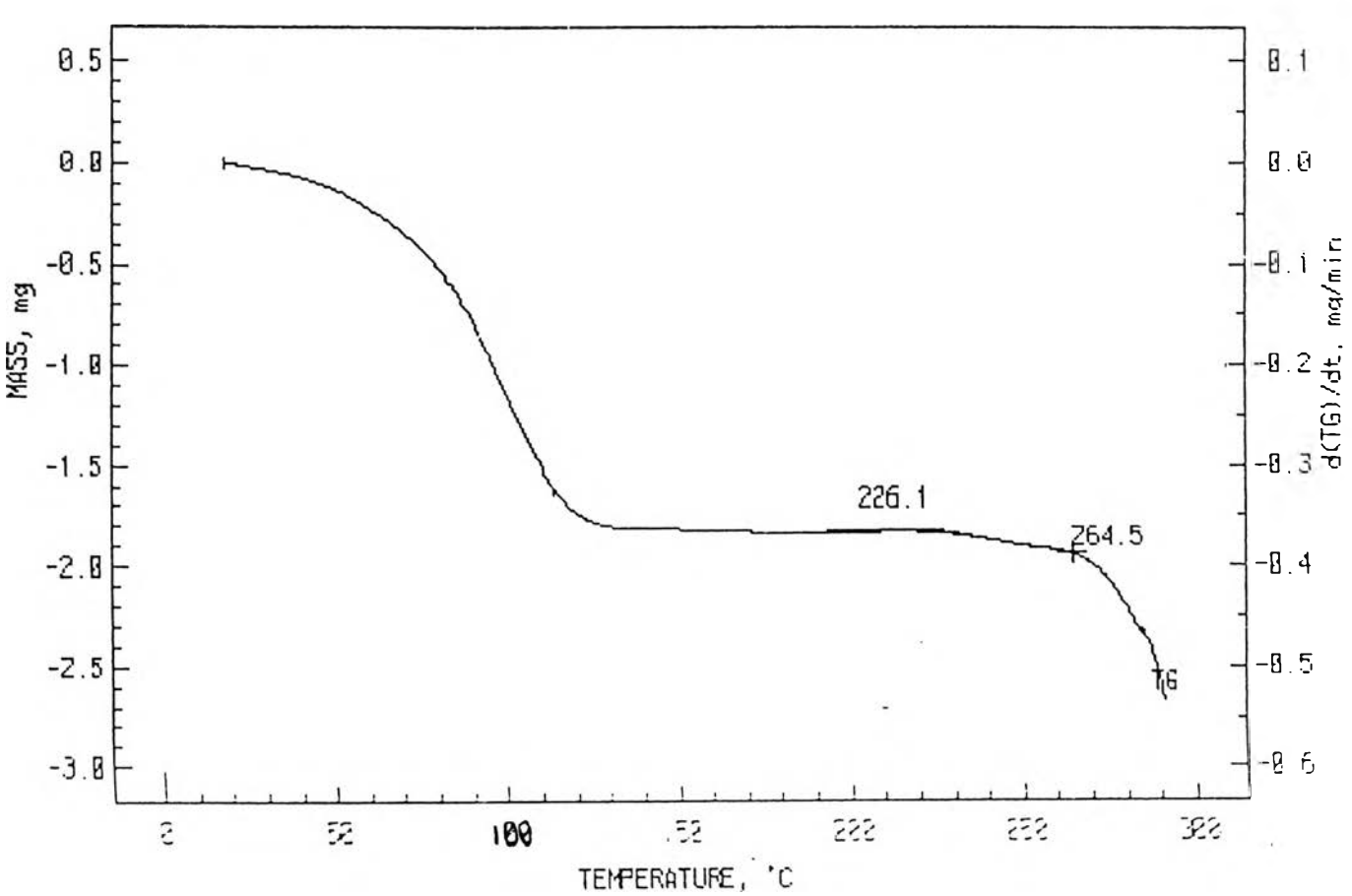

Figure 19 *TGA thermograms of spray dried BCD*

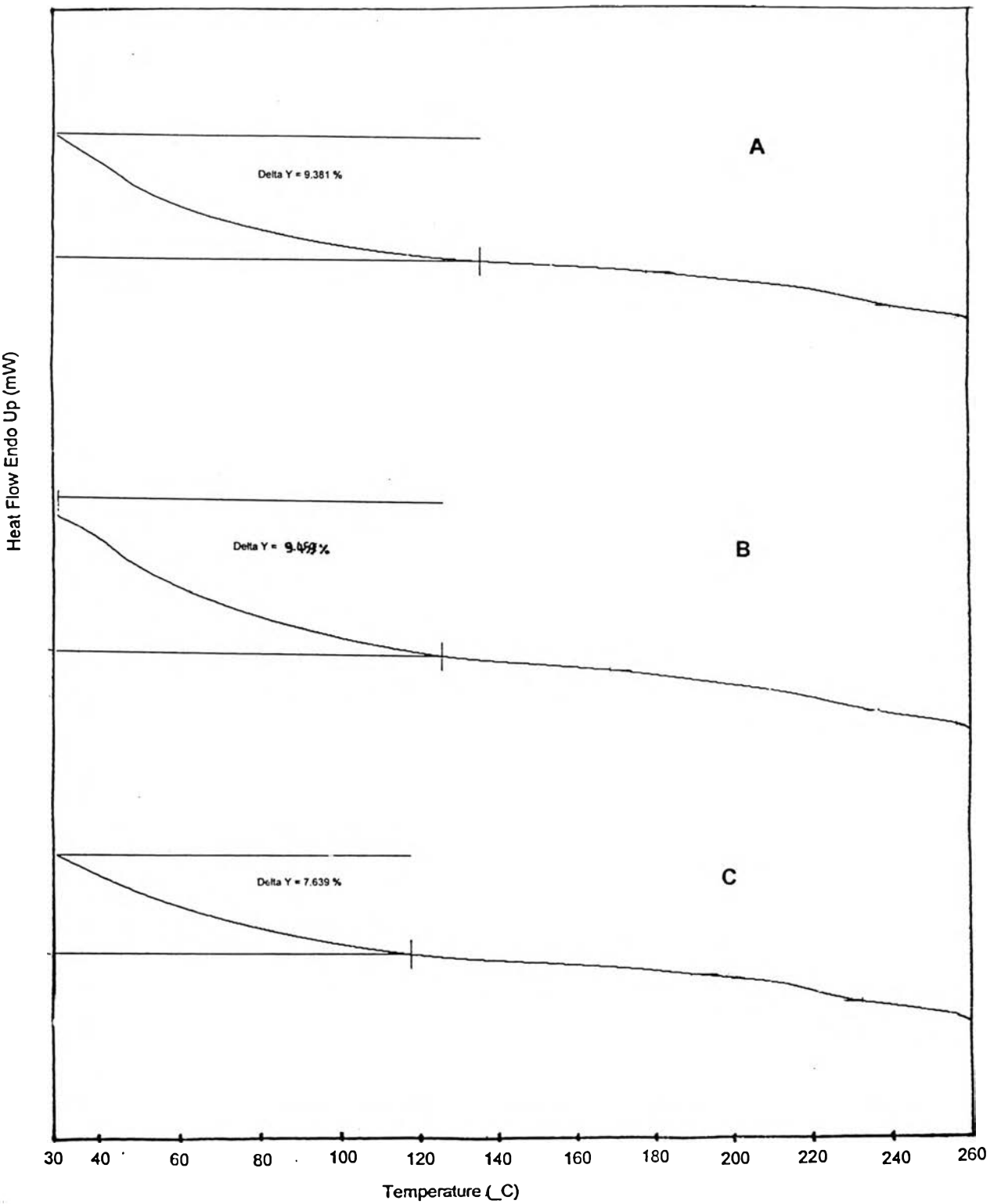

Figure 20 *TGA thermograms of IB prepared by spray drying method, feed rate 15 ml/min [(A) I15B130; (B) II15B140; and (C) I15B150]*

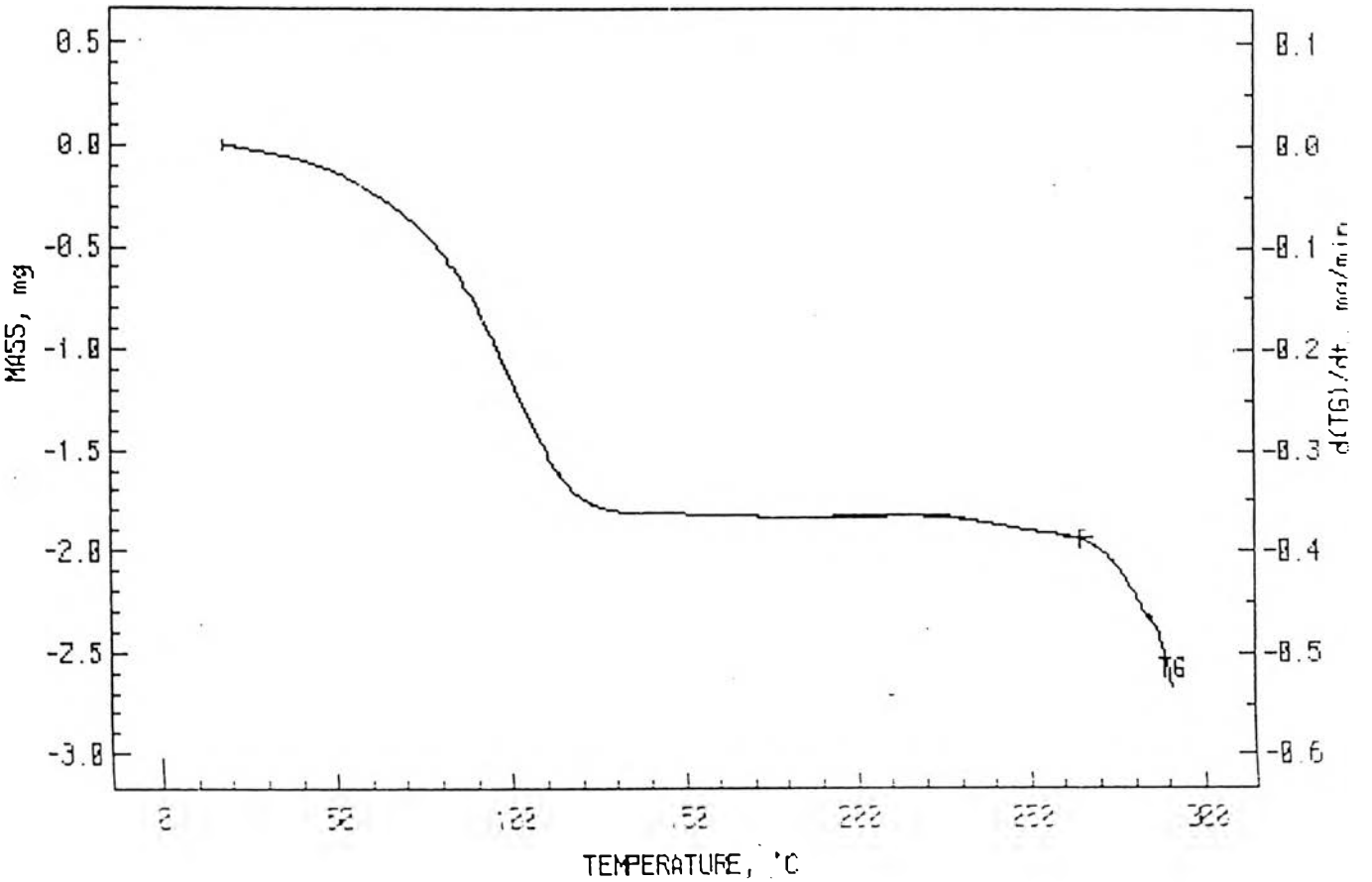

Figure 21 *TGA thermograms of spray dried sodium lauryl sulfate in buffer (spray dried SLS)*

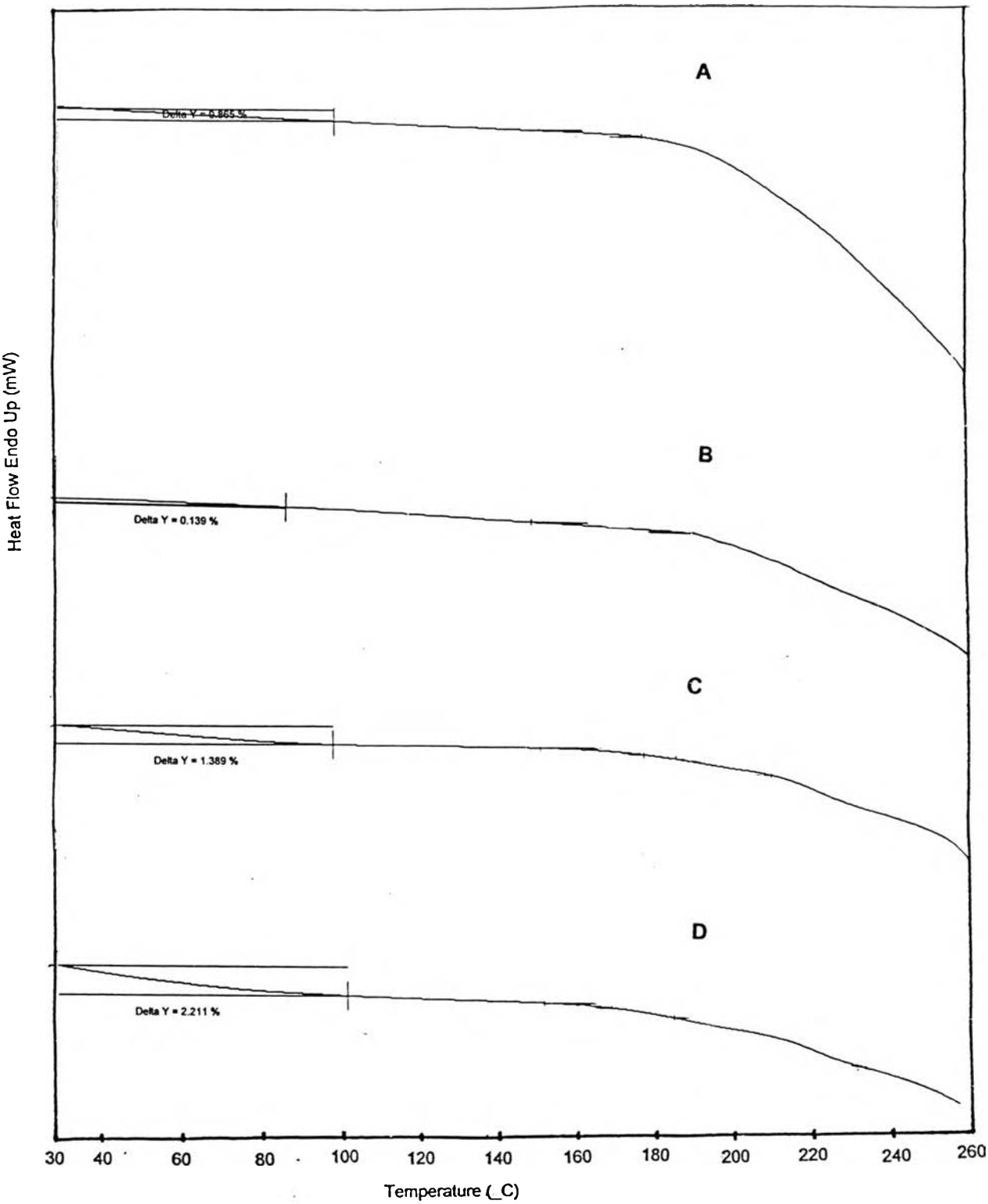

Figure 22 *TGA thermograms of indomethacin and sodium lauryl sulfate prepared by spray drying method[(A) IS13; (B) IS20; (C) IS27 and (D) IS33*

3.5 Differential scanning calorimetry (DSC)

Figure 23 shows DSC curves of IMC, spray dried IMC in water and spray dried IMC in phosphate buffer pH 7.4. It indicates that IMC and spray dried IMC in water were not different. The results were confirmed by X-ray powder diffraction patterns (Figure 31). The sharp endothermic peak at about 161 °C corresponded to IMC. In contrast, no endothermic peak at 161 °C was observed in the DSC thermogram of spray dried IMC in phosphate buffer pH 7.4. Instead, broad endothermic peaks at 85 °C and 228 °C were found. These broad peaks indicate the reduction in crystallinity of IMC attribute to the spray drying treatment. The first endothermic peak was found to be due to the loss of the water or dehydration process (confirmed by TGA thermograms in Figure 17) and the second endothermic peak was the fusion of spray dried buffer as seen in Figure 24C but the melting endotherm of IMC disappeared. Meanwhile, the DSC thermograms of BCD and spray dried BCD (Figure 24A and B) show a broad endothermic peak at approximately 90 °C, which attribute to the loss of the water from BCD (confirmed by TGA thermograms of BCD and spray dried BCD in Figure 18 and 19). A small melting peak at 218 °C of BCD was found (Figure 24A) but this peak was not found in the thermogram of spray dried BCD in phosphate buffer. It was a result of the transformation from the crystalline to the amorphous state of BCD after spray drying process. Instead, a melting endotherm of buffer at 229 °C was found. The reason for small melting peak of spray dried buffer in the thermogram of spray dried BCD in phosphate buffer may be due to the less amount of buffer (1.782%) in spray dried BCD compared with the amount of buffer in spray dried buffer (3.0%).

The endothermic peaks of IMC/BCD physical mixtures (Figure 25) in the molar ratio of 2:1, 1:1 and 1:2 were compared. They show peaks resulting from the simple superimposition of their separate components in the DSC curves. A sharp endothermic peak corresponding to IMC fusion at 161 °C and prominent peaks of BCD at approximately 100 °C and at 222 °C. The endothermic peak of IMC in the physical mixture at 161 °C in the molar ratio of 2:1 show greater area under the curve (AUC) than the molar ratios of 1:1 and 1:2, respectively depending on the amount of IMC in the mixture.

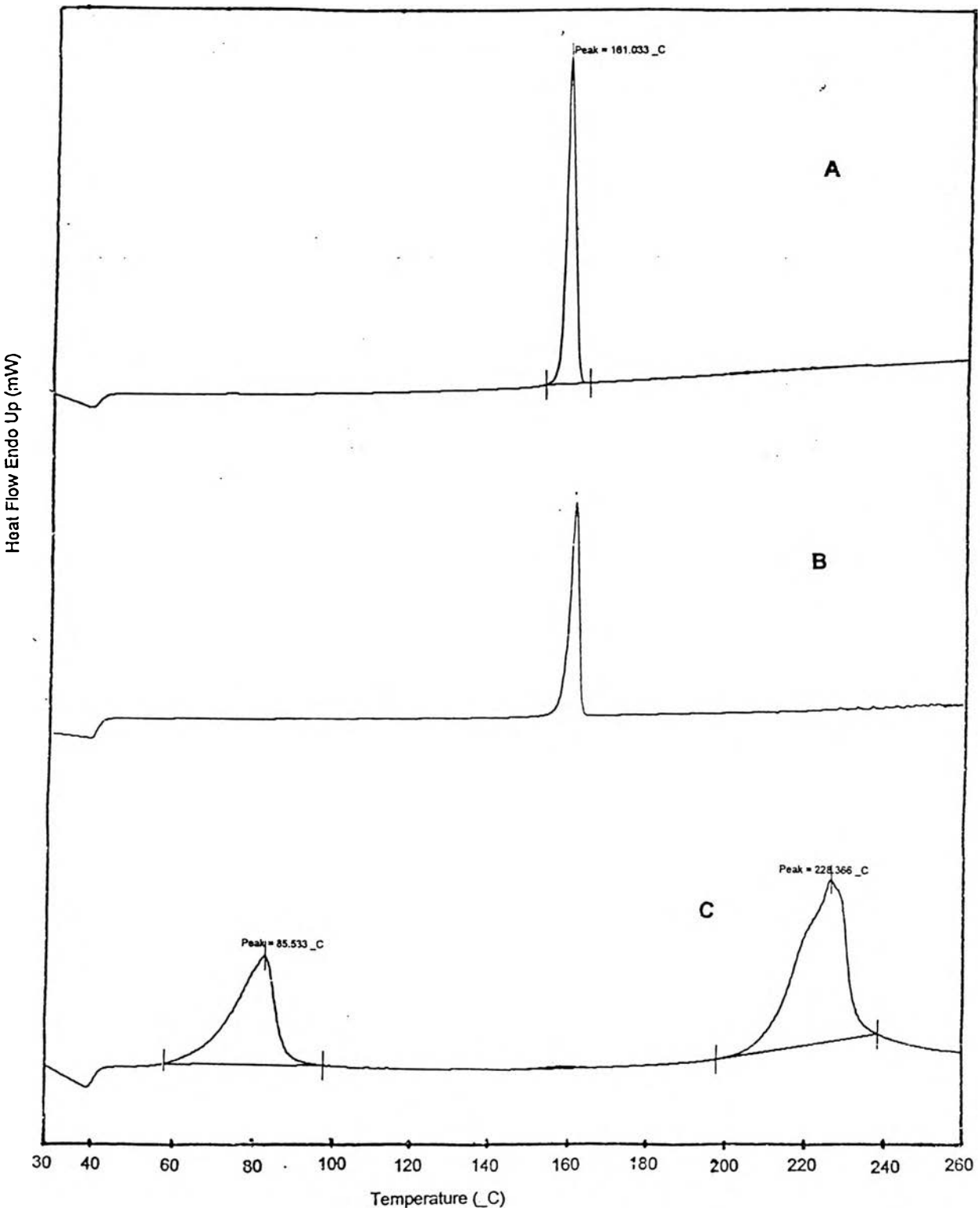

Figure 23 *DSC thermograms of (A) IMC; (B) spray dried IMC in water and (C) spray dried IMC in buffer [spray dried IMC]*

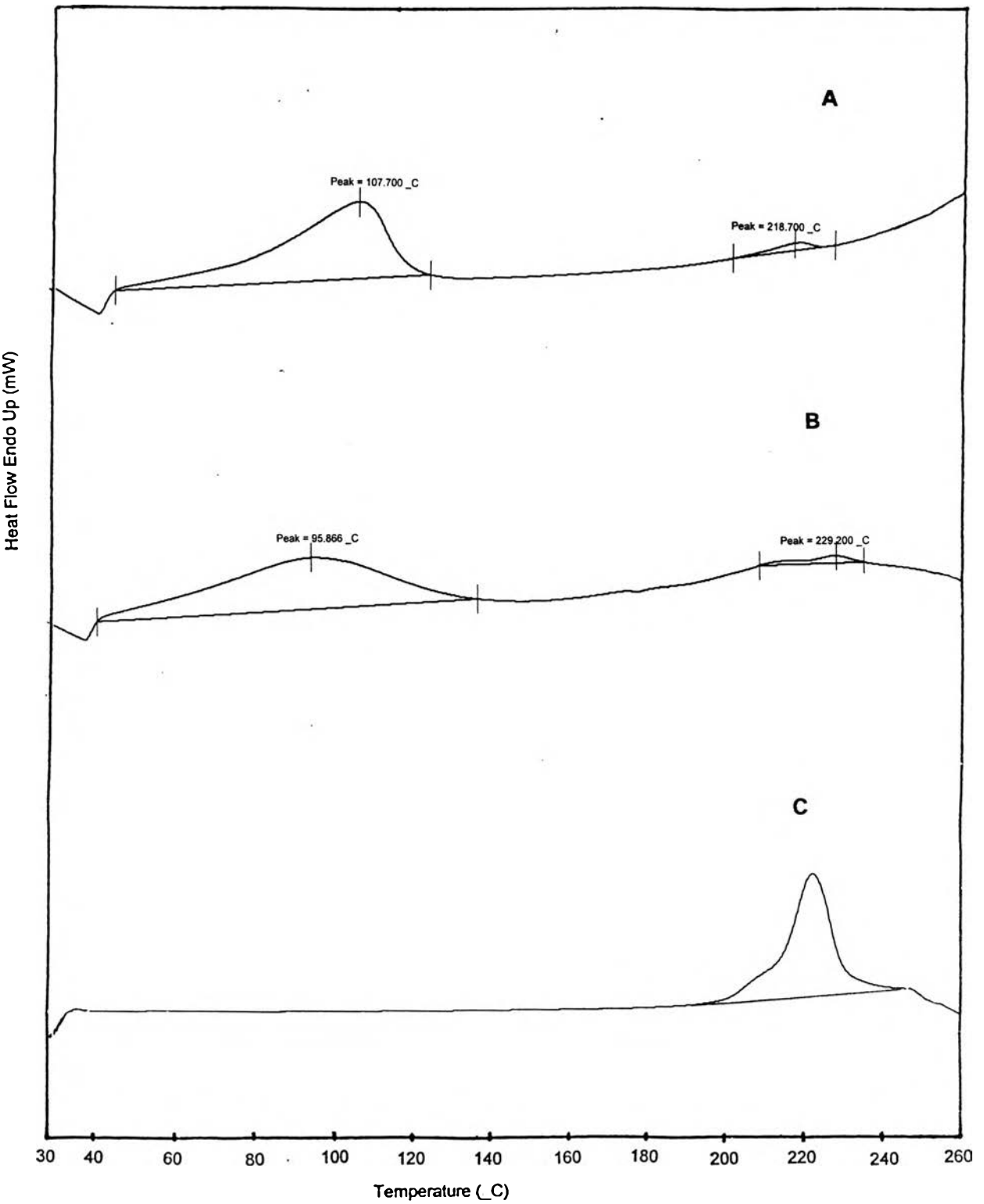

Figure 24 *DSC thermograms of (A) BCD; (B) spray dried BCD in buffer and (C) spray dried buffer*

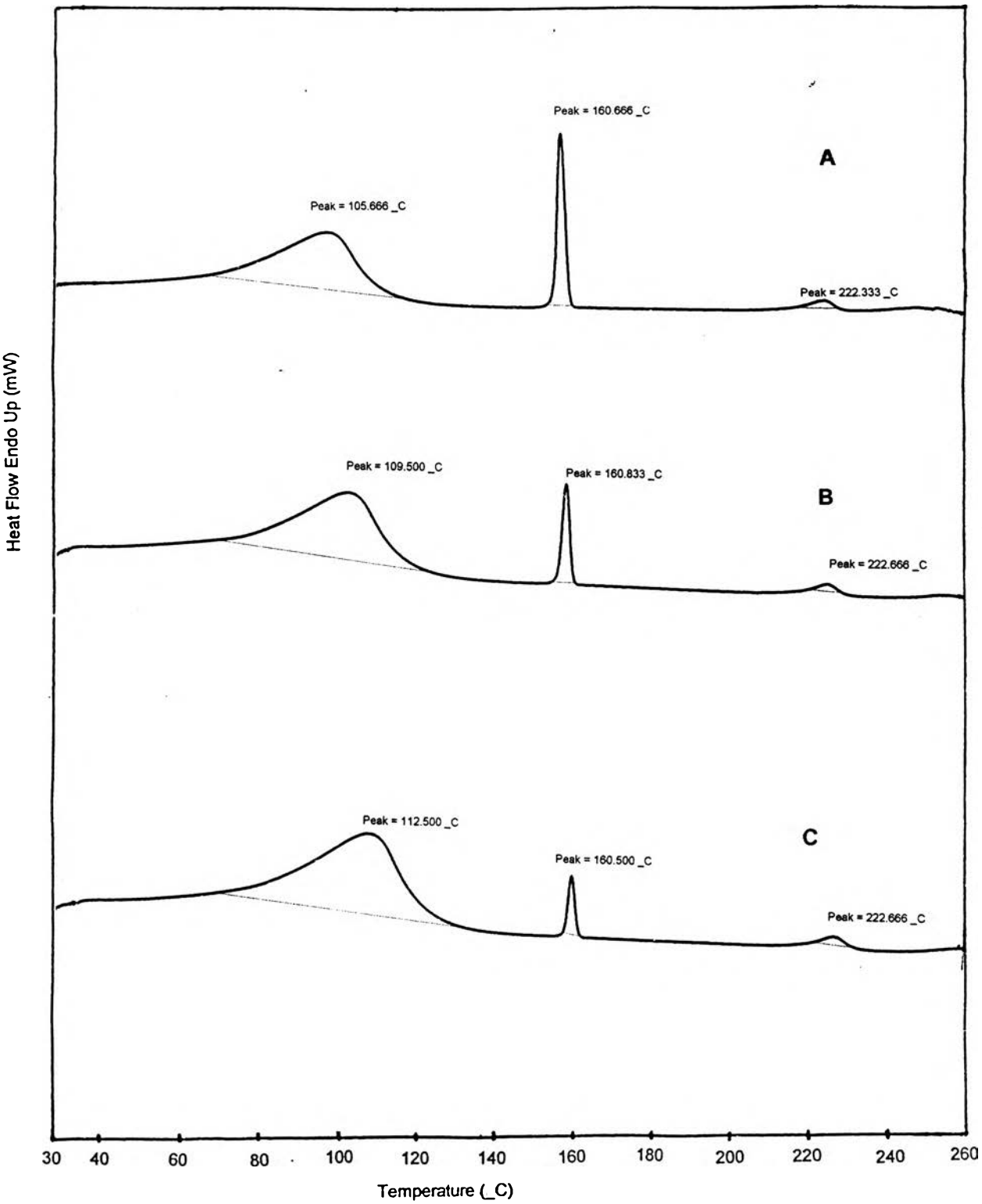

Figure 25 *DSC thermograms of IMC/BCD physical mixtures at molar ratio 2:1; (A) IIB(PM) ; (B) IB(PM) and (C) IBB(PM)*

The DSC curves of spray dried IMC/BCD using various molar ratios and spray dried conditions were observed (Figure 26 and APPENDIX F). There were no endothermic peaks corresponding to fusion of IMC. There were broad endothermic peaks resulting from dehydration between 30 and 120 °C and the fusion peak of spray dried buffer at 199 to 202 °C. The reason for a reduction in the melting peak of solid buffer may be due to high energy input during spray drying which causes the intermolecular bonding of buffer molecules to be weak confirmed by FTIR of spray dried IMC in phosphate buffer pH 7.4 in Figure 44. Thus, this change in buffer arrangement and the introduction of BCD in the system some how cause the molecular rearrangement of the remaining buffer to be different and shifted the fusion endotherm to a lower temperature. The disappearance of the endothermic peak at 161 °C may be due to the total transformation to the amorphous state of IMC and/ or the inclusion of IMC into the cavity of BCD (Lin and Kao, 1989) which performed as if it was at low crystallinty level, compared when detected by X-ray powder diffraction in Figure 36 (confirmed by DSC thermogram of spray dried IMC in buffer in Figure 23C).

Thermograms of SLS and spray dried SLS in buffer are shown in Figure 27. Non spray dried SLS and spray dried SLS both exhibited broad endothermic peaks at approximately 94-99 °C (contribute to dehydration) and a sharp endothermic peak at 188 °C corresponding to fusion of SLS. Figures 28 and 29 show the thermograms of IMC/SLS physical mixtures. They exhibit only the endothermic fusion peak of IMC at 159 °C and failed to show the distinctive peak of SLS at 188 °C possibly due to the very small percentage of SLS used in the mixtures compared with the amount of IMC. Figure 30 exhibits the thermograms of spray dried IMC/SLS in buffer with various percentage of SLS. There were three endothermic peaks in each thermogram. The endotherm of remaining crystalline IMC was observed at approximately 160 °C but with a distinct reduction in intensity due to partial amorphous transformation. Fusion of phosphate buffer occurred at approximately 204 °C (not at originally 229 °C) due to the interaction mentioned previously with IMC/BCD spray dried product and introduction of SLS in the system. A broad endothermic peak was observed in the range of 30-100 °C due to dehydration.

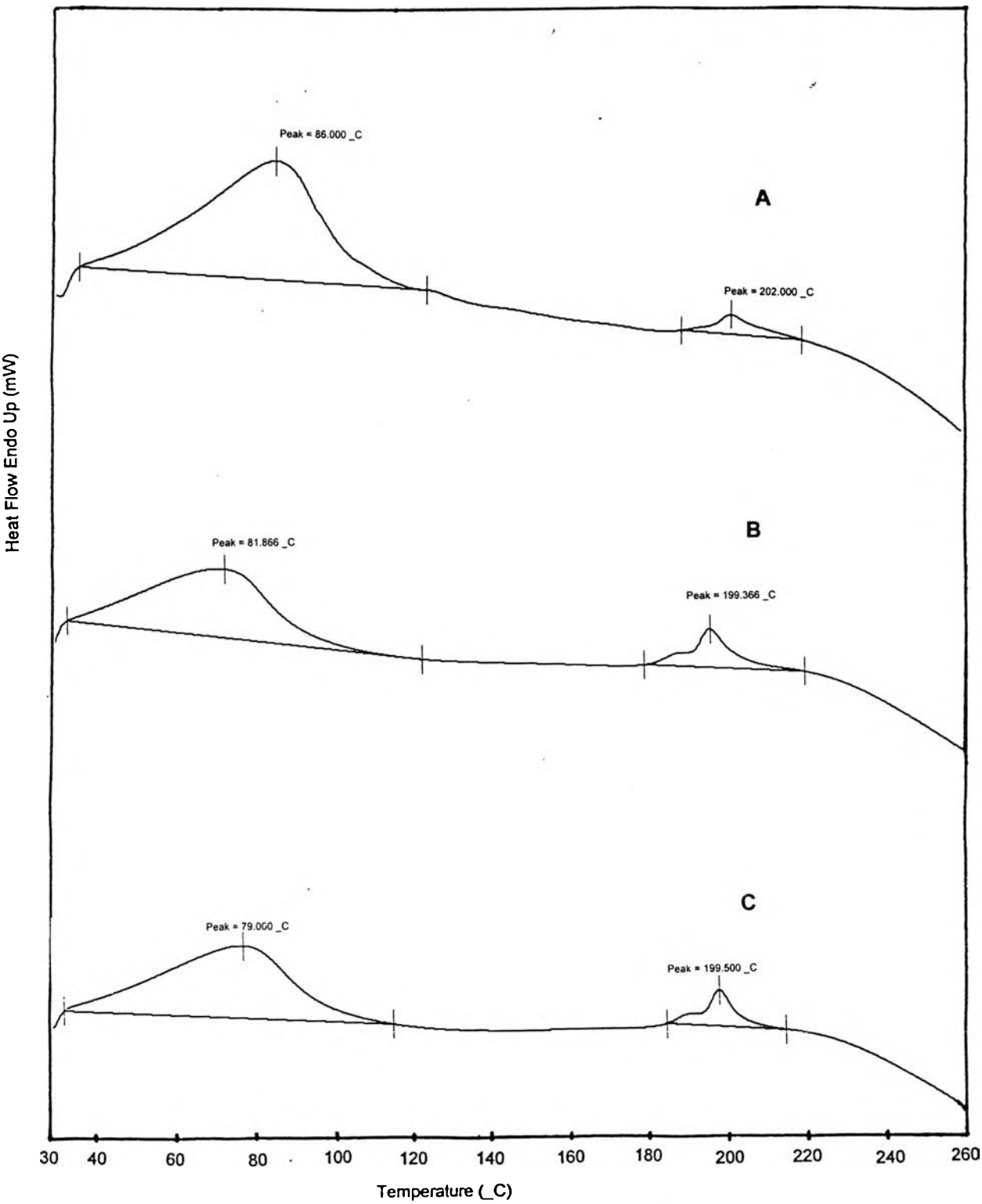

Figure 26 *DSC thermograms of IB, feed rate 15 ml/min [(A) I15B130; (B) I15B140 and (C) I15B150]*

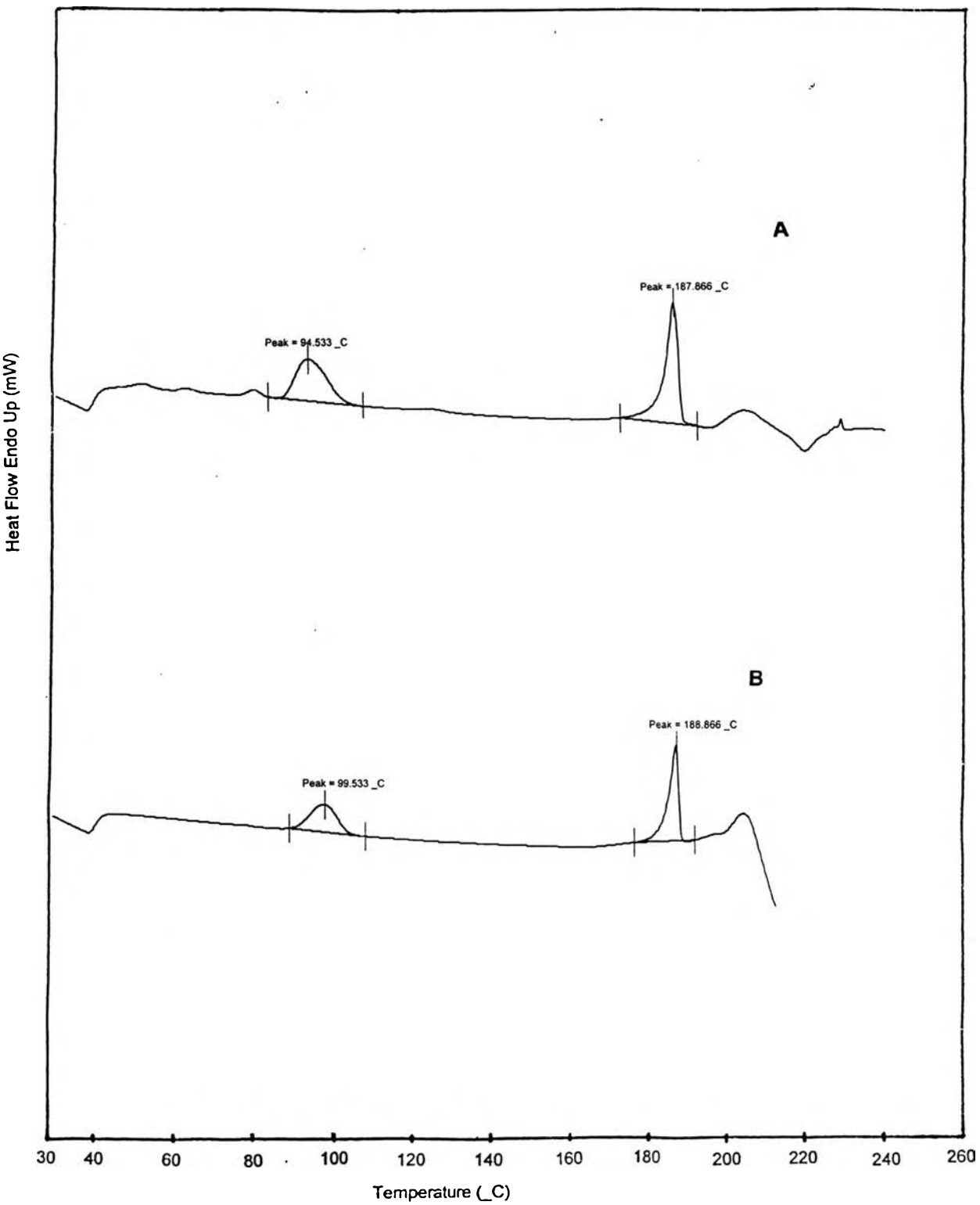

Figure 27 *DSC thermograms of (A) SLS and (B) spray dried SLS*

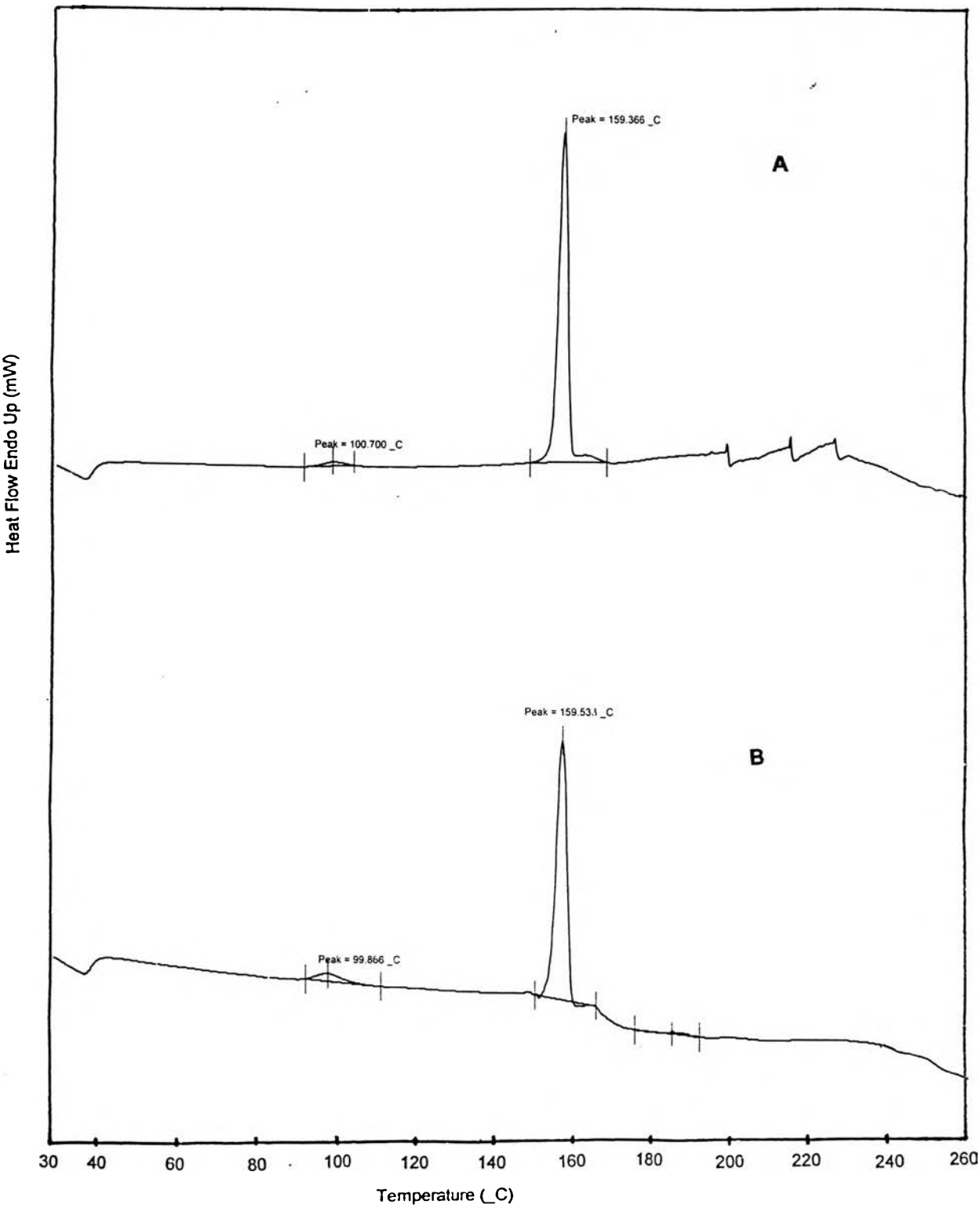

Figure 28 *DSC thermograms of IMC/SLS physical mixtures [(A) S13(PM) and (B) IS20(PM)]*

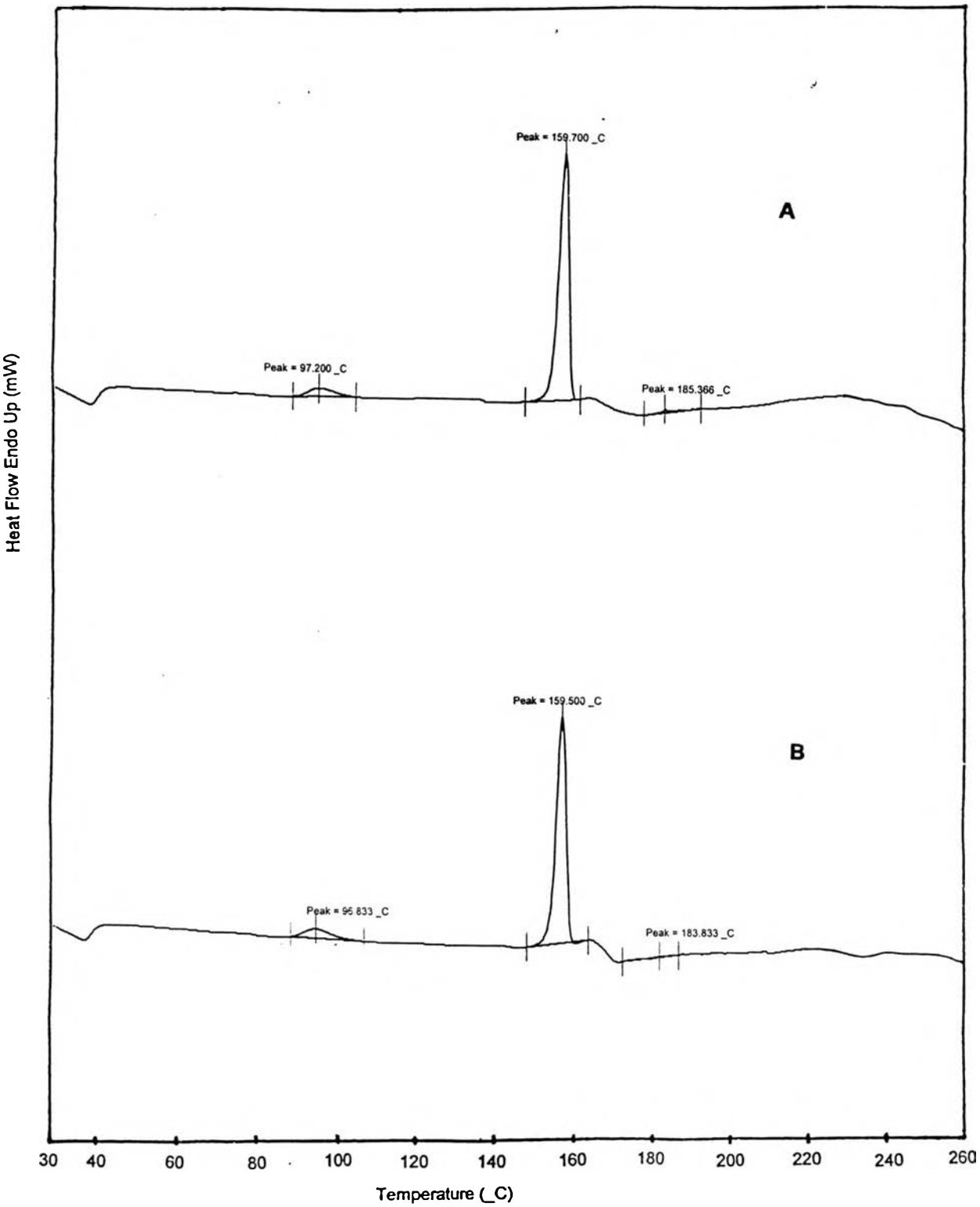

Figure 29 *DSC thermograms of IMC/SLS physical mixtures [(A) IS27(PM) and (B) IS33(PM)]*

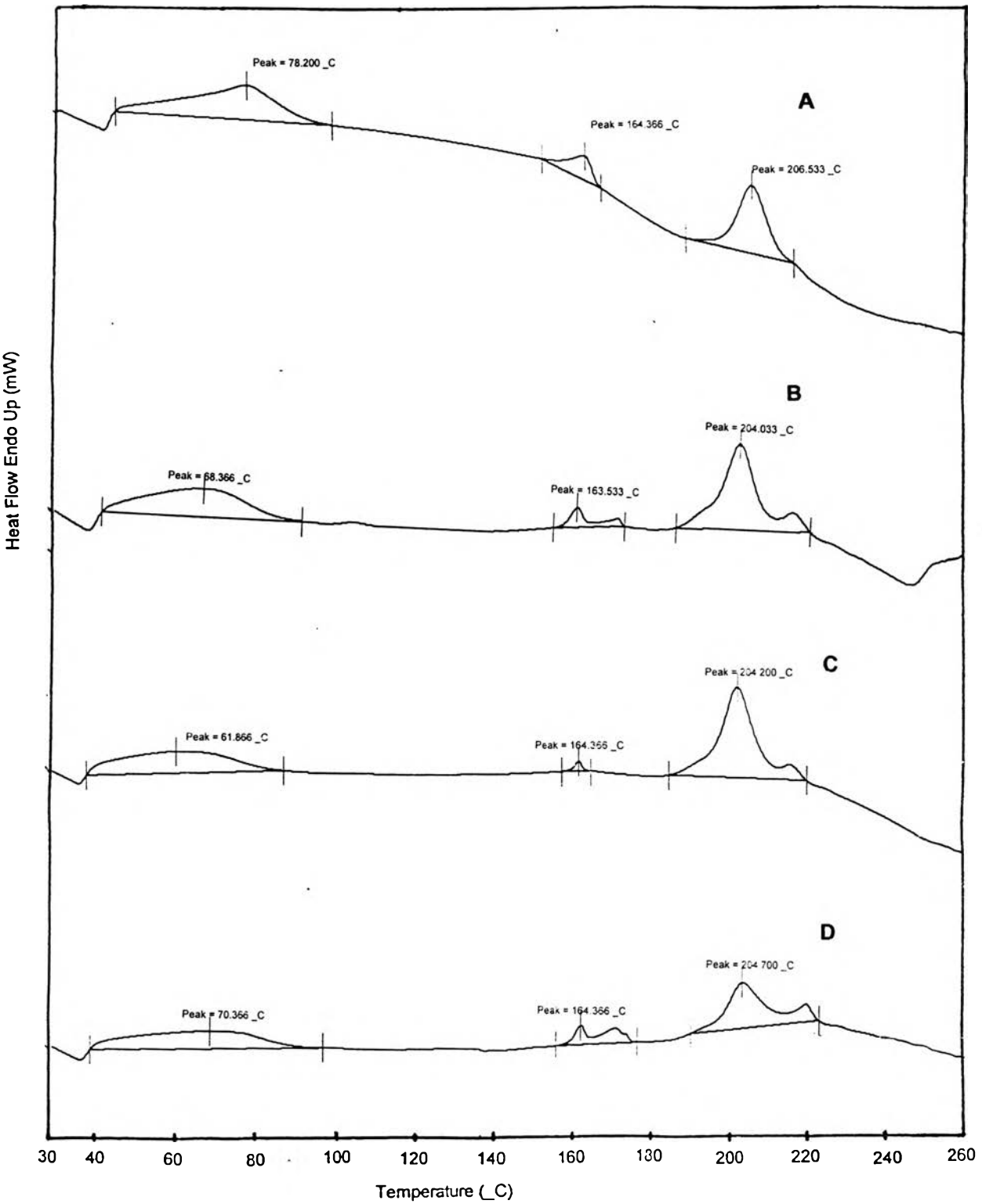

Figure 30 *DSC thermograms of spray dried IMC/SLS [(A) IS13; (B) IS20; (C) IS27 and (D) IS33]*

3.6 Powder X-ray diffraction study

Powder X-ray diffractometry is a useful method for the detection of solid phases. The X-ray powder pattern of each crystalline form of a compound is unique, making this technique particularly suitable for the identification of different polymorphic or other solid forms of a compound. (Suryanarayanan, 1995).

Figure 31 and 32 show powder X-ray diffraction spectra of IMC, spray dried IMC in water and spray dried IMC in phosphate buffer pH 7.4. Major X-ray diffraction peaks of IMC were at 11.64°, 17.04°, 19.64°, 21.80°, 23.12° and 26.72° 2θ, respectively, with major peaks at 11.64° and 19.64° 2θ. (Figure 31). The X-ray diffractograms of pure drug (Figure 31A) and spray dried IMC in water (Figure 31B) were not different. This is due to the fact that particles obtained from spray drying IMC in water was from a suspension due to poor solubility of IMC in water (pH 4.5) as mentioned earlier. The drug then was not totally dispersed in a molecular state making the arrangement of minutely soluble molecules after spray drying to be in the same manner as the original IMC which already existed and suspend in the system. These results showed that for suspension of IMC in water the spray drying process did not alter the solid characteristic of the original solid form of pure drug. The X-ray diffractogram of spray dried IMC in phosphate buffer pH 7.4, however, were different from the X-ray diffractogram of IMC. Major X-ray diffraction peaks of IMC (2θ = 11.64° and 19.64°) disappeared from the X-ray diffractogram of spray dried IMC in phosphate buffer pH 7.4 (Figure 32 and Table 23) but some peaks of IMC (2θ = 10.52° and 17.04° 2θ) decreases in intensities. While some of the new main X-ray diffraction peaks of spray dried IMC in phosphate buffer (2θ = 18.28°, 22.40°, 23.28°, 31.36°, 31.96°, 32.52° and 33.00°2θ) appeared similar to major X-ray diffraction peaks of spray dried phosphate buffer shown in Figure 33 and some peaks are totally new. This observation suggested that the spray-drying process could contribute to a change in solid structure of IMC due to complete molecular dispersion of IMC in phosphate buffer making the random rearrangement of molecules of IMC within phosphate buffer during spray drying possible. The new peaks resulted from the molecular arrangement of sodium salt of IMC which occurred during the solubilization of IMC prior to spray drying, not of acid form.

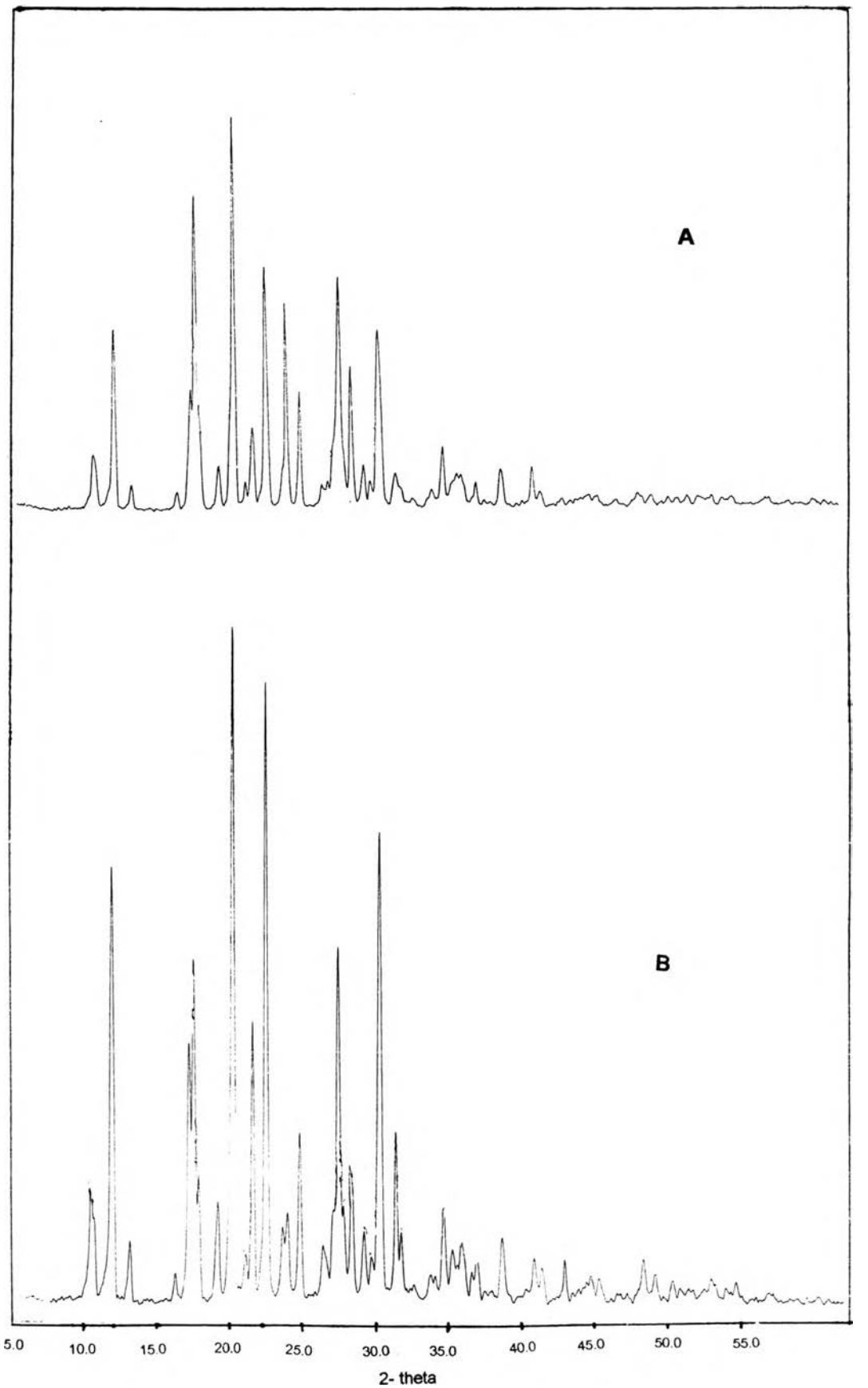

Figure 31 *X-ray powder diffractograms of (A) IMC and (B) spray dried IMC in water*

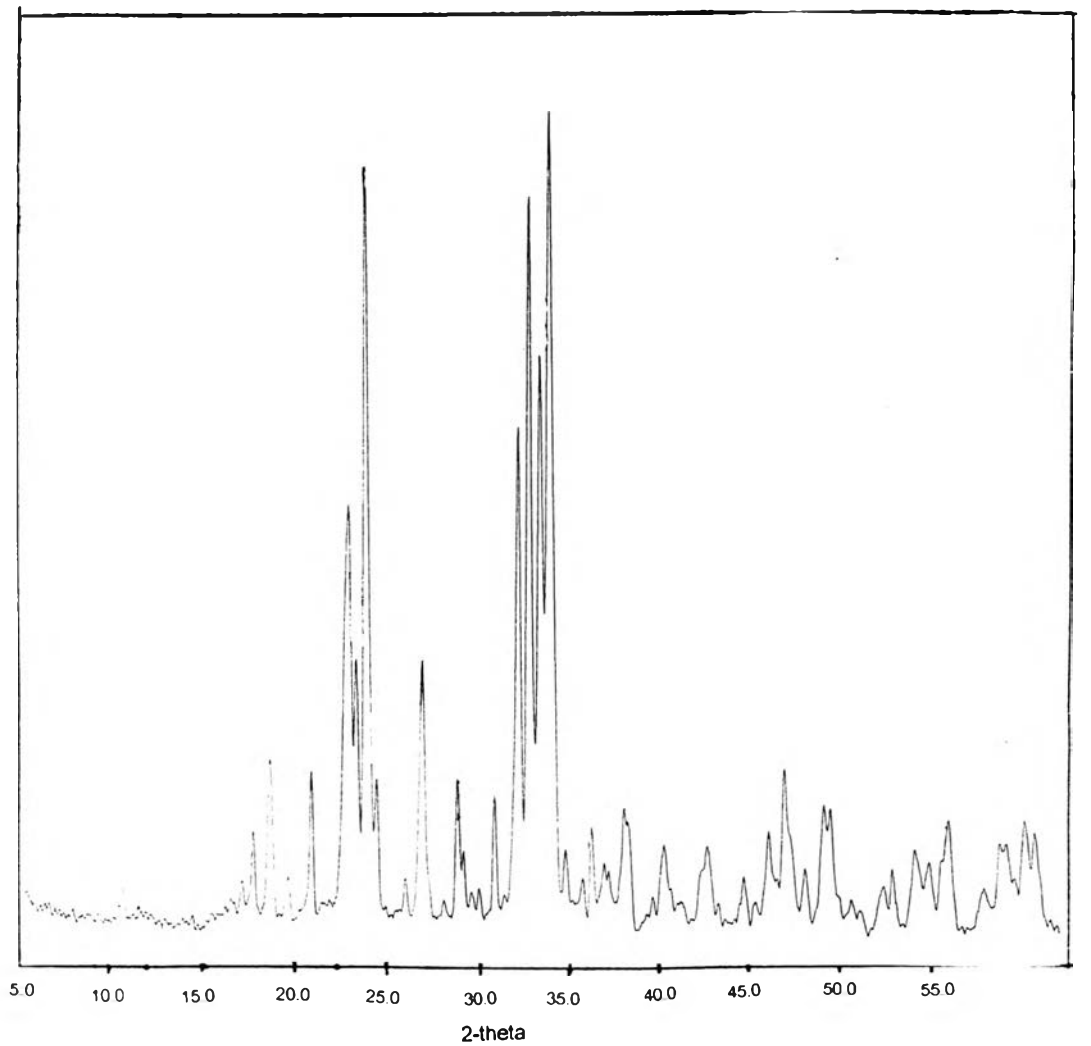

Figure 32 *X-ray powder diffractograms of spray dried IMC in phosphate buffer pH 7.4*

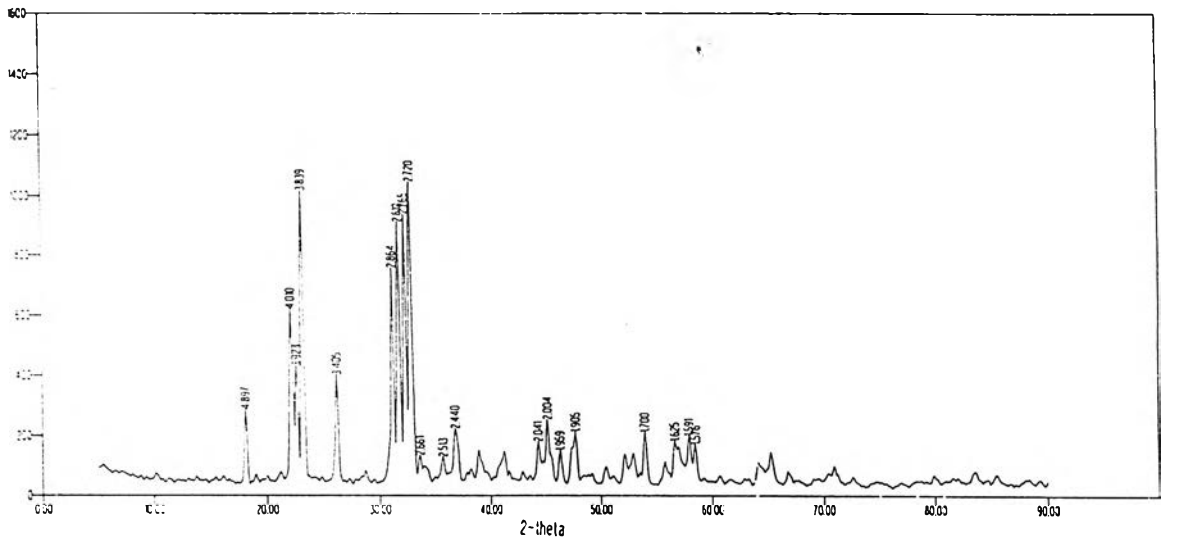

Figure 33 *X-ray powder diffractograms of spray dried phosphate buffer pH 7.4*

Figure 34 displayed powder X-ray diffraction patterns of BCD, spray dried BCD in water (pH 4.5) and spray dried BCD in phosphate buffer pH 7.4. X-ray powder diffractogram of BCD (Figure 34A) exhibited that it was in a crystalline state as demonstrated by the sharp and intense diffraction peaks. The highest peak of BCD is at 12.30° 2θ.

X-ray diffractogram of spray dried BCD in water are highly diffused indicating a complete amorphic transformation. While spray dried BCD in phosphate buffer pH 7.4 did not show any peak of pure phosphate buffer. The reduction in crystallinity of BCD might be attributed to the rapid crystallization by spray drying process (Moyano et al., 1995) which did not allow enough time for arrange molecules to properly.

X-ray diffraction patterns of IMC/BCD physical mixtures are shown in Figure 35 and Table 23. They were simply the superimposition of each component. These data agreed with results obtained from SEM and DSC.

The diffractograms of spray dried IMC/BCD prepared by varying inlet air temperatures and feed rates were different from the original drug. As seen in Figure 36 and Appendix E , at every molar ratios spray dried using various inlet air temperatures and feed rates exhibited very diffused diffraction patterns. These patterns could not be clearly identified as the individual result of IMC, BCD or buffer but believed to be combination of all the components in the formulations. Highly diffused peaks are an indication of disorderliness in the system which was due to the spray drying process (affected BCD and buffer) and/or the inclusion of IMC in the BCD cavities or between BCD molecules (affected IMC). Thus for the latter reason [corresponded to the study of Lin and Kao (1989)], the explanation could be because IMC were unable to arrange themselves in molecular lacttice structure (crystalline) due to the interference of BCD, resulting in very diffused patterns of IMC sodium (as seen in Figure 36 and Appendix E) confirmed by the absence of sharp melting DSC endotherm (as seen in Figure 26 and Appendix F). From the above results, X-ray diffraction patterns of spray dried IMC/BCD prepared by using various inlet air temperatures and feed rates all exhibited low crystallinity than the original drug or

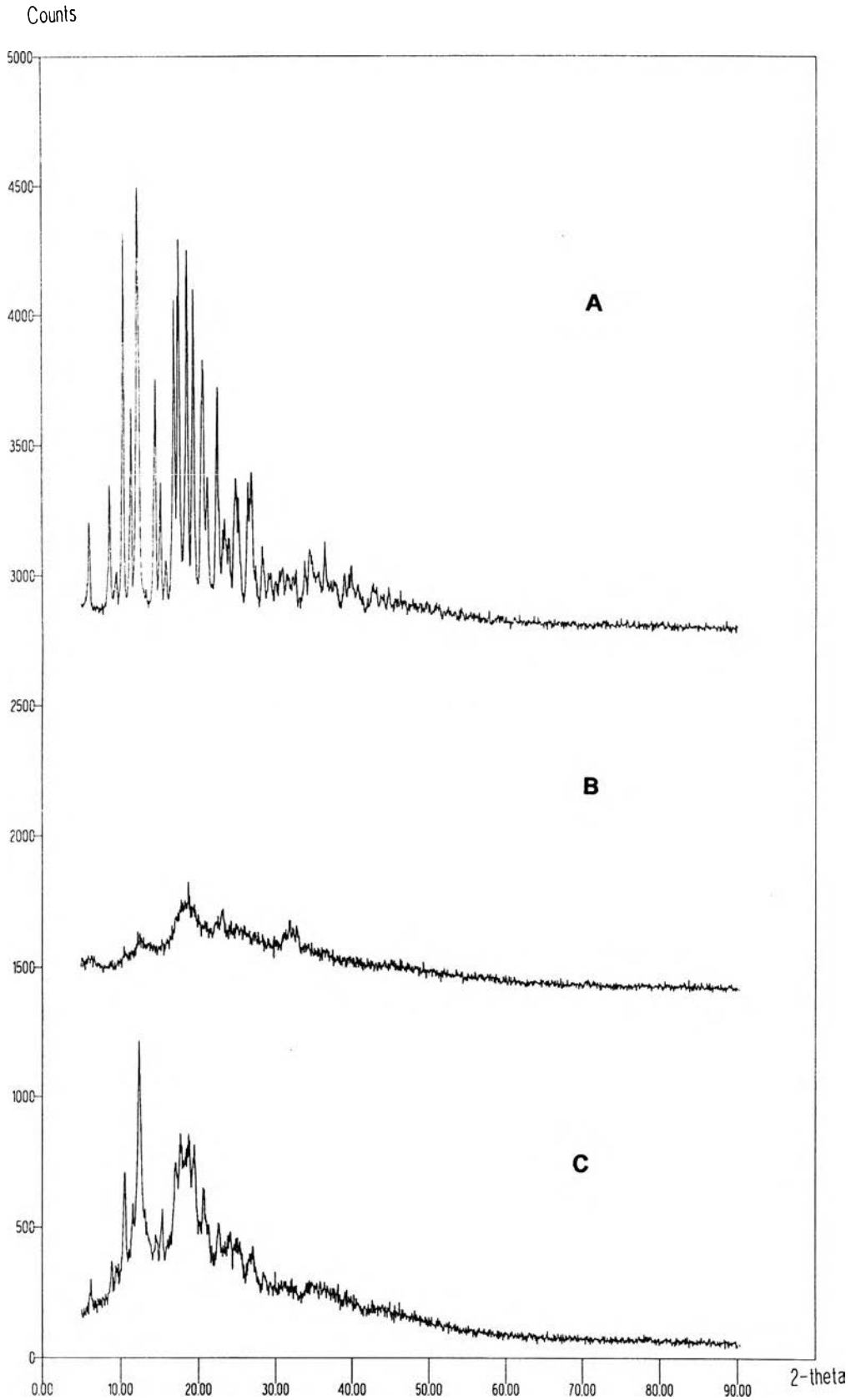

Figure 34 *X-ray powder diffractograms of (A) BCD; (B) spray dried BCD in water and (C) spray dried BCD in buffer*

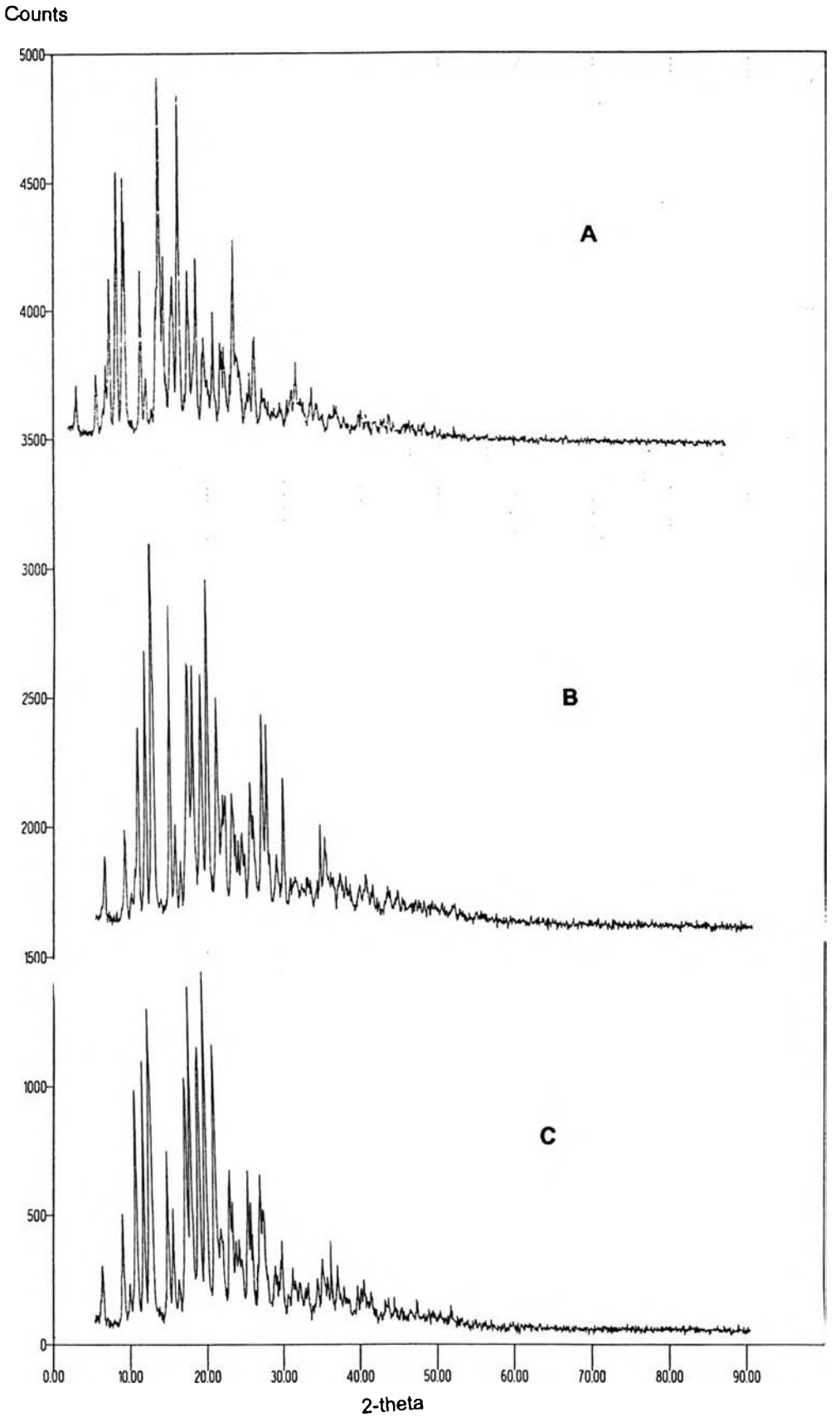

Figure 35 *X-ray powder diffractograms of IMC/BCD physical mixtures: (A) IIB(PM); (B) IB(PM) and (C) IBB(PM)*

Table 23 X-ray powder diffraction patterns of physical mixtures of indomethacin and beta cyclodextrin.

2:1		1:1		2:1	
2θ	I	2θ	I	2θ	I
10.72	932	10.72	1376	10.72	1707
11.72	2188	11.68	2487	11.72	3016
12.56	1519	12.56	2196	12.52	2486
14.72	2058	14.80	2383	14.64	2377
17.08	2647	17.08	2927	17.12	2480
17.76	2231	17.72	3360	17.80	3804
18.80	3061	18.80	4560	18.88	5469
19.72	3889	19.60	2269	19.60	2614
20.76	1962	20.84	2088	20.84	2382
21.80	1291	21.60	1042	21.76	1143
22.76	920	22.68	1375	22.72	1229
23.52	705	23.28	845	23.44	1462
26.72	2249	26.68	2703	26.68	3148

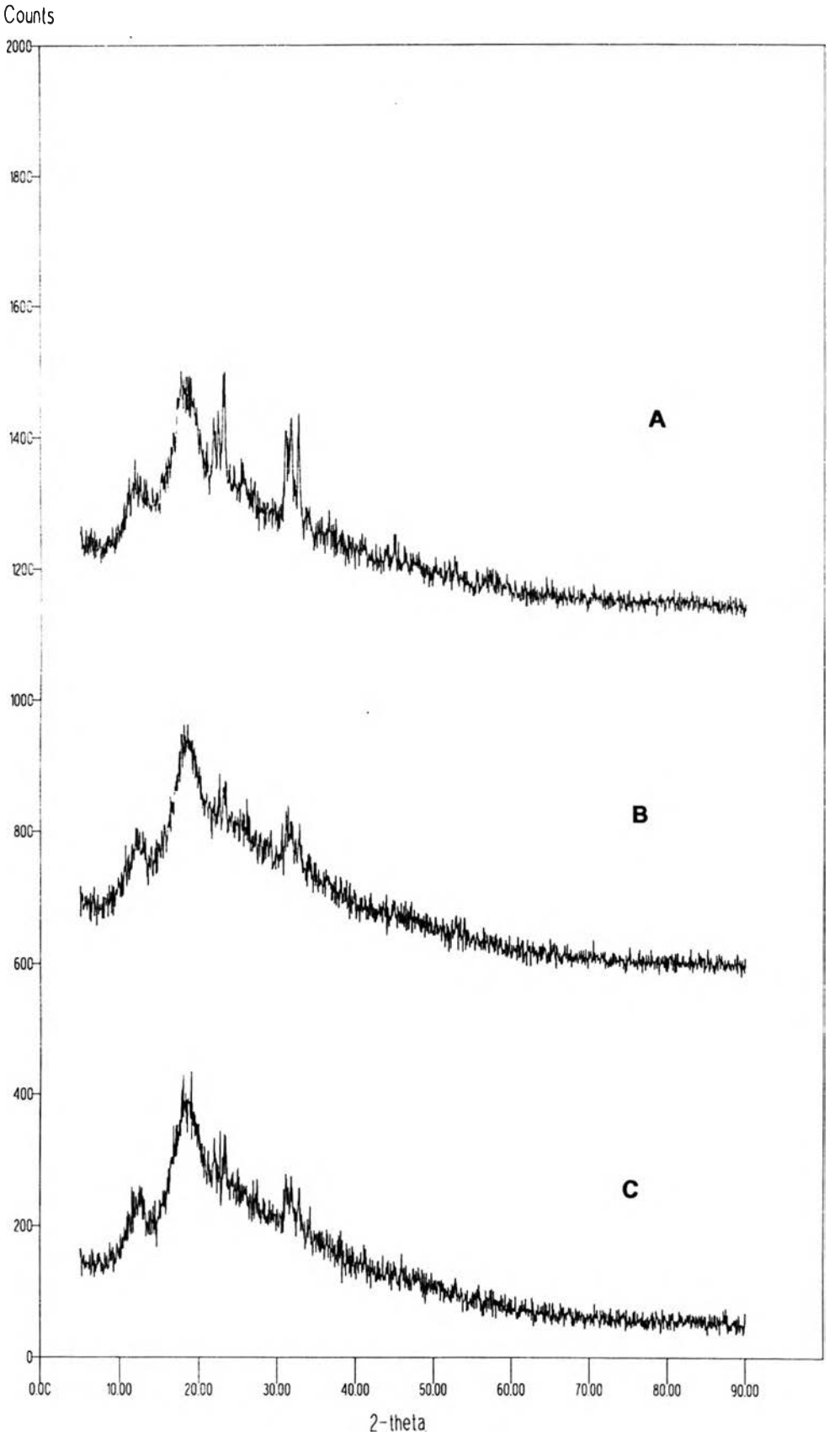

Figure 36 *X-ray powder diffractograms of IB, feed rate 15 ml/min [(A) I15B130; (B) I15B140 and (C) I15B150]*

IMC/BCD physical mixtures. The inlet air temperatures and feed rates did not affect the overall results.

Although the spray-drying conditions may affect the crystallinity of spray dried products, these results failed to correlate the relationship of spray dried conditions (feed rate and inlet air temperature) with crystallinity. Only one conclusive detail was achieved, the disappearance of the main peaks of IMC were evident in all samples with various molar ratios and conditions in this study. The X-ray diffraction patterns of spray dried IMC/BCD confirmed that a new solid phase has been formed. These data were indicative of the transformation of IMC from the crystalline state to the highly energetic amorphous state by formation of amorphous solid and/or the inclusion of IMC in and between BCD (Lin and Kao, 1989). It may result in an increased solubility of IMC as will be discussed later.

Figure 37 shows the diffractograms of SLS (main peak at 7.96° and 20.96°2θ) and spray dried SLS in phosphate buffer pH 7.4. Both shows high degree of crystallinilty with added buffer peaks in Figure 37B (31.36°, 31.80°, 32.28° and 33.08° 2θ). The X-ray diffraction patterns of the IMC/SLS physical mixtures were mainly the patterns of IMC (Figure 38 and 39) corresponded to the results obtained by DSC (Figure 28 and 29). For the X-ray diffractograms of spray dried IMC/SLS systems (Figure 40), they were like the patterns of spray dried IMC in phosphate buffer pH 7.4 (Figure 41) but with diffused baseline. The amount of SLS in these systems were so minute (about 1.782%) compared to amount of buffer that the SLS peaks were not displayed in the X-ray diffractograms of spray dried IMC/SLS. The diffractograms in Figure 40 show only the major peaks of buffer and IMC sodium but with a reduction in intensity due to the spray drying process corresponded to the DSC results obtained previously (Figure 30).

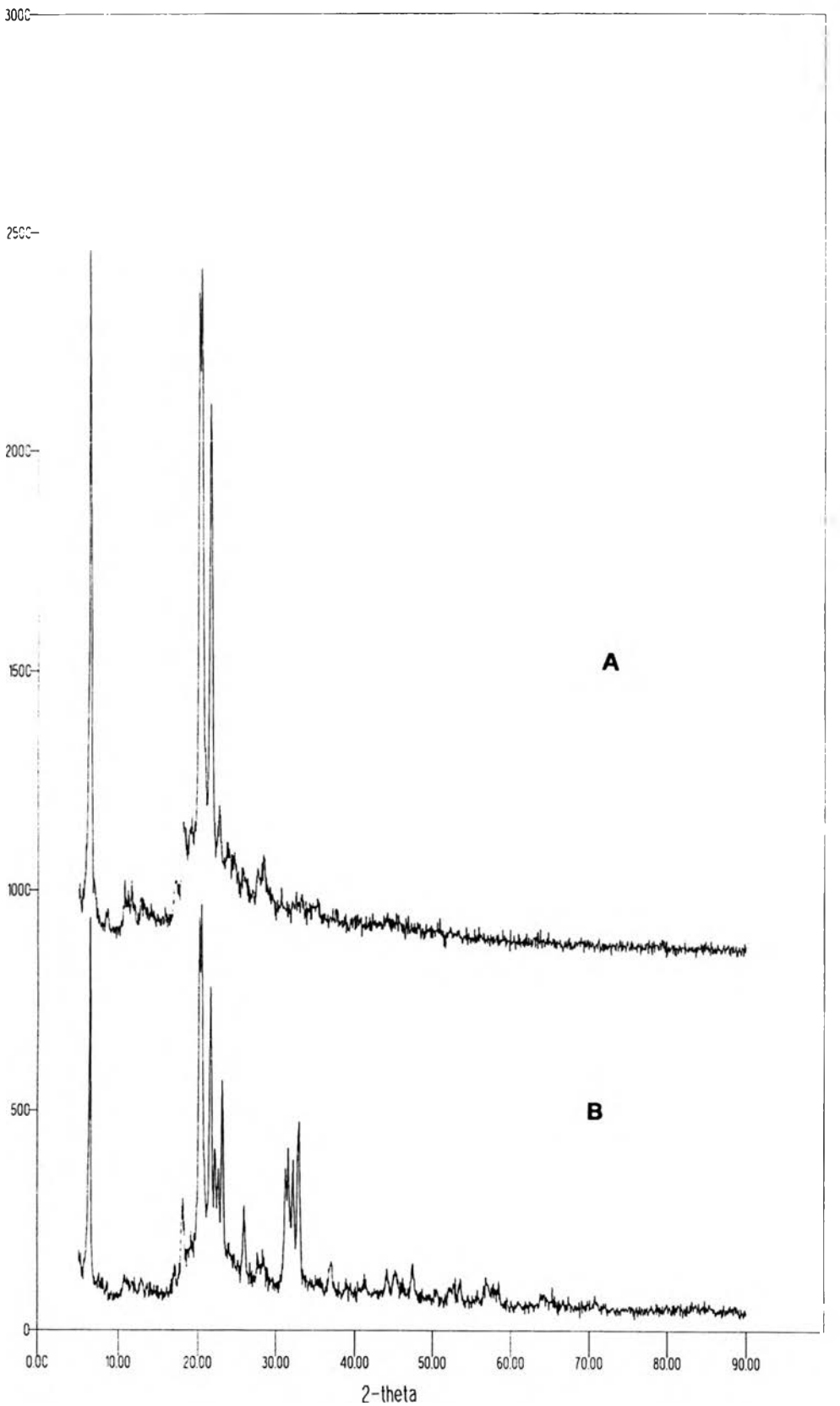

Figure 37 *X-ray powder diffractograms of (A) SLS and (B) spray dried SLS*

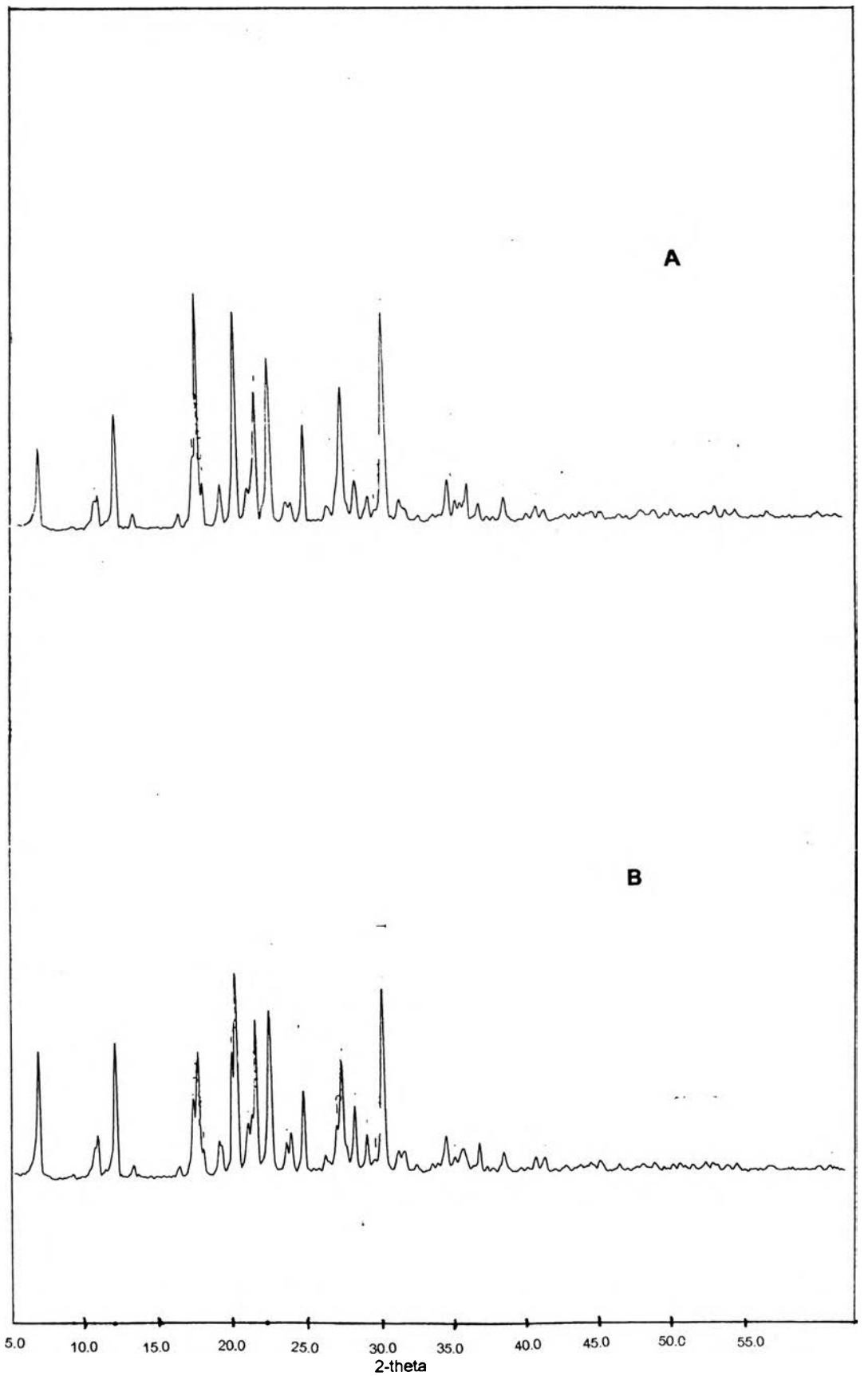

Figure 38 *X-ray powder diffractograms of IMC/SLS physical mixtures: (A) IS13(PM) and (B) IS20(PM)*

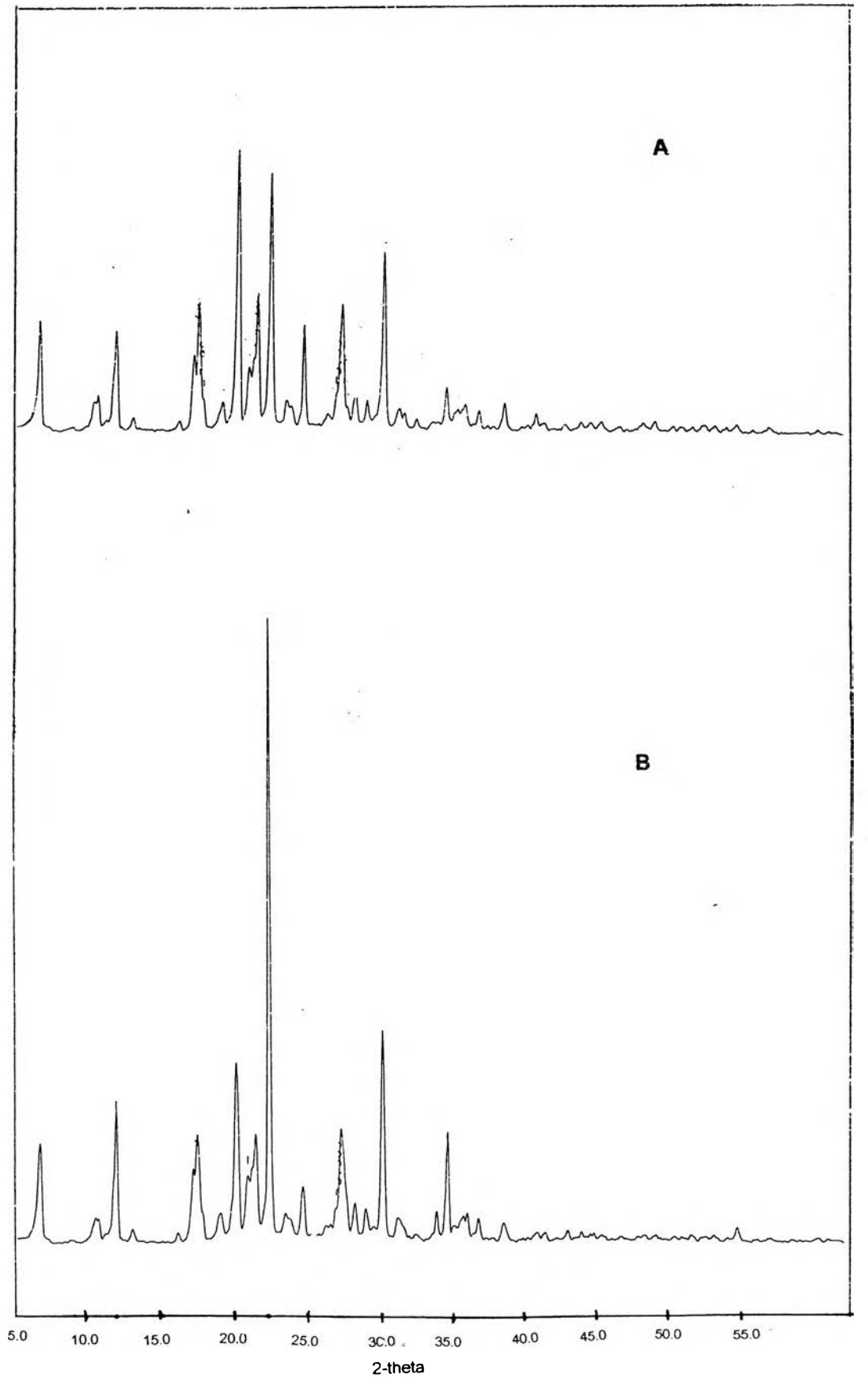

Figure 39 *X-ray powder diffractograms of IMC/SLS physical mixtures : (A) IS27(PM), and (B) IS33(PM), (B)]*

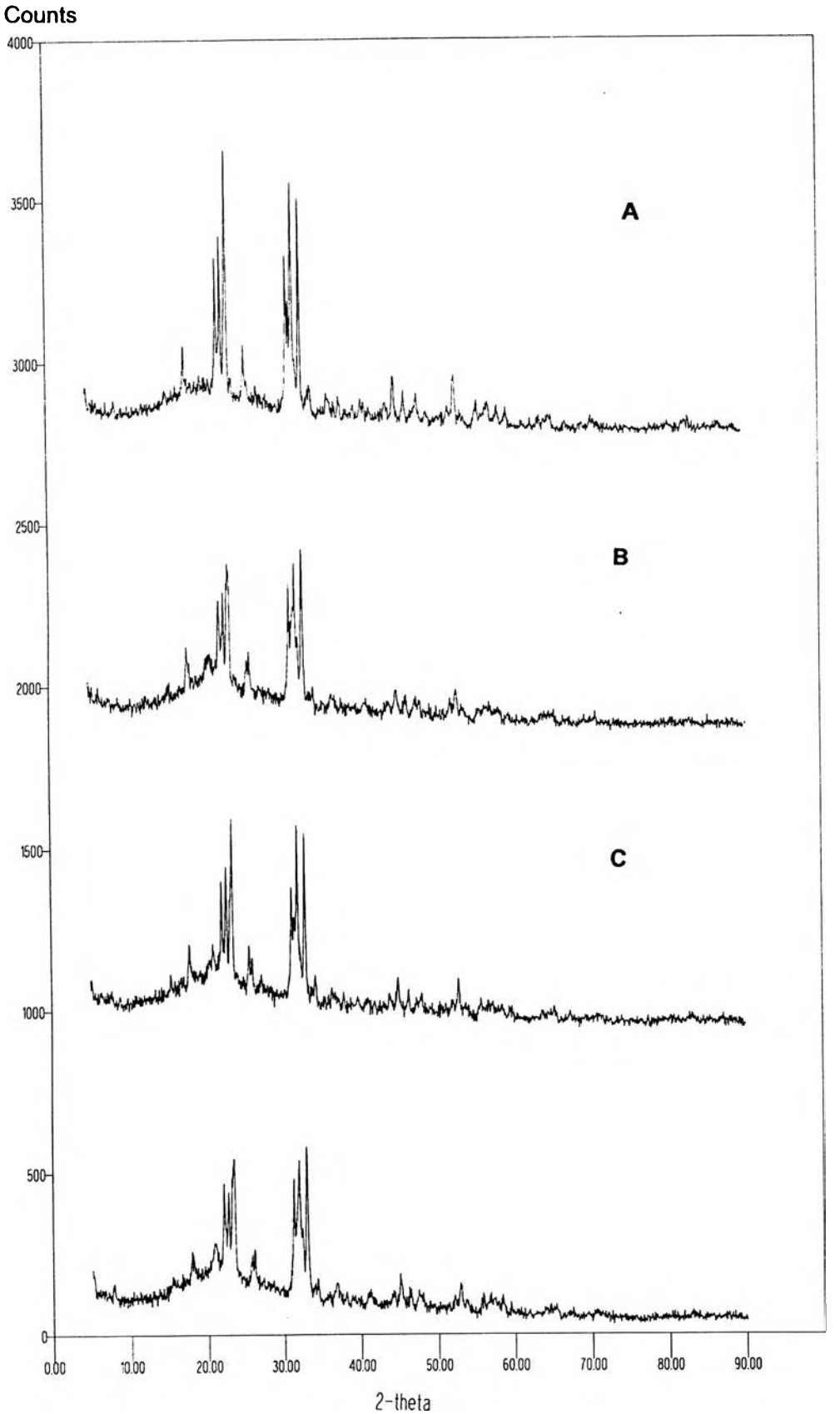

Figure 40 *X-ray powder diffractograms of spray dried IMC/SLS: (A) IS13; (B) IS20, (C) IS27 and (D) IS33*

3.7 Fourier Transform Infrared spectroscopy

The FTIR spectra of IMC, BCD, SLS and spray dried products are separated into related groups and shown in Figures 41-47 and APPENDIX G. The principle characteristic IR bands of IMC are as the following (Mathew, James and Edward, 1984):

~ 3400-2500 cm^{-1}	Aromatic C-H stretch
	Carboxylic acid O-H stretch
1716, 1690 cm^{-1}	C=O stretch of carboxylic group and carbonyl group, respectively
1597 cm^{-1}	Aromatic C=C stretch
1450 cm^{-1}	O-CH3 deformation
923 cm^{-1}	Carboxylic O-H out of plane deformation
900-600 cm^{-1}	Various C-H out of deformation for substituted aromatic

Spray dried IMC in water showed FTIR spectra (Figure 41B) that the position of bands were not different from of FTIR spectra of IMC. It indicated that no IMC changes occurred when it was suspended in water and spray dried. However, spray dried IMC in phosphate buffer pH 7.4 (Figure 41C) showed a reduction in intensity of FTIR bands at C=O stretch (1676 cm^{-1}) when compared with pure IMC may be due to the low amount of IMC in phosphate buffer pH 7.4 and the disappearance of the band at 1716 cm^{-1} which may be due to the ionization of IMC at carboxylic group (Biemann, 1983) to form sodium salt. A decreased intensity of FTIR spectra was due to the low amount of IMC in spray dried IMC.

FTIR spectra of BCD (Figure 42) was characterized by intense bands at 3500-3300 cm^{-1} corresponding to the absorption of hydrogen bonds produced by –OH groups of BCD. It could be seen that the several sharp and intense bands at 1160-1130 cm^{-1} which might be assigned to the stretching vibrations of the C-OH groups. In the 2950-2800 cm^{-1} region corresponding to the vibrations of the –CH and $-CH_2$ groups. It should be noted that BCD contained some moisture, which is characterized by the band at 1639 cm^{-1} (Szejtli, 1982).

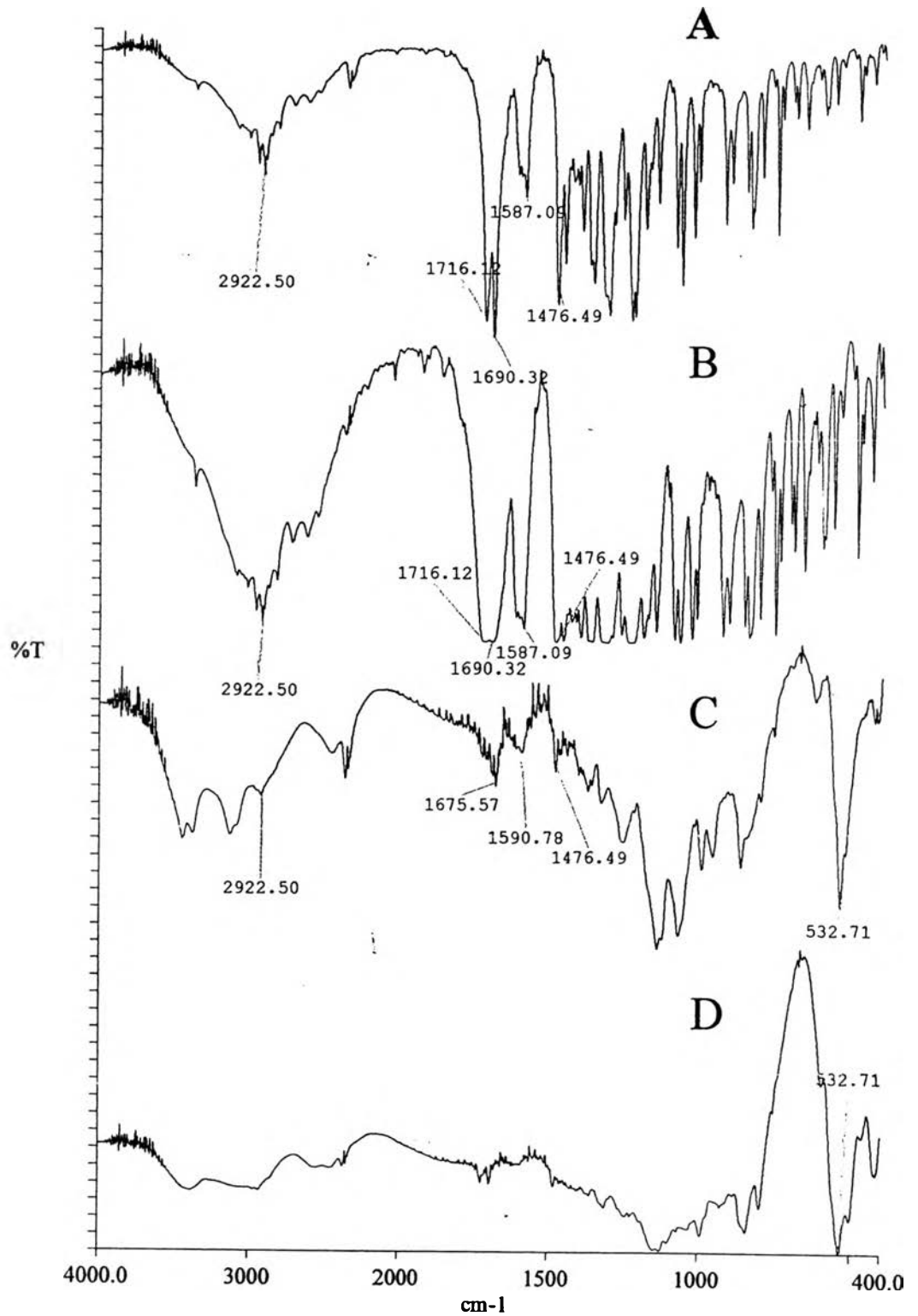

Figure 41 *Infrared spectra in KBr pellet of (A) IMC; (B) spray dried IMC in water; (C) spray dried IMC in buffer and (D) spray dried buffer*

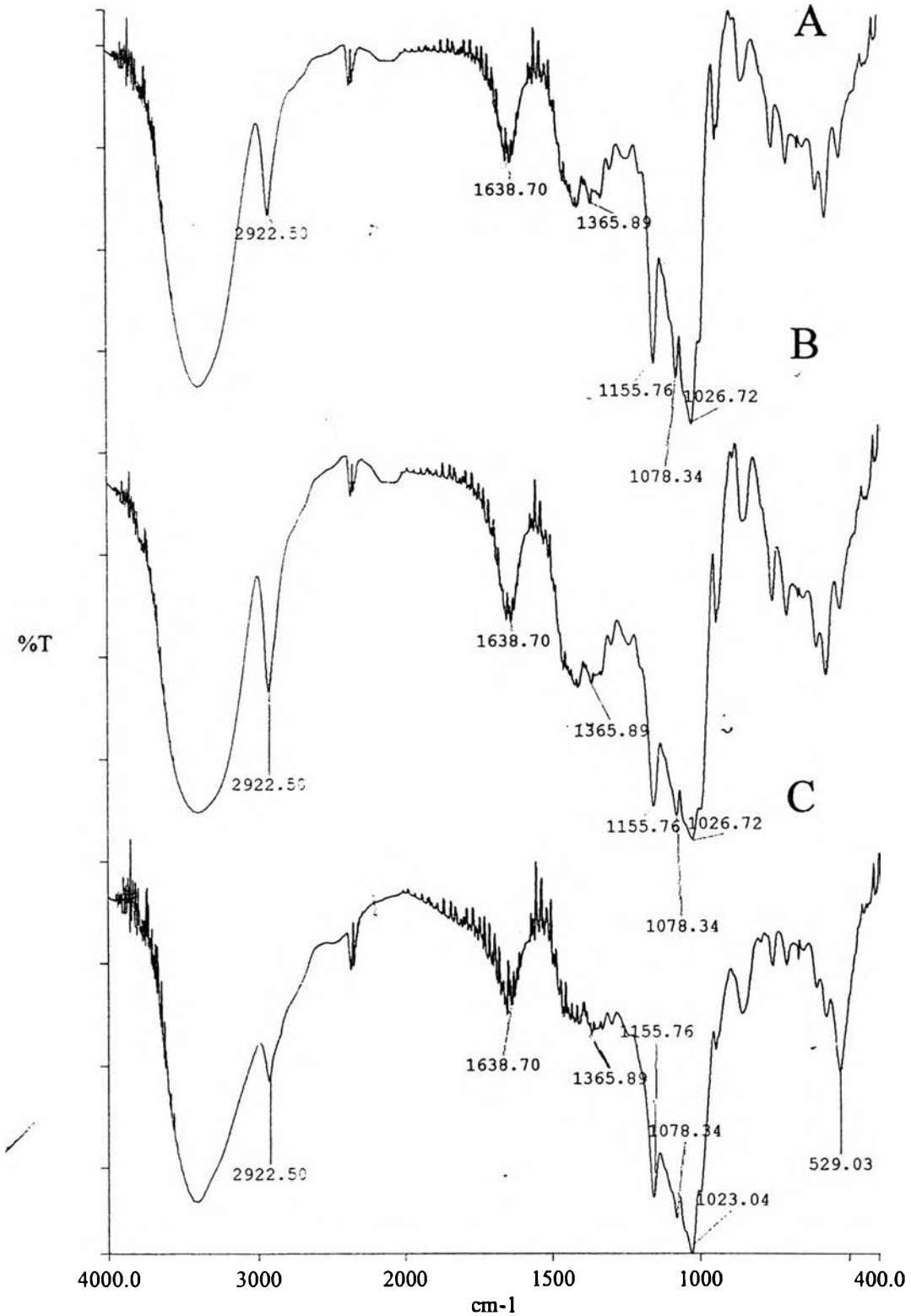

Figure 42 *Infrared spectra in KBr pellet of (A) BCD; (B) spray dried BCD in water and (C) spray dried BCD in buffer*

From the FTIR of the physical mixture of IMC and BCD , they showed bands corresponding to a superimposition of the pure drug and BCD spectra (Figure 43). However, the FTIR spectra of all the spray dried IMC/BCD exhibited some significant differences from those of physical mixtures of drug and BCD (Figures 44). The disappearance of band at 1720 cm^{-1} of IMC be due to the ionization of carboxylic group in phosphate buffer pH 7.4 which indicated by the peaks at 1587 and 1476 cm^{-1} (Biemann, 1983) although these peaks were corresponding to aromatic C=C stretching and O-CH_3 deformation of IMC. A reason for reduction intensity of the carbonyl absorption band (around 1690 cm^{-1}) may be due to the formation of hydrogen bonding between IMC and BCD (Lin, et al., 1991).

Figure 45 showed FTIR spectra of original SLS, spray dried SLS in water and spray dried SLS in buffer. FTIR spectra of SLS and spray dried SLS was characterized by intense band at 1220 cm^{-1} corresponding to stretching vibration of -SO_2 group. In the 2950-2800 cm^{-1} region corresponding to the vibrations of the –CH and –CH_2 groups. From FTIR spectra of spray dried SLS in buffer the FTIR spectra of SLS and spray dried buffer were superimposible. These results showed that spray dried condition did not effect the chemical structure of SLS.

FTIR of physical mixtures of IMC and SLS show spectra corresponding to a simple overlapping of pure drug and SLS spectra (Figure 46). The bands at 1720 and 1692 cm^{-1} corresponding to the carbonyl stretching (C=O) of IMC were dominant in the spectra. This result indicated that there was no change in the chemical structure of IMC in the physical mixtures.

FTIR spectra of spray dried IMC and SLS exhibited some differences from those of physical mixtures of drug and SLS (Figure 47). The band at 1692 cm^{-1} did not shift while the band at 1720 cm^{-1} disappeared and there were the bands about 1587 and 1483 cm^{-1} may be due to the ionization of IMC in phosphate buffer (Biemann, 1983). These results disappeared in the physical mixtures because IMC was in the form of non-ionized form in the physical mixtures.

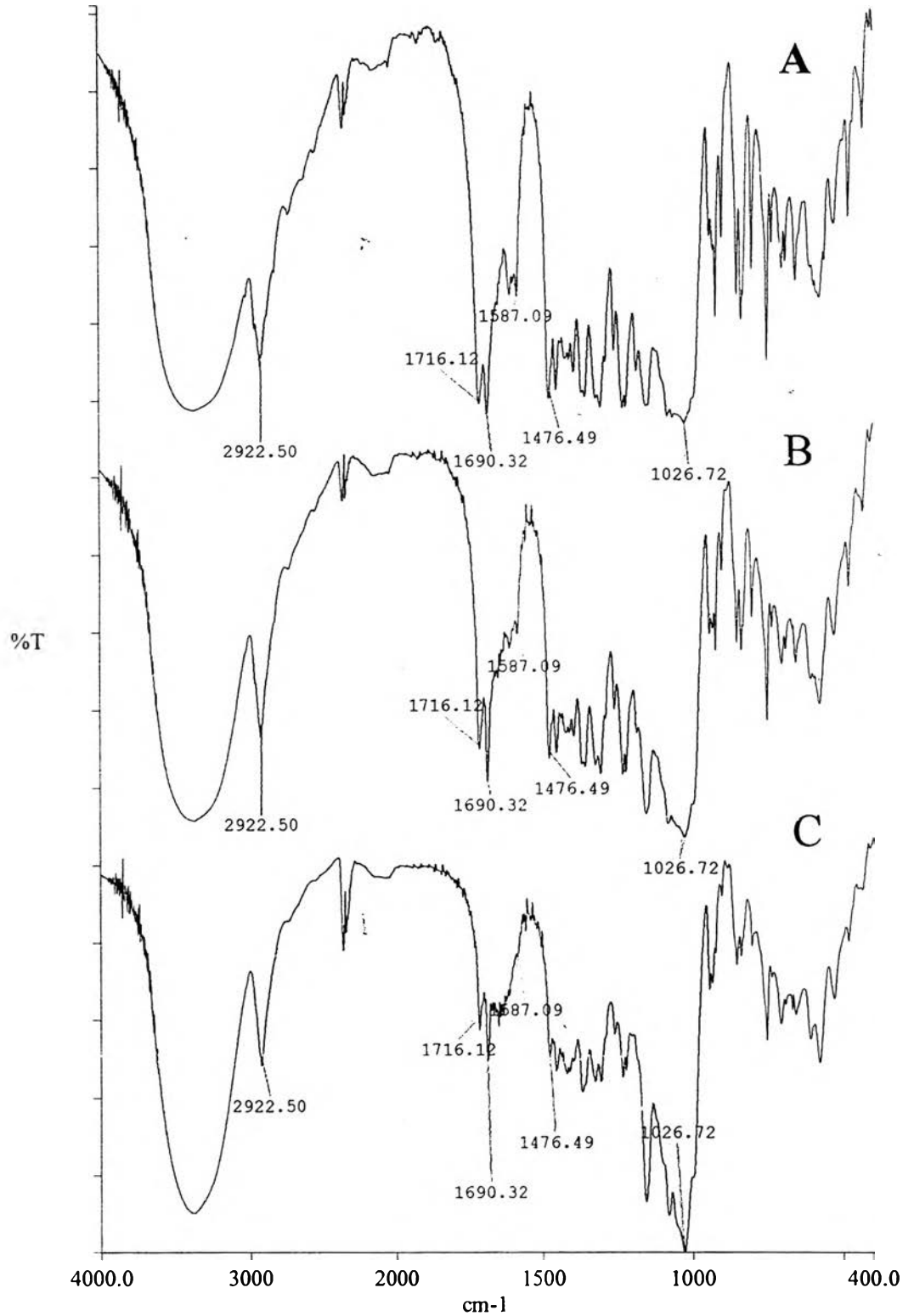

Figure 43 *Infrared spectra in KBr pellet of IMC/BCD physical mixtures: (A) IIB(PM); (B) IB(PM) and (C) IBB(PM)*

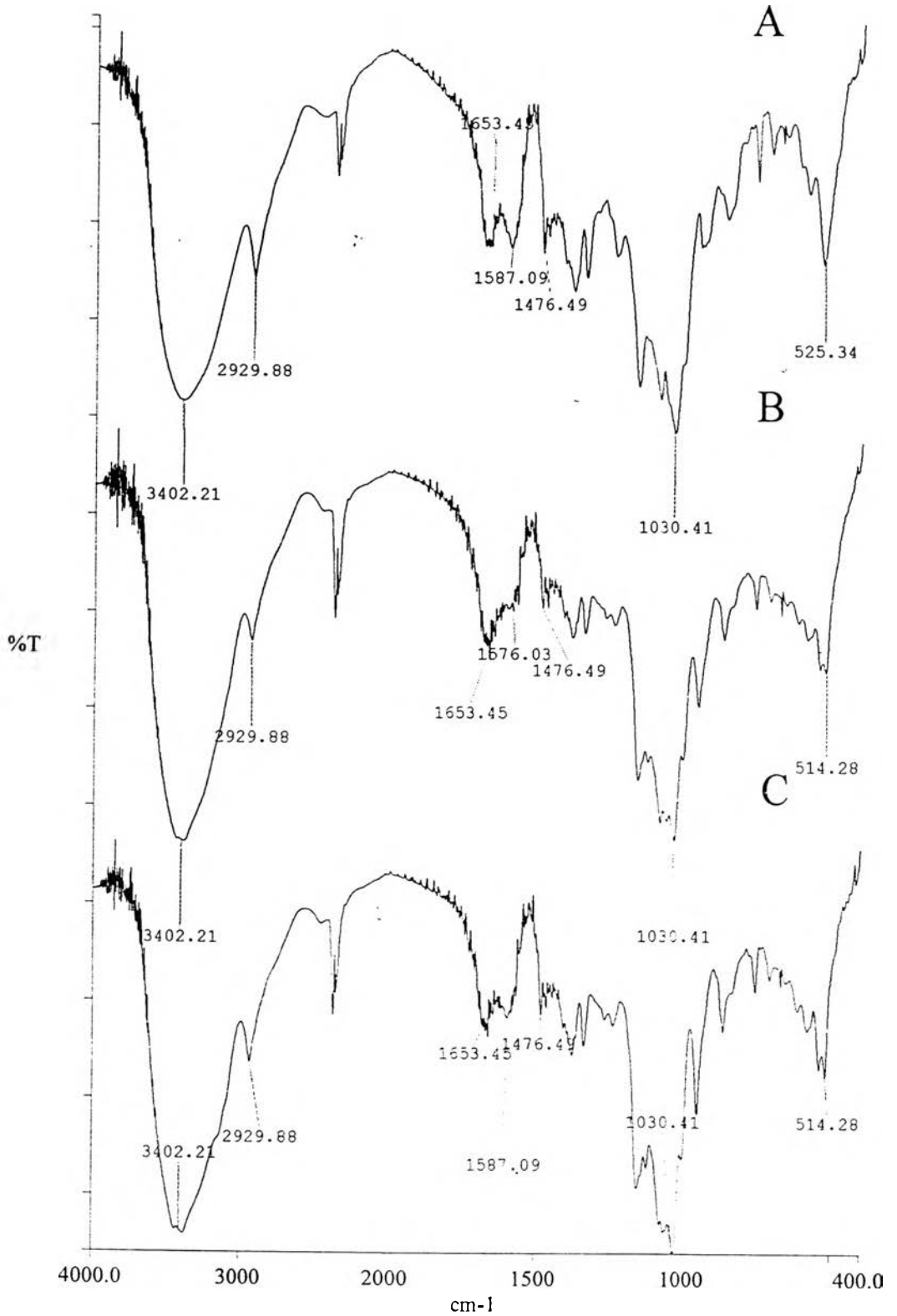

Figure 44 *Infrared spectra in KBr pellet of IB , feed rate 15 ml/min: (A) I15B130; (B) I15B140 and (C) I15B150*

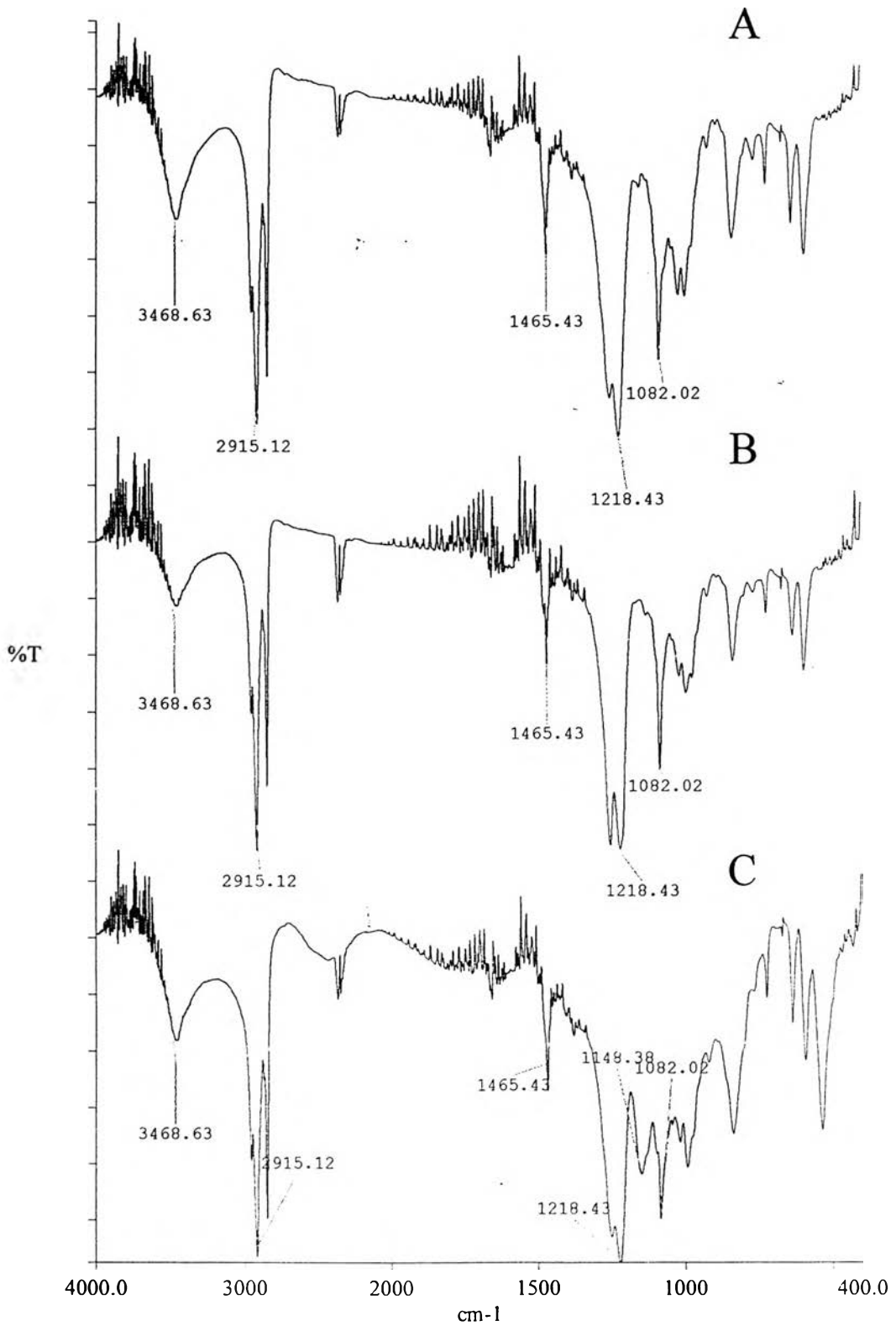

Figure 45 *Infrared spectra in KBr pellet of (A) SLS; (B) spray dried SLS in water and (C) spray dried SLS in buffer*

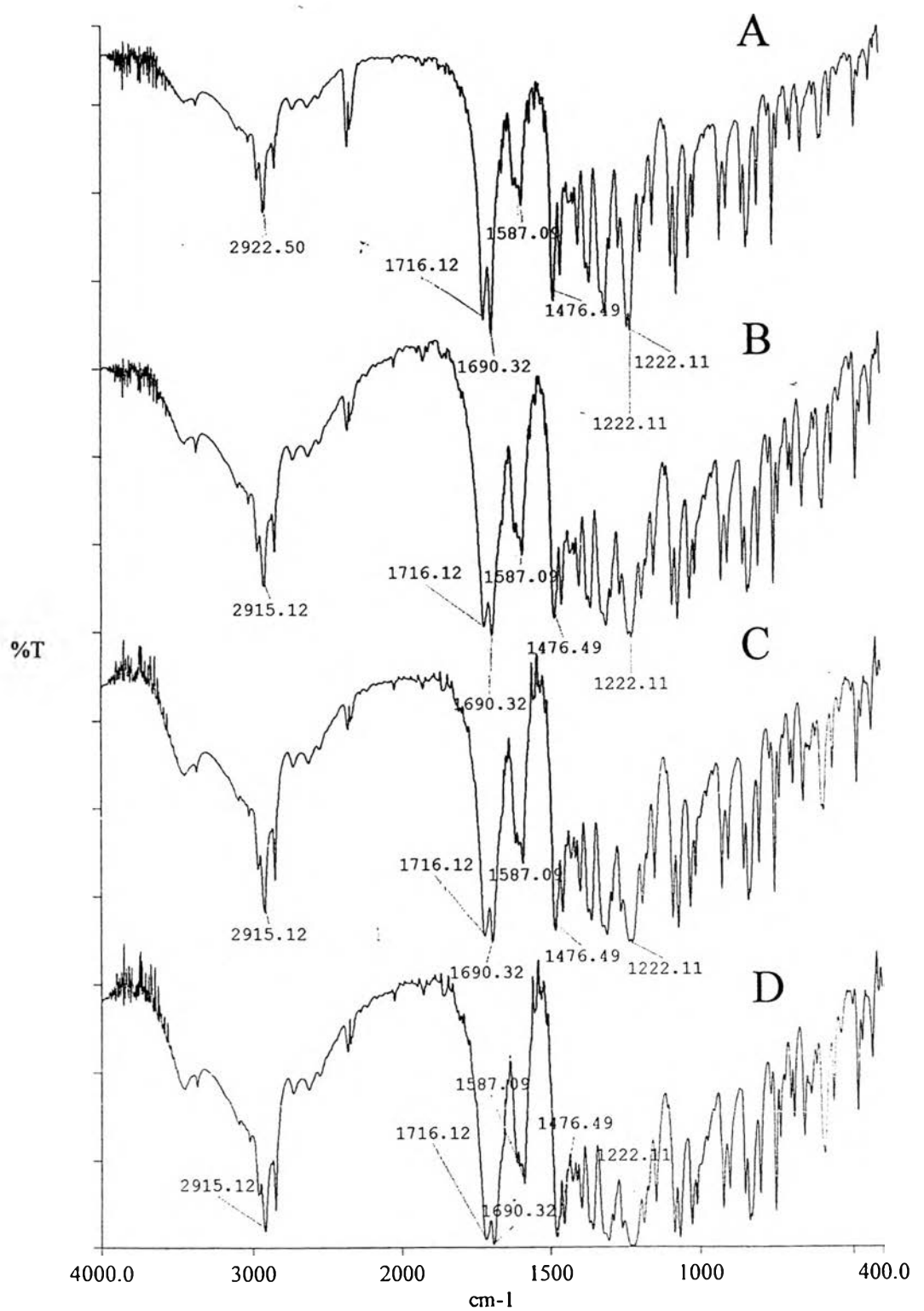

Figure 46 *Infrared spectra in KBr pellet of IMC/SLS physical mixtures; (A) IS13(PM); (B) IS20(PM); (C) IS27(PM) and (D) IS33(PM)*

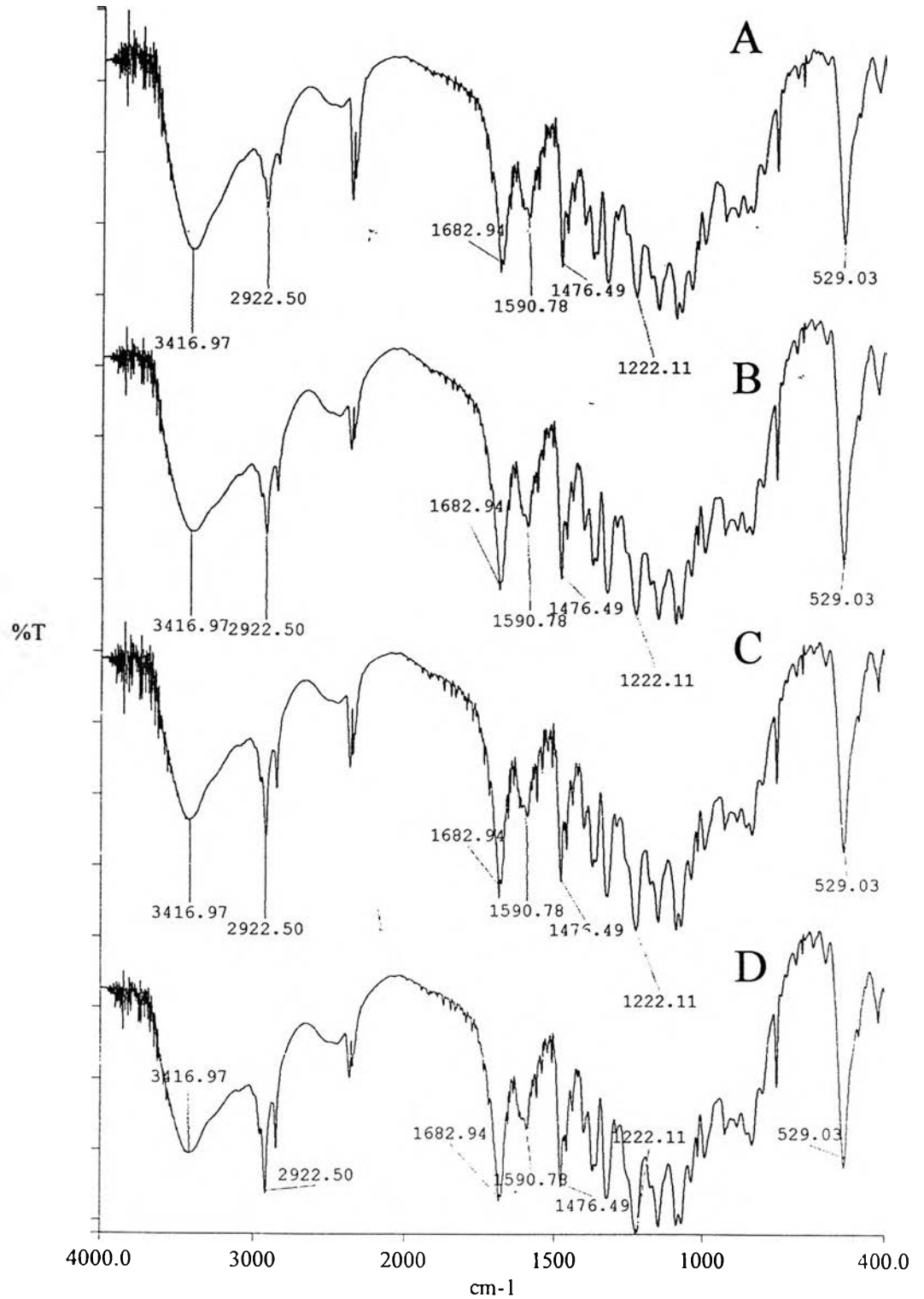

Figure 47 *Infrared spectra in KBr pellet of spray dried IMC/SLS; (A) IS13; (B) IS20; (C) IS27 and (D) IS33*

3.8 Quantitations of Indomethacin in spray dried powders using HPLC

HPLC analysis (Table 24) shows the determination of percent drug content of IMC prepared by spray drying method. In this case, the IMC buffered solution which contains BCD must be confirmed that the presence of BCD and buffer components did not interfere with the determination of IMC which was shown to not interfere with this analytical procedure (see the specificity of HPLC determination in page 152).

Table 24 compares the percent content of IMC in spray dried products with or without BCD. When BCD was used in the formulation at three different molar ratios, the percent content of IMC was shown to be approximately the same (for 2:1) or higher (for 1:1 and 1:2, respectively) than that when spray dried IMC in buffer solution alone (89.53%). These observed results is thought to be due to the fact that the drug was included in the BCD cavity or protected by the surrounding BCD and was protected against deteriorating effect of basic hydrolysis at pH 7.4 (Backensfeld, 1990). The addition of BCD to the formulations thus, stabilized IMC and the stabilizing effect increased with increasing amount of BCD in the preparation (each molar ratio of spray dried IMC/BCD).

The results on the stability of IMC in various ratios of spray dried IMC/BCD are also summarized in Table 24. It could be concluded that the percent amount of IMC in the spray dried products of the same molar ratio were not significantly different when changes in the inlet air temperature and feed rate in the spray drying process occured. At molar ratio of 2:1, the percent amount of IMC were in the range of 84.36 to 89.72 (Table 24: II10B130-II20B150). While other two different molar ratios of spray dried IMC/BCD 1:1 and 1:2, percent amount of IMC/BCD were higher than IMC and BCD at molar ratio 2:1. The percent amounts of 1:1 and 1:2 molar ratios were an average of 97.81 and 95.76, respectively. The percent amount IMC in the 1:1 and 1:2 molar ratios were higher may be due to the excess of IMC in the 2:1 system which was not protected by BCD from the basic hydrolysis during in the spray drying process. The probable reason for the higher percent amount of protected IMC in the 1:1 and 1:2 molar ratio was because there was enough amount of BCD for the protection against the basic hydrolysis during the spray drying process.

Table 24 HPLC analysis of spray dried products and physical mixtures

Sample	Percent drug content		
	1	2	Average
II10B130	88.7	86.42	87.56
II10B140	85.4	84.23	84.82
II10B150	87.98	87.59	87.79
II15B130	82.88	89.53	86.21
II15B140	85.35	89.05	87.20
II15B150	87.01	88.46	87.74
II20B130	89.72	87.47	88.60
II20B140	85.67	83.04	84.36
II20B150	85.91	85.54	85.73
I10B130	97.38	99.54	98.46
I10B140	99.42	97.94	98.68
I10B150	95.92	94.91	95.42
I15B130	99.47	99.76	99.62
I15B140	96.26	95.14	95.70
I15B150	96.77	97.46	97.12
I20B130	99.32	98.35	98.84
I20B140	99.98	99.43	99.71
I20B150	97.23	96.31	96.77
I10BB130	97.94	99.97	98.96
I10BB140	99.56	99.95	99.76
I10BB150	98.89	95.59	97.24
I15BB130	99.93	91.33	95.63
I15BB140	92.52	96.11	94.32
I15BB150	95.46	93.88	94.67
I20BB130	94.55	93.48	94.02
I20BB140	95.52	95.86	95.69
I20BB150	92.03	91.08	91.56

Table 24 (continue) HPLC analysis of spray dried products

And physical mixtures

Sample	Percent Drug Content		
	1	2	Average
IIB(PM)	99.98	-	99.98
IB(PM)	98.87	-	98.87
IBB(PM)	98.96	-	98.96
IS13	83.01	76.51	79.76
IS20	87.37	73.47	80.42
IS27	82.85	81.42	82.14
IS33	78.96	81.18	80.07
IS13(PM)	99.95	-	99.95
IS20(PM)	98.89	-	98.89
IS27(PM)	98.56	-	98.56
IS33(PM)	99.96	-	99.96
Spray dried IMC	92.77	86.29	89.53

Table 24 shows HPLC analysis of IMC/BCD physical mixtures [IIB(PM)-IBB(PM)]. The result indicated that the percent of IMC at three different concentrations of BCD were not different and they were close to 100 percent. The reason why IMC content was higher than the spray dried systems indicated earlier was because IMC in the physical mixture at various molar ratios were in the physical mixture, it did not come in contact with the slightly basic buffer solution used during the spray drying process which induced any possible basic hydrolysis of IMC.

The effect of SLS on the stability of IMC are also shown in Table 24. The amount of IMC at different concentrations of SLS in the physical mixtures were close to 100 percent [IS13(PM)-33(PM)]. The result was similar to the high amount of IMC (close to 100 percent) of IMC/BCD physical mixtures. However, the amount of IMC in spray dried IMC/SLS was found to be low in the range of 75.07 to 82.14% (IS13-IS33). These results indicated that anionic micelles of SLS could not

inhibit the basic hydrolysis during spray drying due to the increased pH of spray drying solution when SLS dissolved. Thus, it can not stabilize IMC in the formulation.

4. Solubility of the mixtures

Evaluation of the concentration-time profiles

The concentration-time profiles of IMC in phosphate buffer pH 7.4 at 37°C (Figure 50) show a steady increase in the amount of IMC until reaching a plateau concentration (1.602 mcg/ml) after about 6 hours. The spray dried product shows an initial surge solubility of approximately 12 mcg/ml until about 6 hours, then this solubility declines to a lower plateau of about 11 mcg/ml. The plateau observed in this case was higher than that obtained for IMC. The increase in this solubility was due to combination of many reasons as will be discussed. One of the reason was probably due to the ionization of IMC in phosphate buffer pH 7.4 and formed sodium salt in the solution during the spray-drying process which was indicated by the disappearance of FTIR band at 1720 cm^{-1} and exhibited the bands at 1591 and 1477 cm^{-1} as shown in previous section. The initial solubility surge of the spray dried product resembled the characteristic concentration-time profile of a metastable solid form produced by the milling process (Elamin, A.A., et al., 1994). It indicated that after spray drying a metastable phase was present and in this case was confirmed to be an amorphous transformation as seen in X-ray diffractogram (Figure 32) and the disappearance of melting peak of IMC in DSC thermogram (Figure 23). The other reason for increased solubility of spray dried IMC may be the reduction of particle size after the spray drying process as indicated in particle size determination in Table 21. Thus, from the above reasons the solubility of spray dried IMC in phosphate buffer was more than that of pure IMC in phosphate buffer.

The solubility profiles of IIB are not shown in this study because the concentration of IMC did not change after shaking in phosphate buffer pH 7.4 after 24 hours duration. Instead a separation of the composition of the spray dried product was observed, indicated by the white precipitate on the bottom and gel-like structure on the top. Each composition was subjected to X-ray diffractometry for identification. X-ray diffraction pattern of gel-like composition (Figure 49) is similar to that of spray dried

BCD but the X-ray diffraction pattern of white precipitate (Figure 48) could only be mostly identified as a partial amorphous solid. The formation of gel-like structure of BCD indicated in this study would need further investigation on many aspects, such as the lower solubility of BCD at very high concentrations of IMC or condition(s) suitable for BCD polymerization. In this study we did not persue the investigation on this phenomenon any further.

Figure 51 shows the plateau solubility of IIB(PM), IB(PM) and IBB(PM) which are about 8.956, 9.719 and 7.995 mcg/ml, respectively. These results show that the solubility of physical mixtures of IMC and BCD at various molar ratios are not significantly different ($p>0.05$). However, the solubility of these physical mixtures were higher than the solubility of intact IMC due to the surfactant-like properties of BCD when IMC dissolved in buffer (Guyot et., al 1995). The solubility of spray dried IMC however is 12.149 mcg/ml (Figure 50), which was higher than the solubility of the physical mixtures of IMC and BCD due to the changes occurred during the spray drying process such as the smaller particle size (confirmed by particle size determination in Table 21) and the ionization of IMC to sodium salt in phosphate buffer pH 7.4 during spray-drying (confirmed by FTIR). The additional reason for the higher solubility of spray dried IMC compared to the physical mixture might be the low crystallinity of spray dried product which was in high-energetic state as shown in X-ray diffraction pattern.

The concentration-time profiles of IB , IBB and IS were similar to that of the spray dried IMC. However, the equilibrium solubility concentration of spray dried IMC/BCD were much higher (as presented in Figure 52 – 56) than spray dried IMC. These results may be due to many reasons. One major reason for the improvement of solubility may be due to the formation of inclusion compound between IMC and BCD. The low crystallinity of spray dried IMC/BCD, indicated by X-ray powder diffraction, suggested the possible formation of the inclusion of IMC into the cavity of BCD (Lin and Kao, 1989) or between BCD molecules. The diffraction patterns failed to show the main peaks of IMC (Figure 36) because IMC are molecularly dispersed in BCD cavities or between, but they exhibited the main peak of IMC when analysing the spray dried IMC in phosphate buffer when BCD were not used. The other explanations for the possible inclusion of IMC into the cavity of BCD were the lost of endothermic peak of

IMC at 161°C as shown in DSC thermogram (Figure 26), and the disappearance of carbonyl stretching absorption band (1690 cm^{-1}) in FTIR spectra (Figure 44). Another possibility for solubility improvement may be because of the formation of sodium salt between IMC and phosphate buffer, indicated by the disappearance of FTIR carbonyl stretching (around 1720 cm^{-1}) of IMC and exhibited the peaks around 1587 and 1476 cm^{-1}.

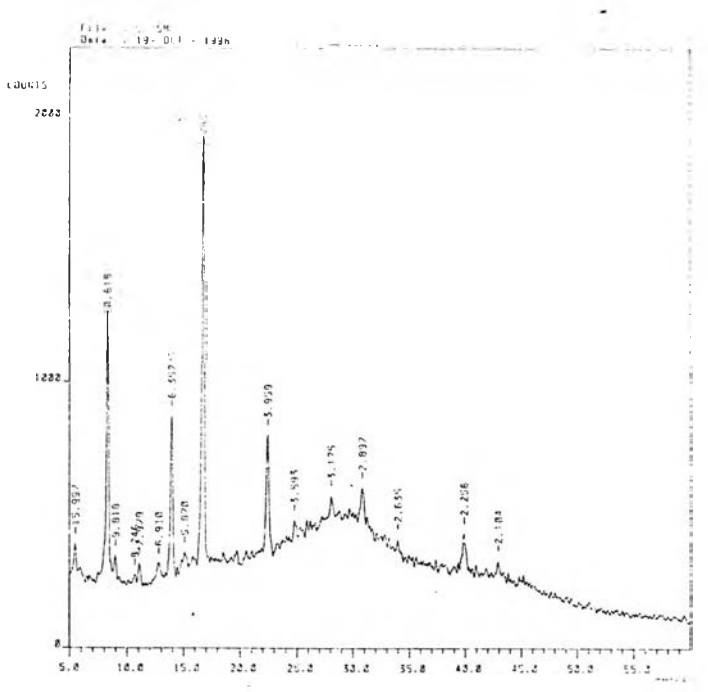

Figure 48 *X-ray diffraction pattern of the crystalline precipitate of IIB*

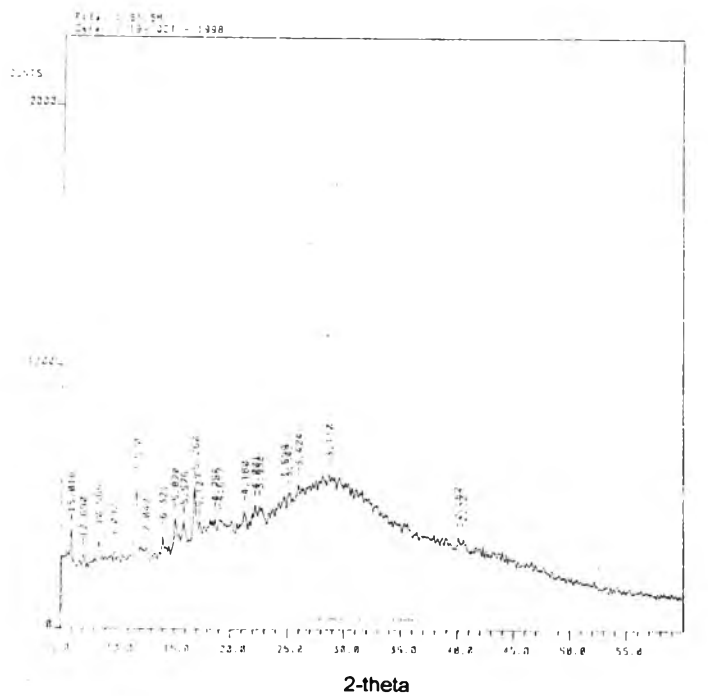

Figure 49 *X-ray diffraction pattern of the gel like composition of IIB*

The initial increased in solubility attained by the spray dried IMC and spray dried IMC/BCD (Figure 50-56) may correspond to the solubility of an 'activated state' (Elamin, A.A., et al., 1994). At the activated states, the samples are in the form of higher-energy metastable states (Buckton and Beezer, 1992), which tend to form more thermodynamically stable, lower energy, crystalline product during solubility studies or during storage states. Hence, an initial peak surge was seen. The time required by these spray dried products to reach the plateau was much longer (more than 24 hours). It is probably due to the high-energetic amorphous state of spray dried products (as shown in X-ray diffractograms and DSC thermograms) which needed time to form stable lower-energetic state before equilibrium solubility can occur.

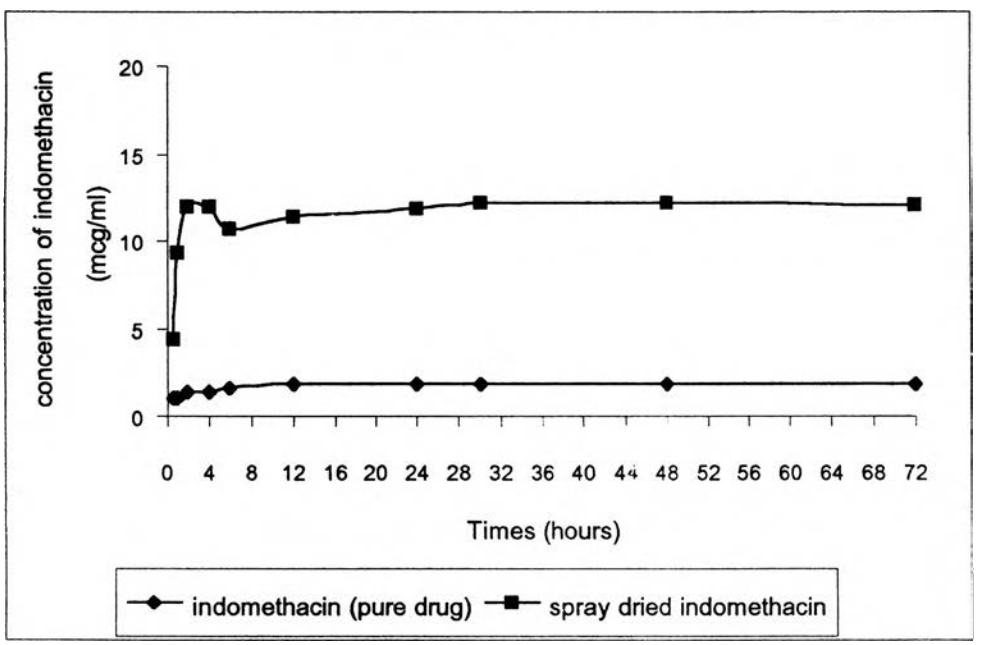

Figure 50 *Concentration-time profiles of pure indomethacin and spray dried IMC in phosphate buffer pH 7.4 at 37 °C*

The equilibrium solubility values of each formulation of IB (Figure 52-54) are not significantly different ($p > 0.05$) when varied the inlet air temperature and feed rates. This result is also the same for the saturated solubility values of each formula of IBB [Figures 55 – 57]. The reasons for these conclusions were that there were no significantly different ($p > 0.05$) particle size of each formula in each molar ratio (confirmed by determination of particle size in Table 21) and the similar amorphous patterns of spray dried products as shown in X-ray diffraction analysis. It can be concluded that although the spray dried IMC/BCD, at the same molar ratio, were prepared by various spray-drying conditions the solubility of spray dried products were not significantly different ($p>0.05$).

However, a comparison spray dried IMC/BCD at molar ratio 1:1 with 1:2 showed that the average solubility of IB [about 45 mcg/ml] was more than the solubility of IBB [about 20 mcg/ml]. A comparison with the X-ray diffraction patterns of IB and the X-ray diffraction patterns of IBB indicated the disappearance of the main peak of IMC for both molar ratios. The lower average solubility of IBB may be due to the excess amount of BCD in the IBB. If one assumed that there was as inclusion formation, when the inclusion formation was completed the excess BCD which had the higher solubility than IMC will be dissolved and compete with the solubility of IMC inclusion product. Thus reduction of the solubility of IMC was shown.

The final conclusion for the solubility values of pure IMC, spray dried IMC, physical mixtures of IMC and BCD and spray dried IMC and BCD at various molar ratios and spray-drying conditions are as follows:

Spray dried IMC/BCD (1:1) > spray dried IMC/BCD (1:2) >spray dried IMC in buffer > physical mixtures > IMC

It is important to note that the spray drying process had higher impact on the solubility values than the influence of BCD in the formulation or the formation of sodium salt of IMC.

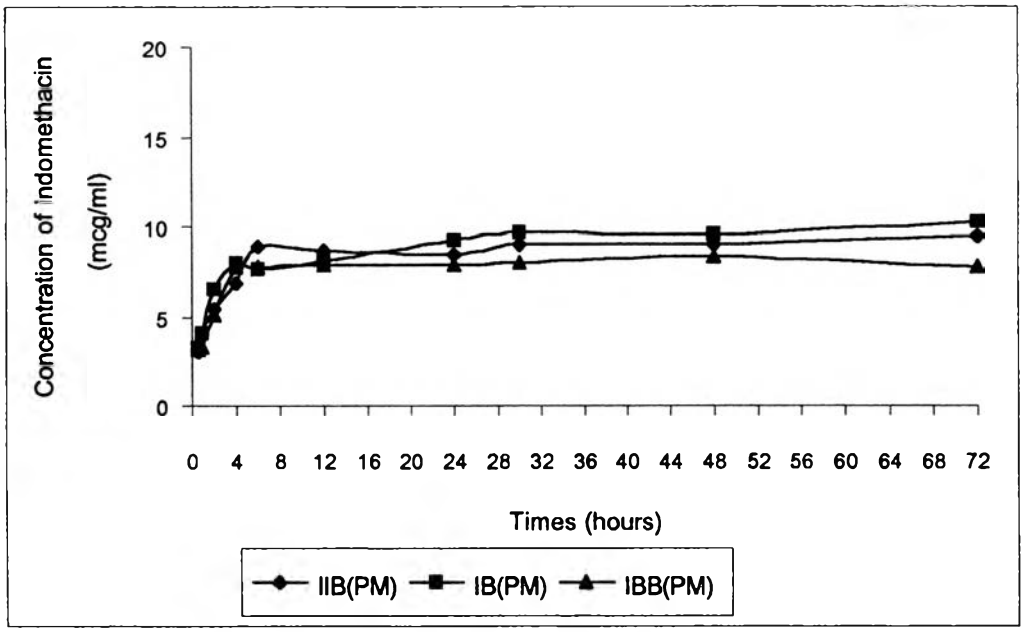

Figure 51 *Concentration-time profiles of IMC/BCD physical mixtures in phosphate buffer pH 7.4 at 37 °C*

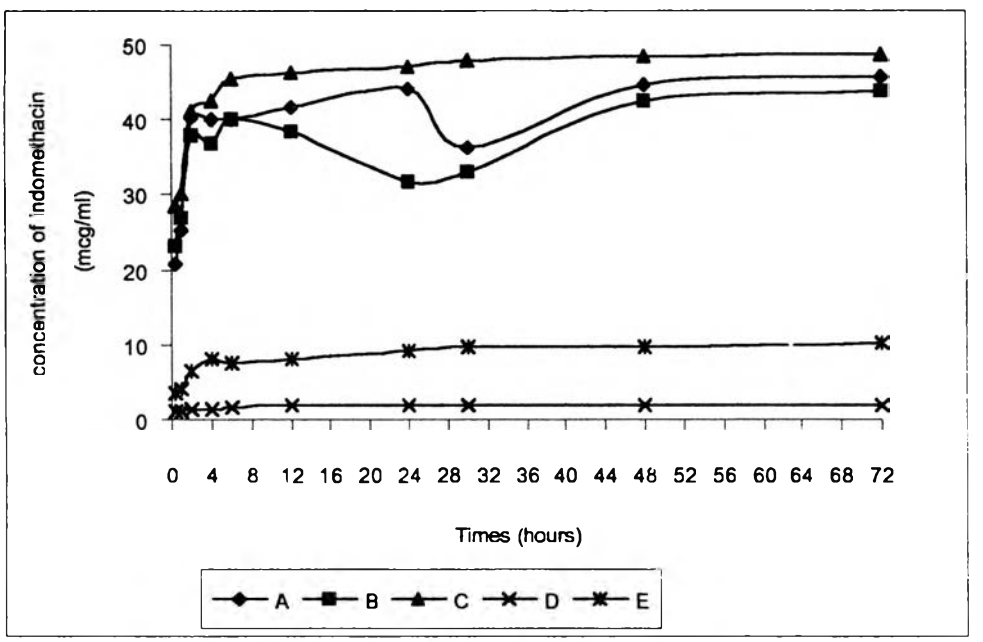

Figure 52 *Concentration-time profiles of spray dried IMC/BCD (1:1) in phosphate buffer pH 7.4 at 37 °C prepared using spray drying at feed rate 10 ml/min [(A) I10B130, I10B140, (C) I10B150, (D) IMC and (E) IMC/BCD physical mixture (1:1).*

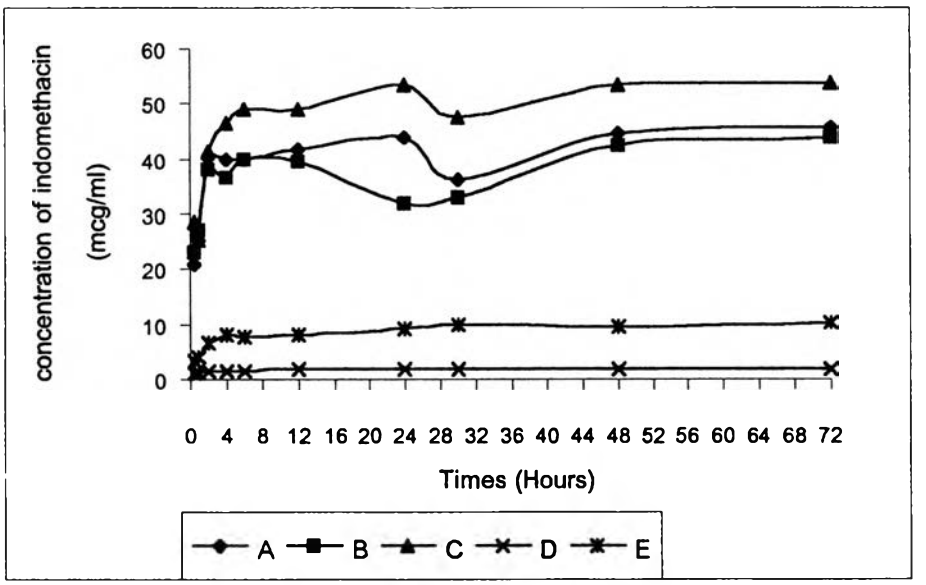

Figure 53 *Concentration-time profiles of spray dried IMC/BCD (1:1) in phosphate buffer pH 7.4 at 37 ℃ prepared using spray drying at feed rate 15 ml/min [(A) I15B130, (B) I15B140, (C) I15B150, (D) IMCand (E) IMC/BCD physical mixture (1:1).*

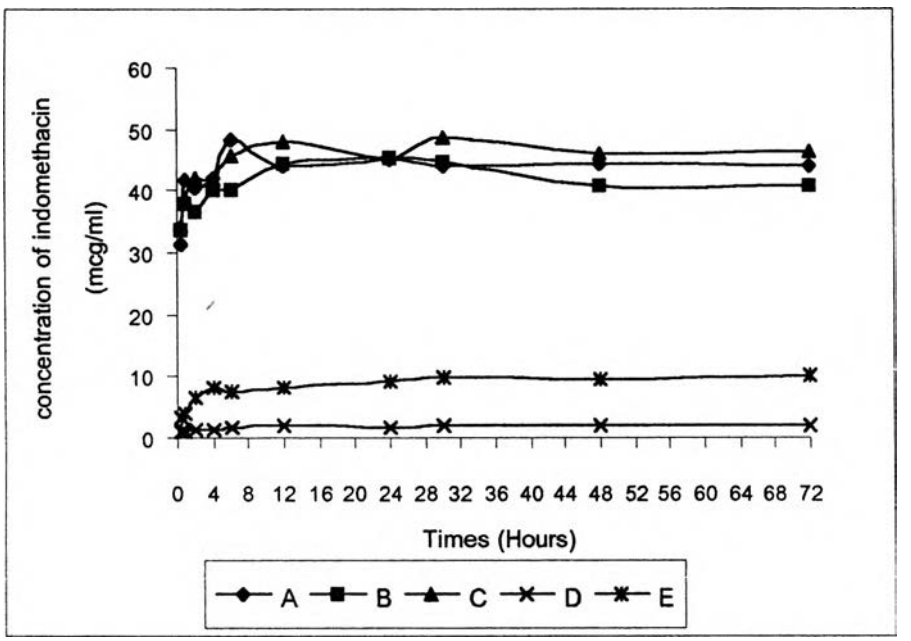

Figure 54 *Concentration-time profiles of spray dried IMC/BCD (1:1) in phosphate buffer pH 7.4 at 37 ℃ prepared using spray drying at feed rate 20 ml/min [(A) I20B130, (B) I20B140, (C) I20B150, (D) IMC and (E) IMC/BCD physical mixture (1:1).*

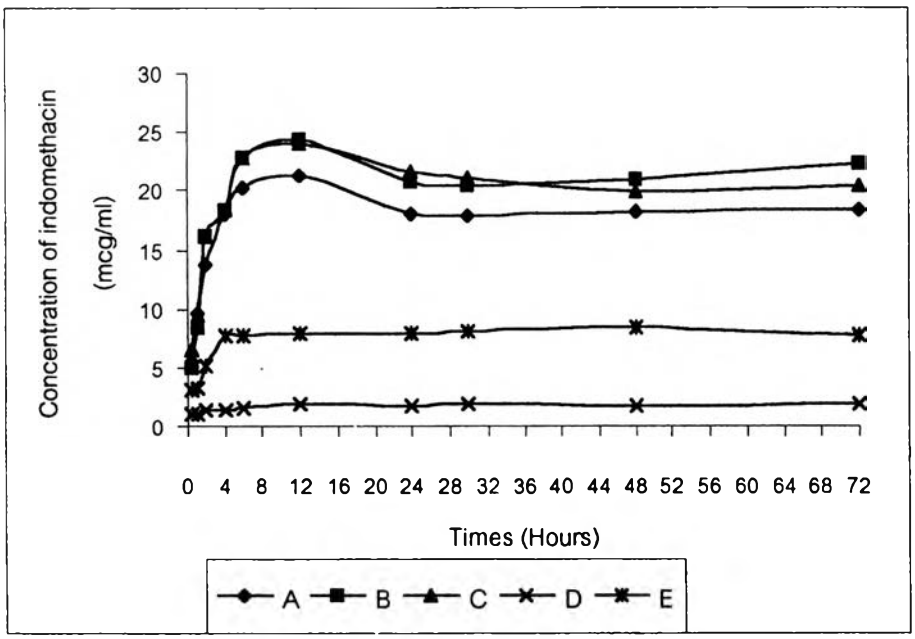

Figure 55 *Concentration-time profiles of spray dried IMC/BCD (1:2) in phosphate buffer pH 7.4 at 37 °C prepared using spray drying at feed rate 10 ml/min [(A) I10BB130, (B) I10BB140, (C) I10BB150, (D) IMC and (E) IMC/BCD physical mixture (1:2).*

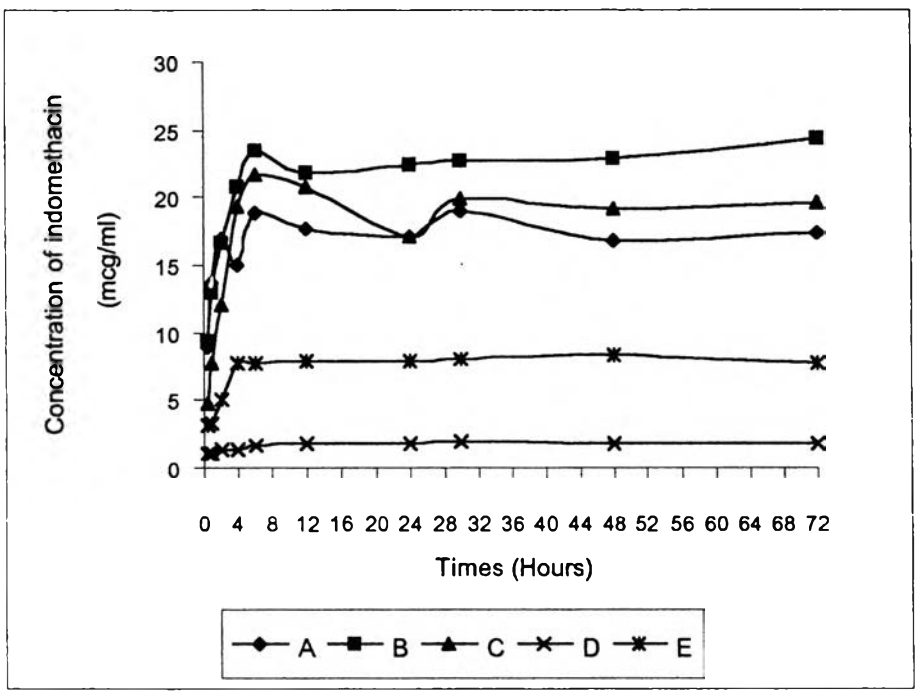

Figure 56 *Concentration-time profiles of spray dried IMC/BCD (1:2) in phosphate buffer pH 7.4 at 37 °C prepared using spray drying at feed rate 15 ml/min [(A) I15BB130, (B) I15BB140, (C) I15BB150, (D) IMC and IMC/BCD physical mixture].*

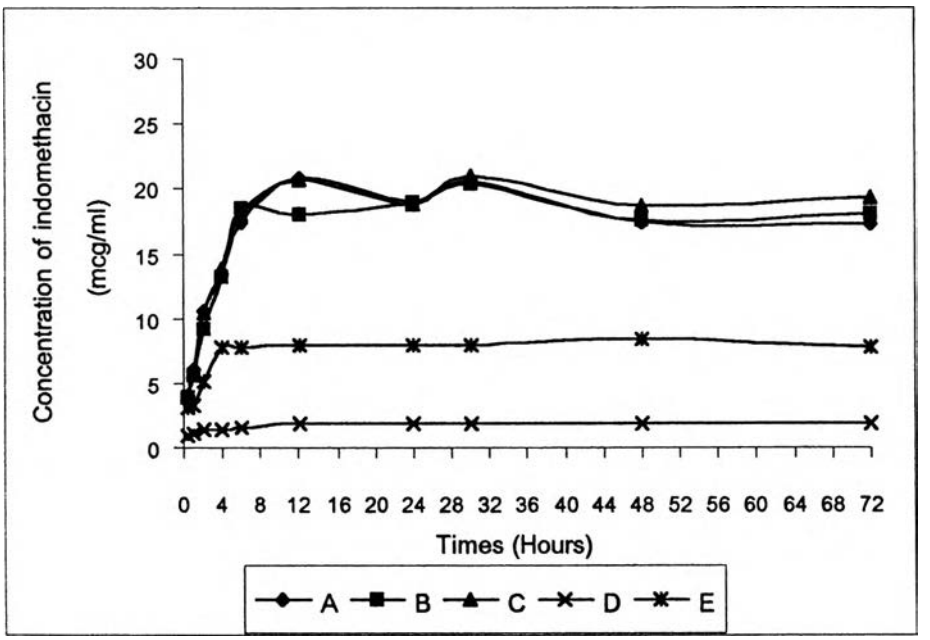

Figure 57 *Concentration-time profiles of spray driedIMC/BCD (1:2) in phosphate buffer pH 7.4 at 37 °C prepared using spray drying at feed rate 20 ml/min [(A) I20BB130, (B) I20BB140, (C) I20BB150, (D) IMC and (E) IMC/BCD physical mixture (1:2)].*

The solubility values of IMC/SLS physical mixtures are shown in Figure 58. This result, which was statistically tested, showed that the equilibrium solubility of IS13(PM), IS20(PM), IS27(PM) and IS33(PM) are not significantly different ($p>0.05$). The increase in the solubility of IS(PM) when compared to intact IMC are due to the micellar solubilization of SLS when IMC was dissolved in phosphate buffer pH 7.4 and the solubility increased as the amount of SLS increased in every SLS concentrations when compared with IMC.

The results of equilibrium solubility of spray dried IMC with various concentrations of SLS phosphate buffer in pH 7.4 (Figure 59) show that they are not significantly different ($p>0.05$) [about 18 mcg/ml]. In this Figure it was shown that there was an initial solubility surge at the beginning then the solubility of spray dried products declined to plateau level. These results are due to the recrystallization from metastable state of IMC when suspended in the medium as mention previously. However, the solubility of spray dried products are higher than the solubility of IMC. It was due to the micellar formation of SLS and the ionization of IMC in phosphate buffer pH 7.4 as shown by the disappearance of the carbonyl stretching (1720 cm^{-1}) of IMC in FTIR spectra (Figure 47). The additional reason for the increased in solubility

these spray dried products is the smaller size of the spray dried products as shown in particle size determination in Table 21.

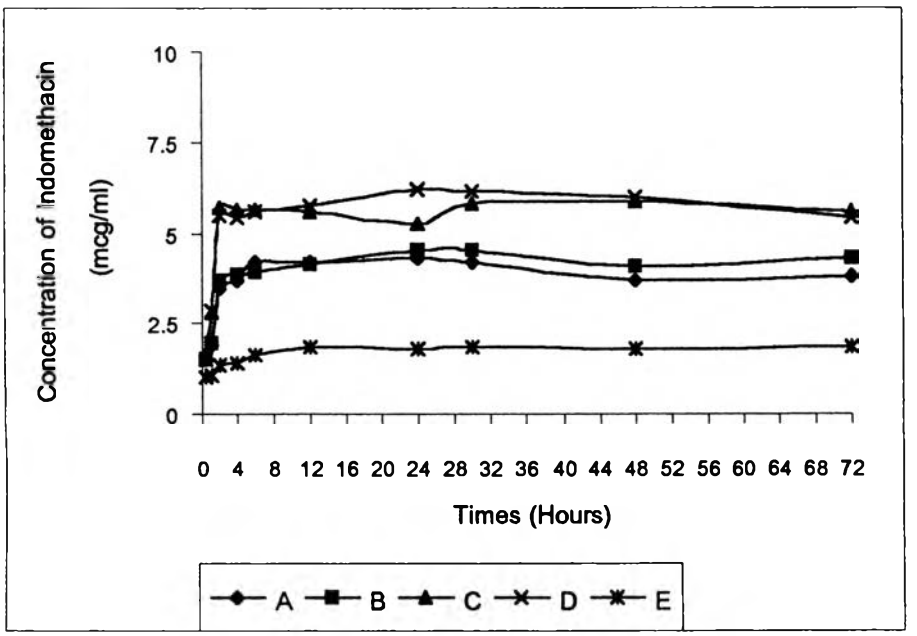

Figure 58 *Concentration-time profiles of IMC/SLS physical mixtures in phosphate buffer pH 7.4 at 37 ℃ [(A) IS13(PM); (B) IS20(PM);(C) IS27(PM); (D) IS33(PM) and (E) IMC]*

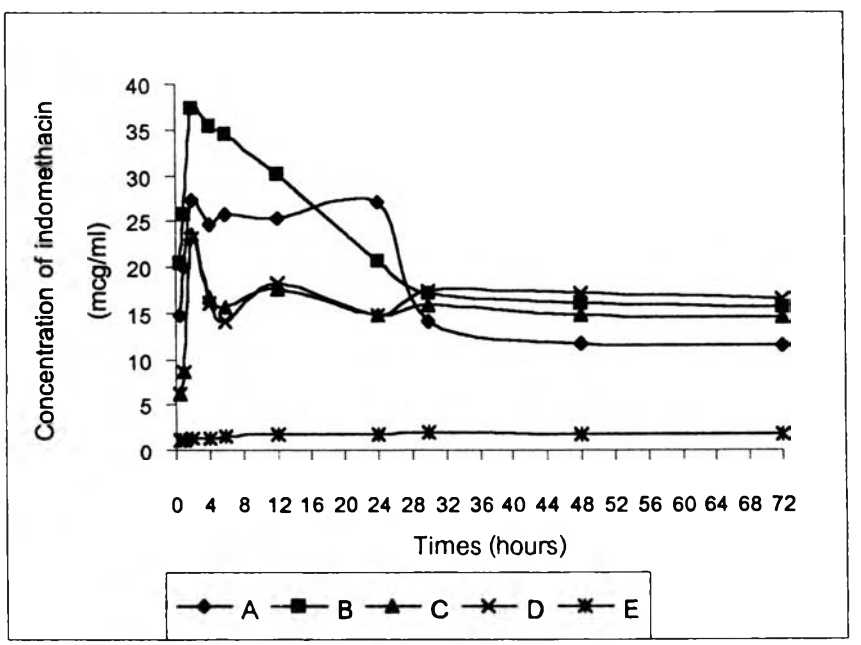

Figure 59 *Concentration-time profiles of spray dried IMC/SLS in phosphate buffer pH 7.4 at 37 ℃ [(A) IS13; (B) IS20; (C) IS27; (D) IS33 and (E) IMC]*

5. Dissolution of indomethacin capsule

The dissolution profiles are plotted between percent of drug dissolved against time. The dissolution data are shown in Appendix I.

All preparations were produced by filling into capsules (as equivalent to 25.00 mg of drug). They were evaluated in phosphate buffer pH 7.4 for 60 minutes. Percentage of drug dissolved was calculated by comparison of the cumulative percentage of amount of drug at the time of sampling with total amount of drug used in the dissolution study.

The percentages of drug dissolved in the medium from all spray dried products was approximately equal or more than 85% within 20 min. This dissolved level passed the criteria for percent drug dissolved from indomethacin capsule stated in USP XXIII.

The drug dissolution data of IMC and spray dried IMC in capsules are listed in Appendix I and dissolution drug profiles are shown in Figure 60.

The percentage of drug dissolved in phosphate buffer pH 7.4 of IMC capsule and spray dried IMC capsule at 20 minutes were 67.71% and 83.91%, respectively and the initial dissolution rate (Table 25) of spray dried IMC (calculated by the slope of the dissolution profile in the range of 0 minute and the initial equilibrium time) was more than that of IMC regardless of spray dried conditions used. This result indicated that spray dried IMC was more soluble than IMC due to the higher solubility of this powder as indicated in the solubility study of spray dried IMC and IMC in section 4. Other explanations for the increase in dissolution rate of these spray dried products were the solubility improvement by sodium salt formation of spray dried IMC (indicated in FTIR in Figure 41) the effect of smaller particle size of spray dried IMC produced by the spray-drying process. The smaller particle size has higher chemical potential (partial molar free energy) of the molecules in the particle will be, and hence the greater the solubility (Grant and Brittain, 1985). Moreover, the low crystallinity (as shown in the X-ray diffraction pattern in Figure 33) of the spray dried IMC confirmed the formation of higher-energetic state and improving the dissolution rate of spray dried IMC.

The dissolution profiles of physical mixtures and spray dried IMC/BCD at various molar ratios are shown in Figures 61-70 (Table 2I-28I,Appendix I). Each point represents the average value from three determinations at a given sampling time.

As shown in the dissolution profiles of spray dried IMC/BCD, they exhibited instantaneous dissolution. Complete dissolution from all spray dried products was reached within 20 min. At this time, dissolution of IMC was only 67.71% from pure drug, 72.93% from IIB(PM), 86.31% from IB(PM), 86.26% from IBB(PM) and 83.91% from spray dried IMC.

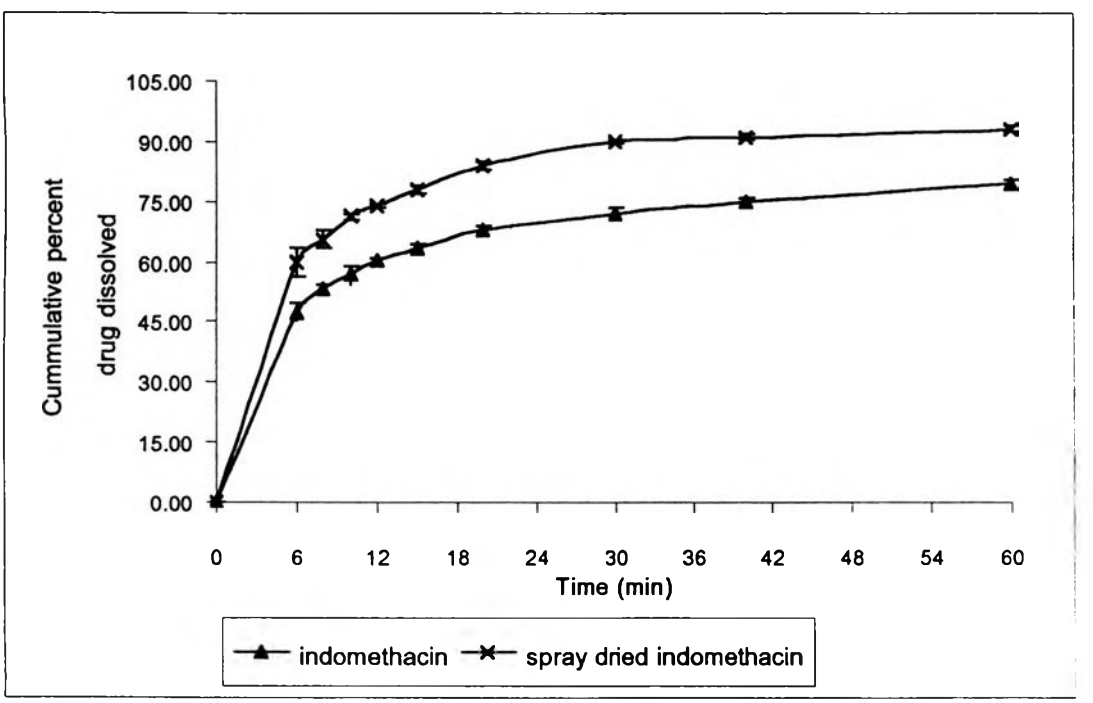

Figure 60 *Dissolution profiles of IMC and spray dried IMC in phosphate buffer*

The analysis of all dissolution data was evaluated by the initial dissolution rate (Table 24-27). Initial dissolution rate indicated the dissolution rate of drug just until before reaching the plateau of the dissolution profile. The time used to reach this point may vary depending on the composition. The amount of drug dissolved before 6 minutes was too low for analysis by UV/visible spectrophotometry. Thus, can not be detected. According to Beer's law the absorbance for the proper sensitivity of detection by this method should be in the range of 0.200-0.800. Although

HPLC method is a suitable and sensitive method for analysis of small amount of drug dissolved, it is time-consuming for the quantitation of drug dissolved very fast.

Table 24 Initial dissolution rate (%mg/min) of indomethacin and spray dried indomethacin in buffer.

Sample	Initial dissolution rate (%mg/min)
IMC	7.91
Spray dried IMC	9.96

Table 25 Initial dissolution rate (%mg/min) of spray dried products

Sample	Inlet air temperature (°C)		
	130	140	150
1) IMC/BCD (2:1)			
Feed rate : 10 ml/min	8.55	11.95	10.76
15 ml/min	8.10	9.19	8.96
20 ml/min	9.19	12.84	10.31
2) IMC/BCD (1:1)			
Feed rate : 10 ml/min	9.32	10.03	10.33
15 ml/min	11.78	10.34	12.11
20 ml/min	9.87	7.57	8.78
3) IMC/BCD (1:2)			
Feed rate : 10 ml/min	10.27	13.29	10.72
15 ml/min	11.30	8.80	10.24
20 ml/min	11.03	10.08	12.77
4) IMC with SLS:			
13% SLS		6.26	
20% SLS		7.68	
27% SLS		7.91	
33% SLS		6.88	

Table 26 Initial dissolution rates (%mg/min) of IMC/BCD physical mixtures

Sample	Initial dissolution rate (%mg/min)
IIB(PM)	9.83
IB(PM)	9.30
IBB(PM)	8.16

Table 27 Initial dissolution rates (%mg/min) of IMC/SLS physical mixtures

Sample	Initial dissolution rate (%mg/min)
IS13(PM)	7.84
IS20(PM)	7.85
IS27(PM)	8.19
IS33(PM)	7.60

From the dissolution profiles of the IMC/BCD physical mixtures (Figure 61) and pure IMC the initial dissolution rates of the physical mixtures are more than that of pure drug. This result can be explained by a local solubilization action of BCD operating in the microenvironment or the hydrodynamic layer surrounding the drug particles in the early stages of dissolution process. BCD dissolves in a short time thus improving the wettability, and hence dissolution, of the drug particles (Hassan, et al.,1990). Although the initial dissolution rate of IIB(PM) is similar to that of the IB(PM) but the dissolution values were not alike (Figure 61) the percent indicated by drug dissolved in IIB(PM) at a certain time was less than that of IB(PM) in later period. It is possibly due to the excess amount of IMC in IIB(PM). Thus after the local solubilization of BCD with part of IMC in the early stage, the remaining undissolved drug in the physical mixture of IMC and BCD at molar ratio of 2:1 dissolved with the low dissolution rate in the medium similar to that of pure IMC. A comparison between the final % drug dissolved of IBB(PM) and IB(PM) showed no significant difference. It may be because there were adequate amount of BCD in this physical mixture to increase the dissolution of IMC which are limited especially in IBB(PM). Also, Figure 61 shows that initial dissolution rates of IB(PM) is higher than IBB(PM). The explanation for this occurance may be because of excess BCD. Instead of helping to dissolve IMC initially, it act as if it formed coating of IMC and prevented IMC from coming into contact with water during this early stage, resulting in a slower rate.

Table 25 shows the initial dissolution rate of spray dried products. Statistic test for comparison between the effect of spray drying conditions (inlet air temperature and/or feed rate) and initial dissolution rate by ANOVA test indicates no significant difference ($p>0.05$) of the initial dissolution rate of each IIB. In contrast, the initial dissolution rate of each IB exhibits significant difference ($p<0.05$). This result is similar to IBB. Both inlet air temperatures and feed rates affect the initial dissolution rate of IBB while only feed rates affect the initial dissolution rate of IB.

Further evidence obtained from dissolution profiles of spray dried IMC/BCD (as shown in Figure 62-70 and Table 2E-29E, Appendix E) presents higher cummulative percent drug dissolved at 60 minutes than pure IMC, spray dried IMC and physical mixtures were shown. The above results indicated that spray drying process, in addition to having BCD in the component, affect the initial dissolution rate of spray dried IMC/BCD. The spray drying process introduced the higher energetic amorphous state of IMC particles in spray dried IMC/BCD as shown in X-ray diffraction study (Figure 36) and DSC thermograms (Figure 26) (Lin and Kao, 1989). The low crystallinity of the spray dried IMC/BCD having a higher lattice free energy will tend to dissolve fast, since the release of a higher amount of stored lattice free energy will increase the solubility and hence the driving force for dissolution (Grant and Brittain, 1995). Furthermore, the smaller particle size was produced spray drying, as shown in the determination of particle size (Lin and Kao, 1989), giving rise to higher dissolution rates of the spray dried product.

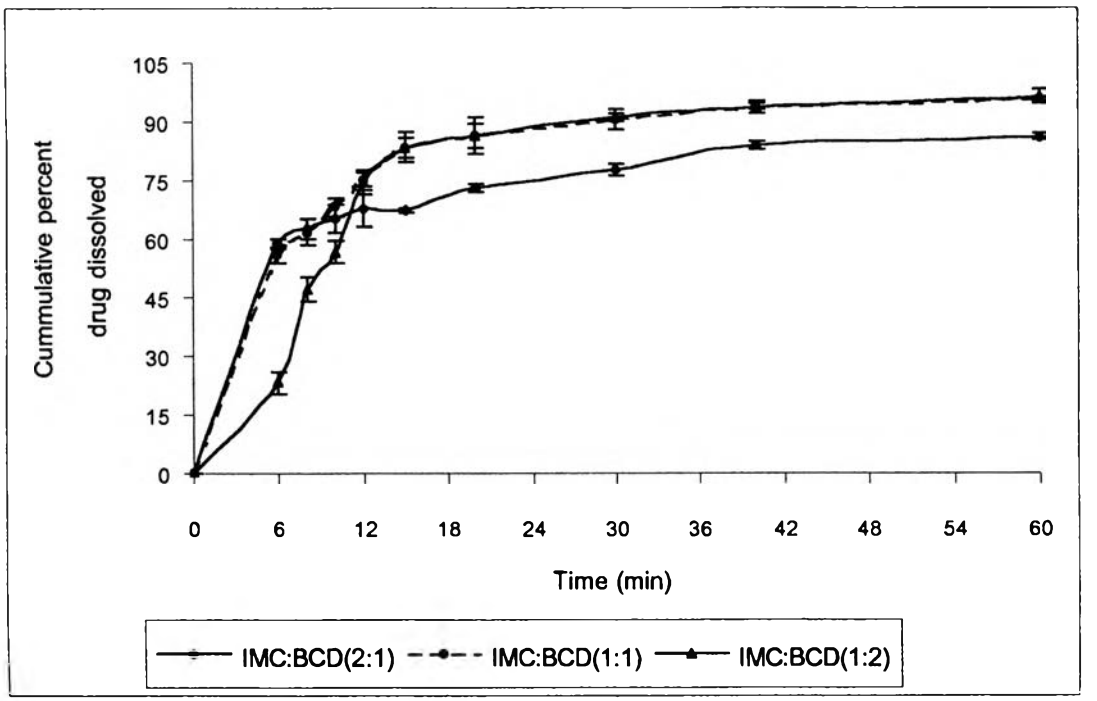

Figure 61 *Dissolution profiles of IMC/BCD physical mixtures*

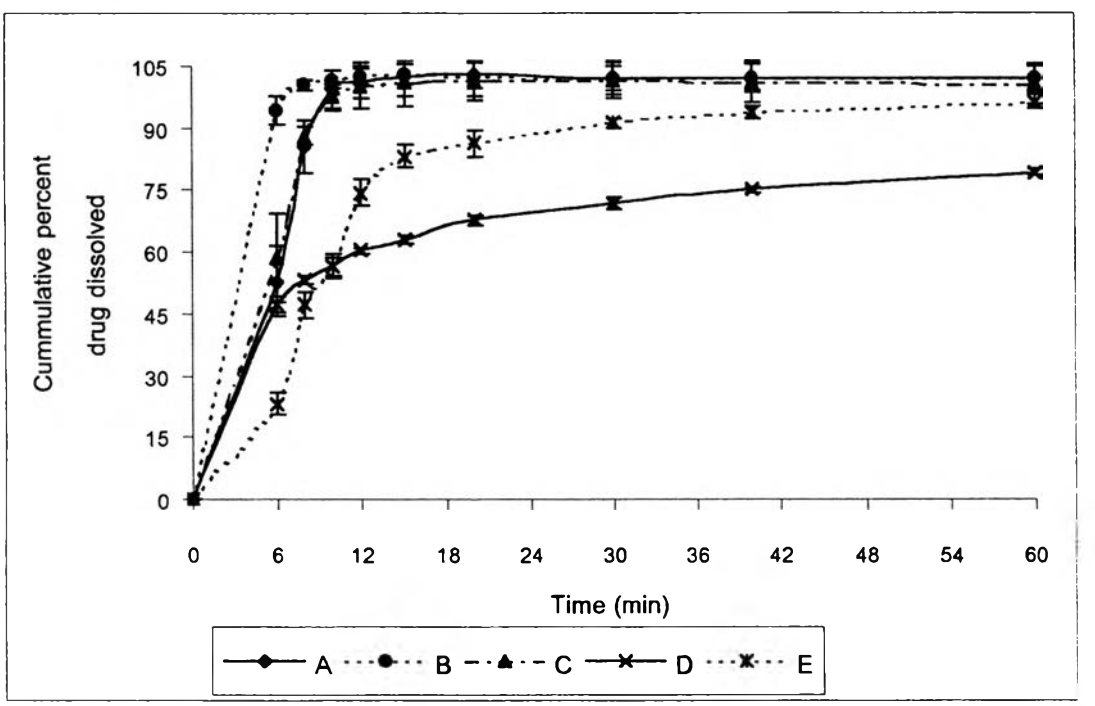

Figure 62 *Dissolution profiles of spray dried IMC /BCD (2:1) at feed rate 10 ml/min and inlet air temperature 130 °C, II10B130, (A); 140 °C, II10B140, (B); 150 °C ,II10B150,(C); IMC, (D) and IIB(PM), (E)*

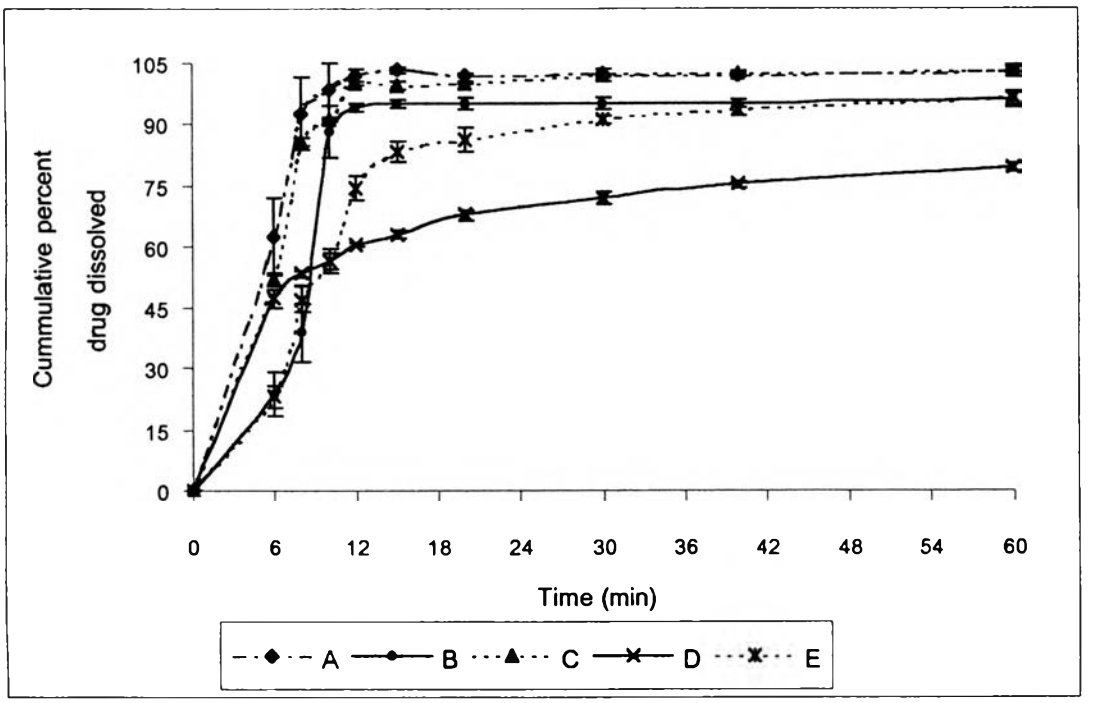

Figure 63 *Dissolution profiles of spray dried IMC /BCD (2:1) at feed rate 15 ml/min and inlet air temperature 130 °C, II15B130, (A); 140 °C, II15B140, (B); 150 °C, II15B150,* (C); *IMC, (D) and IIB(PM), (E)*

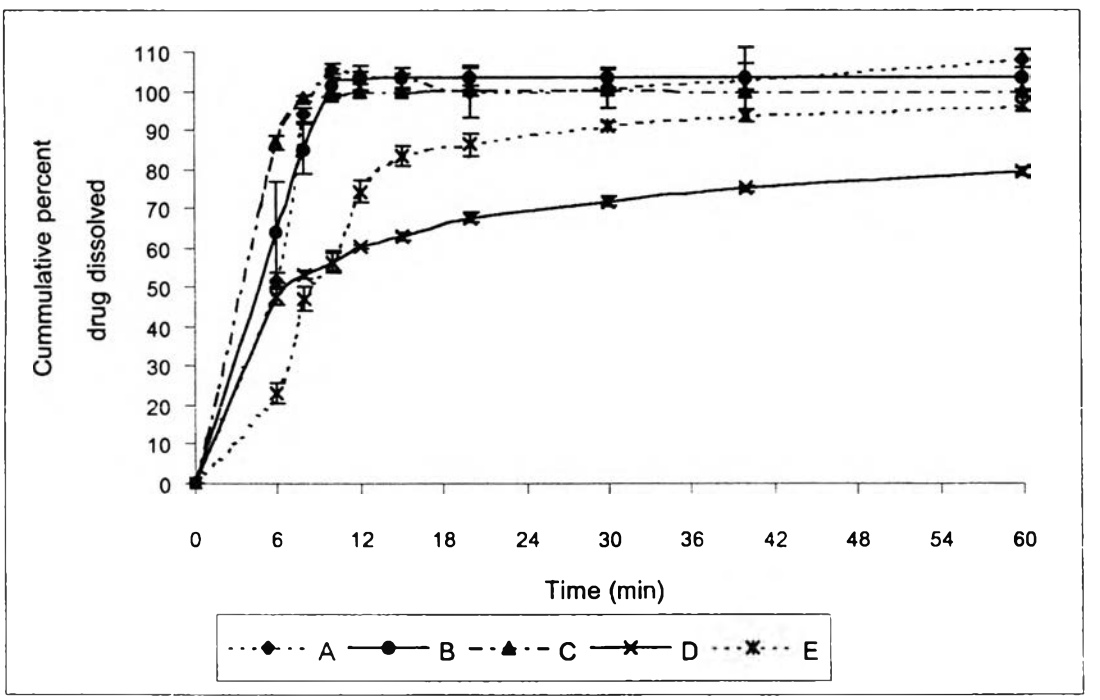

Figure 64 *Dissolution profiles of spray dried IMC/BCD (2:1) at feed rate 20 ml/min and inlet air temperature 130 °C, II20B130, (A); 140 °C, II20B140, (B) ;150 °C, II20B150, (C) ;IMC, (D) and IIB(PM), (E)*

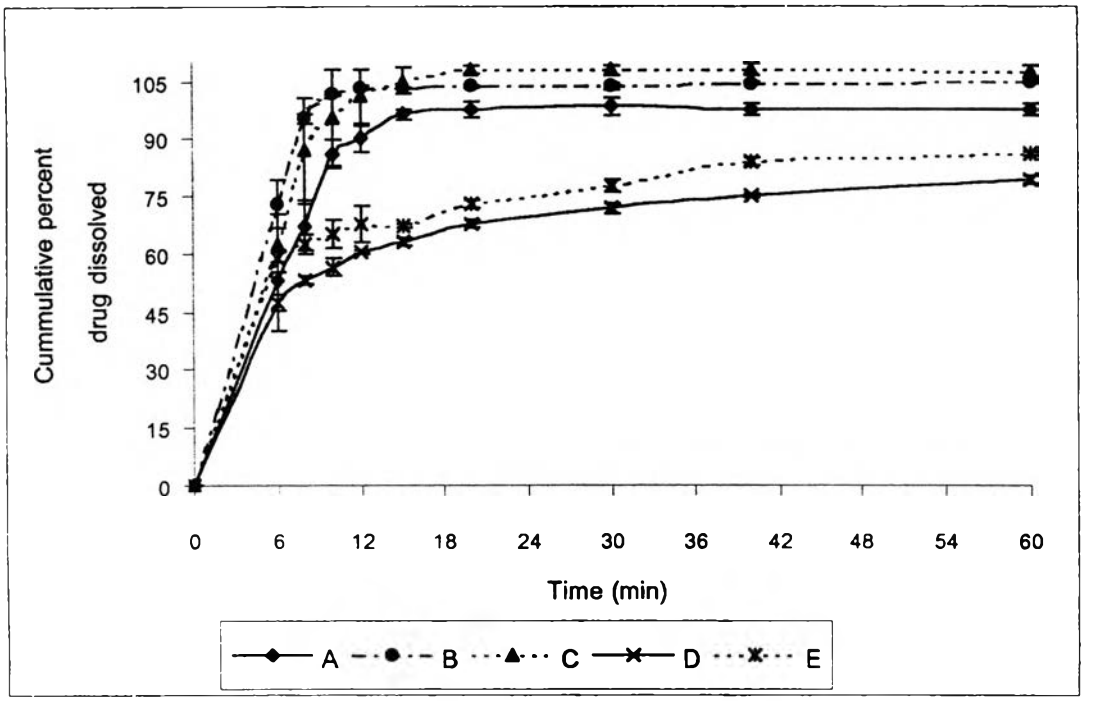

Figure 65 *Dissolution profiles spray dried IMC/BCD (1:1) at feed rate 10 ml/min and inlet air temperature 130 °C,I10B130, (A); 140 °C, I10B140, (B); and 150 °C, I10B150 (C); IMC, (D) and IB(PM), (E).*

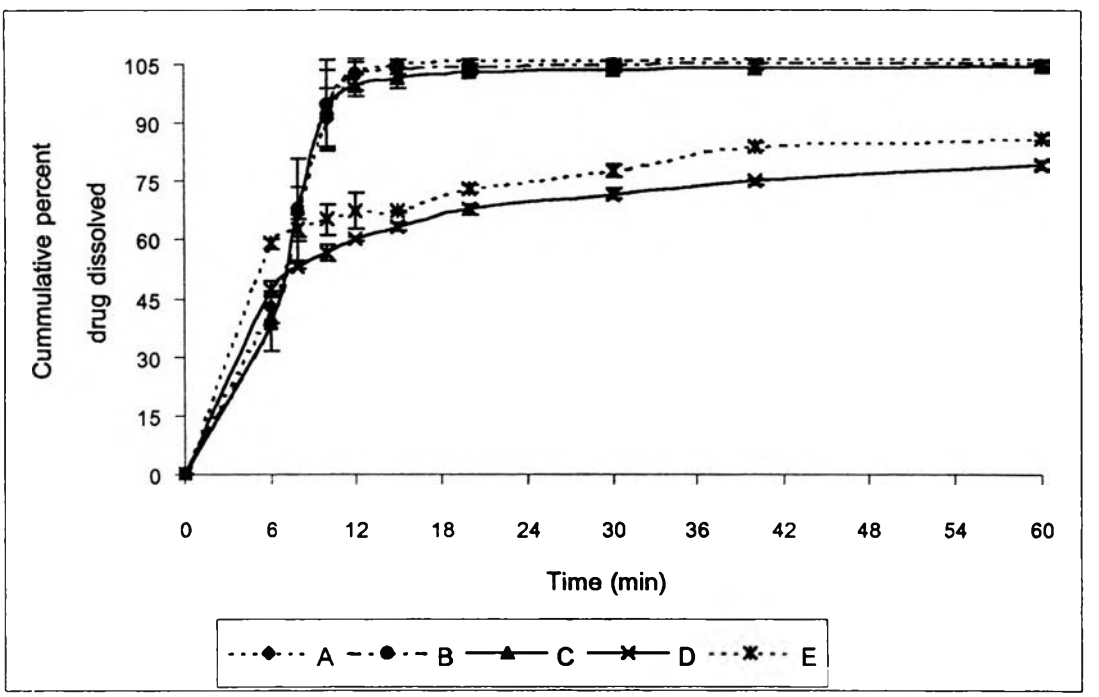

Figure 66 *Dissolution profiles of spray dried IMC/BCD (1:1) at feed rate 15 ml/min and inlet air temperature 130 °C, I15B130, (A); 140 °C, I15B140, (B); 150 °C, I15B150, (C); IMC, (D) and IB(PM), (E).*

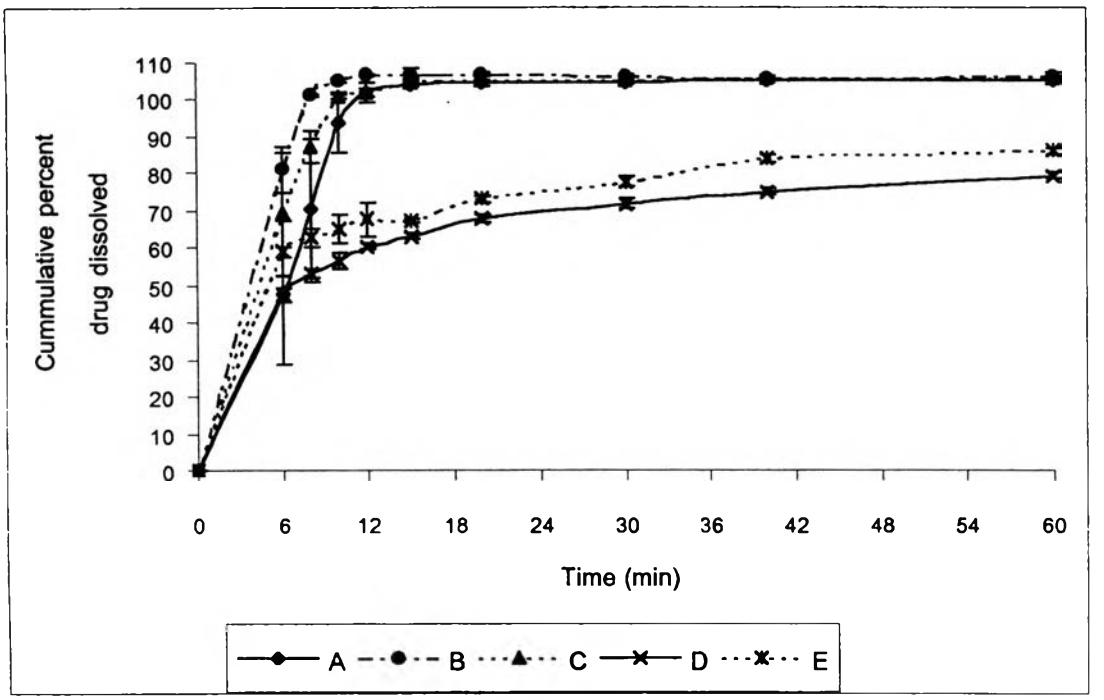

Figure 67 *Dissolution profiles of spray driedIMC /BCD (1:1) at feed rate 20 ml/min and inlet air temperature 130 °C, I20B130, (A); 140 °C, I20B140, (B); 150 °C, I20B150, (C); IMC, (D) and IB(PM), (E).*

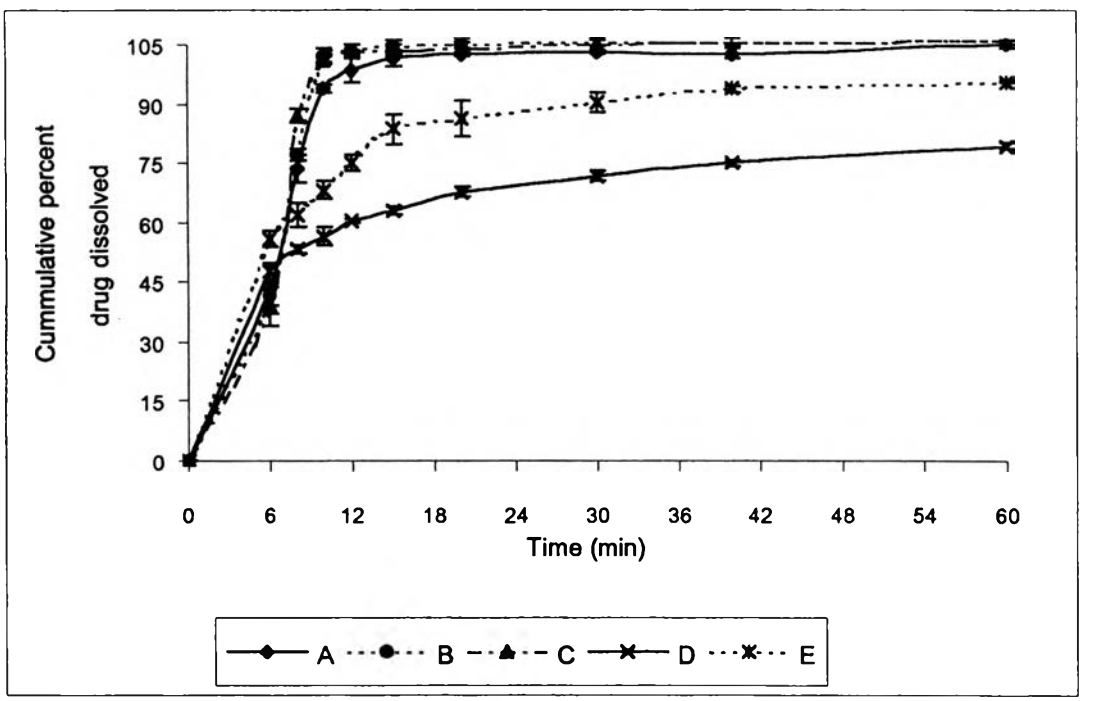

Figure 68 *Dissolution profiles of spray dried IMC /BCD (1:2) at feed rate 10 ml/min and inlet air temperature 130 °C, I10BB130, (A); 140 °C, I10BB140, (B); 150 °C, I10BB150, (C); IMC ,(D) and IBB(PM), (E).*

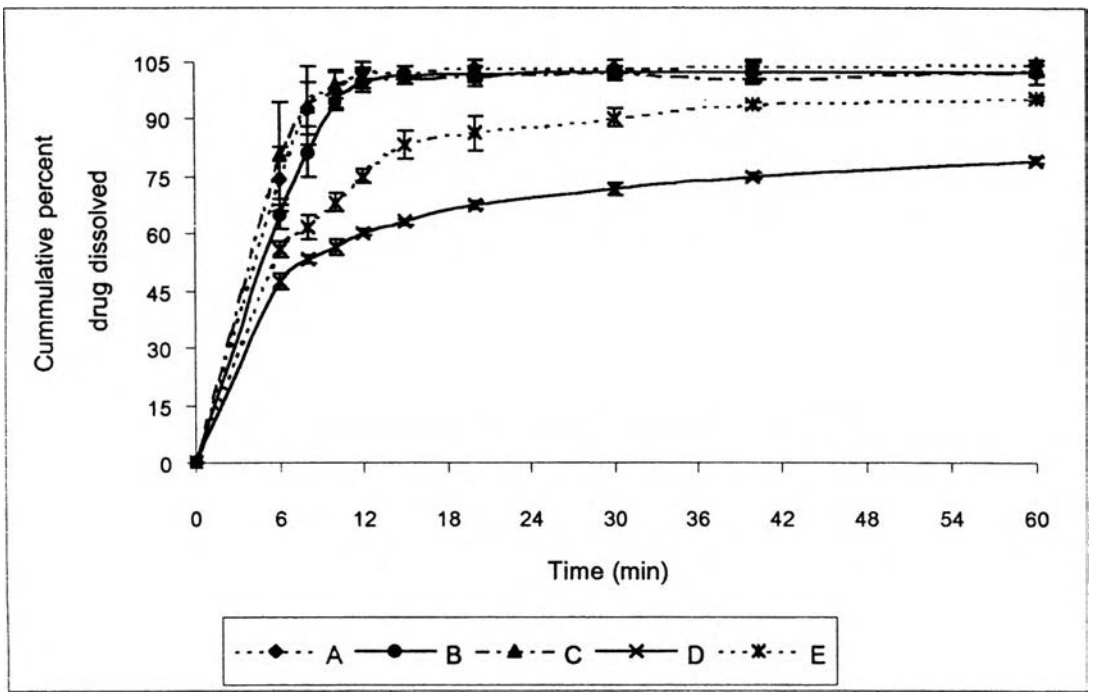

Figure 69 *Dissolution profiles of spray dried IMC /BCD (1:2) at feed rate 15 ml/min and inlet air temperature 130 °C, I15BB130, (A); 140 °C, I15BB140, (B); 150 °C, I15BB150, (C) ; IMC, (D) and IBB(PM), (E).*

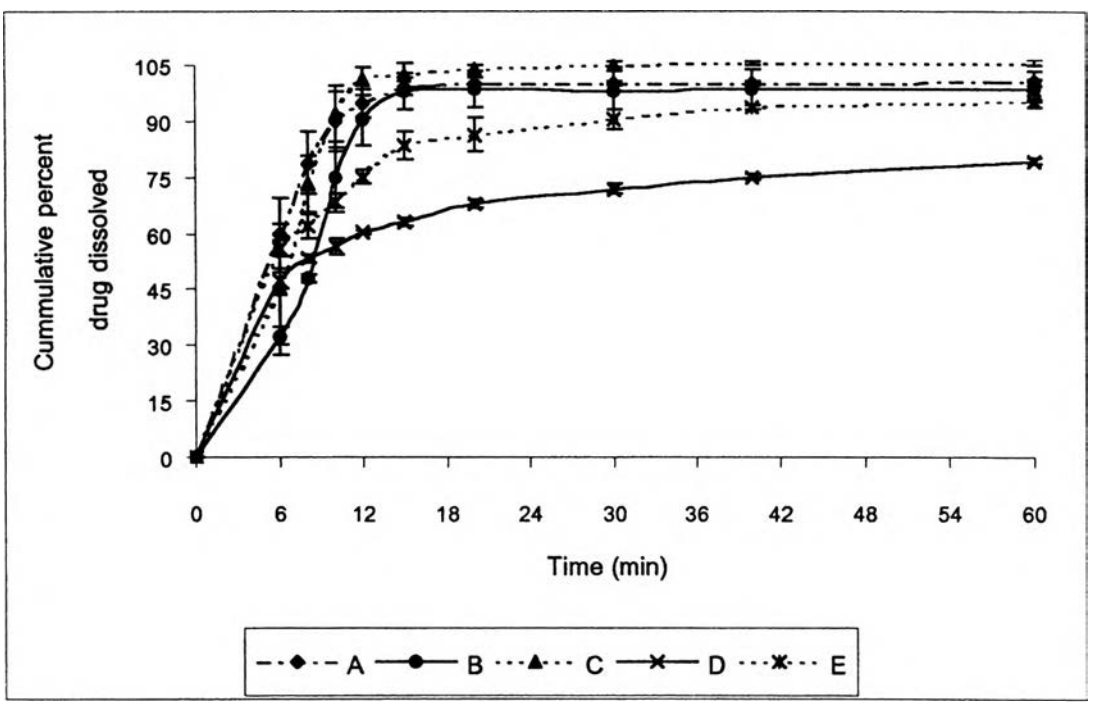

Figure 70 *Dissolution profiles of spray dried IMC /BCD (1:2) at feed rate 20 ml/min and inlet air temperature 130 °C, I20BB130, (A); 140 °C, I20BB140, (B); 150 °C, I20BB150, (C); IMC, (D) and IBB(PM), (E).*

Figure 71 and 72 illustrate the dissolution profiles plotted from the experimental values of IMC/SLS physical mixtures, and its spray dried products. The dissolution profiles of varying ratios of the physical mixtures did not show significant differences ($p>0.05$) either in the dissolved amount, the dissolution time used or initial dissolution rate. In addition SLS in physical mixtures did not affect the initial dissolution rate and the dissolved amount of IMC due to the high amount of SLS in the system.

The dissolution profiles of spray dried IMC/SLS exhibit faster initial dissolution rates than the physical mixture. The dissolution values at 60 minutes of spray dried IMC/SLS was superior to that of the physical mixtures due to the fact that solubilities of the physical mixtures were lower than the spray dried products. This result indicated that the dissolution rate of drug was affected by the spray drying process. Complete dissolution of samples was achieved within 20 minutes. The increase in initial dissolution rate when increased the SLS concentration was not significantly different ($p > 0.05$) with all the spray dried IMC/SLS. The dissolution rate enhancement of spray dried products when compared to the physical mixtures or pure IMC might be due to many reasons. One was the incorporation of SLS surfactant and able to reduce the interfacial tension between the solid and the dissolution medium and hence improving the wettability of the drug particles (Sjokvist et al., 1992). This might be due to solid-state molecular interaction between the drug and surfactant which in turn affects the enthalpy of the solid and the solubility of the drug (Otsuka and Matsua, 1995), confirmed by DSC (Figure 30). Other reasons were the smaller particle size, resulting from the increased in surface area of particles, and the low crystallinity of spray dried products (as shown in X-ray diffraction patterns) might also improved the solubility of drug. Moreover, the formation of sodium salt during the spray drying process indicated by FTIR may increase the solubility of this spray dried products.

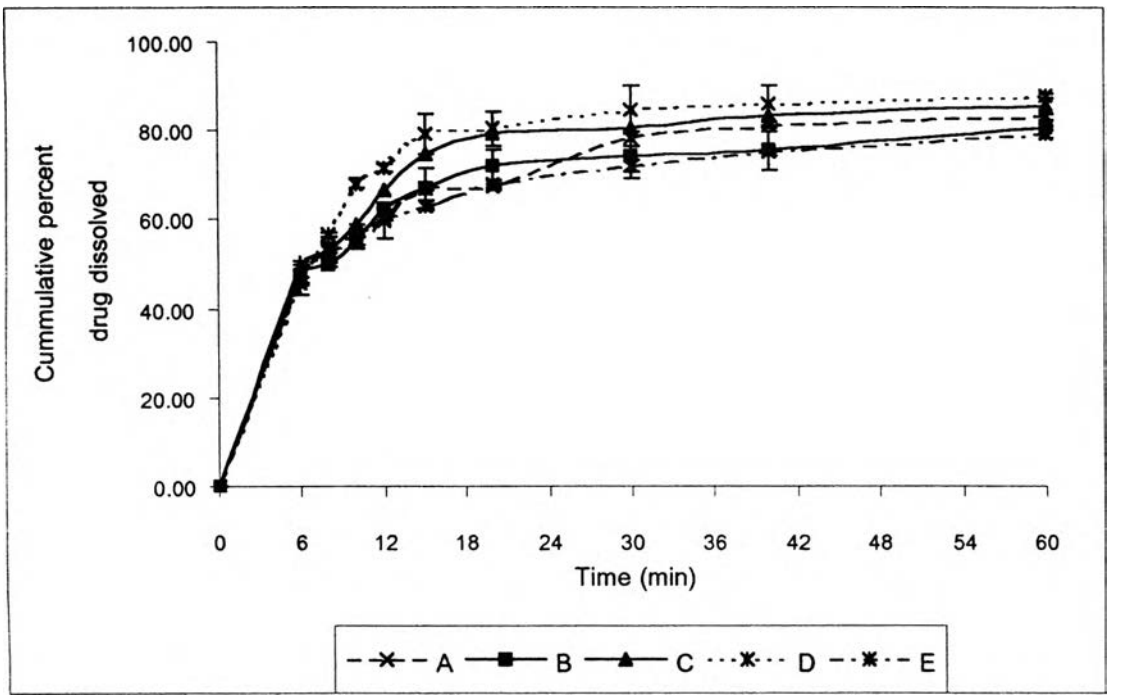

Figure 71 *Dissolution profiles of IMC/SLS physical mixtures : IMC+13% SLS, !S13(PM), (A); IMC+20% SLS, IS20(PM), (B); IMC+ 27% SLS, IS27(PM), (C); IMC+ 33% SLS, IS33 (PM), (D) and IMC, (E)*

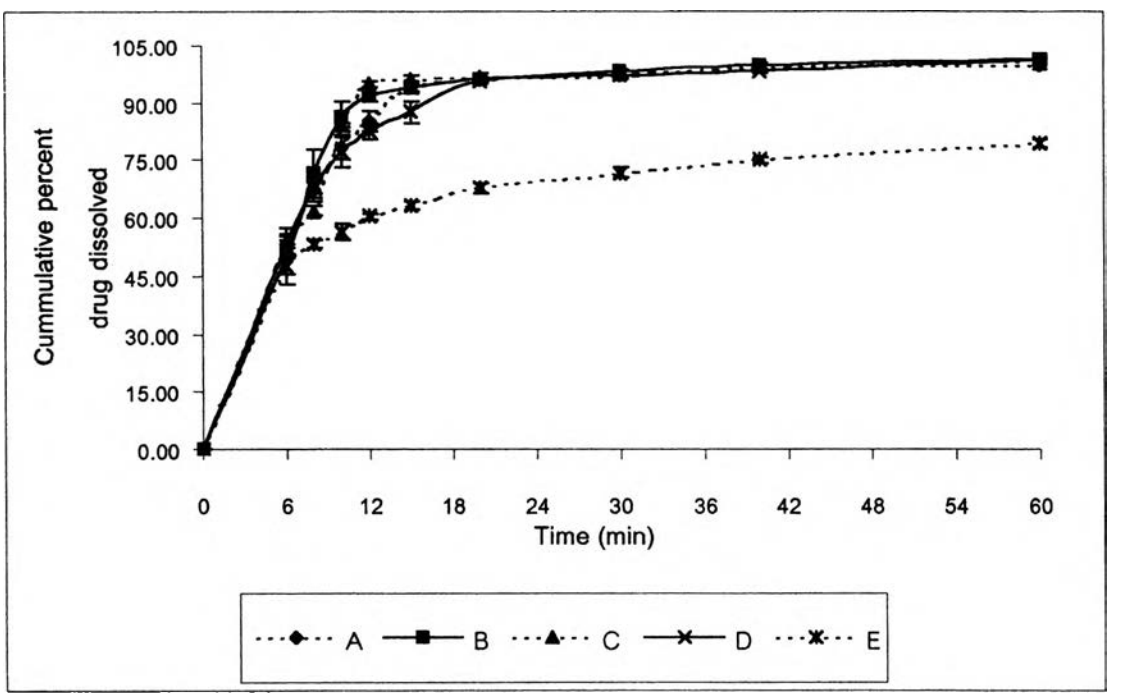

Figure 72 *Dissolution profiles of spray dried IMC/SLS: IMC+13% SLS, IS13, (A); IMC+20% SLS, IS20, (B); IMC+ 27% SLS, IS27, (C); IMC+ 33% SLS, IS33, (D) and IMC (E)*